Aus dem Institut/der Klinik für Tissue Engineering Laboratory & Berlin-Brandenburg Center for Regenerative Therapies, Department of Rheumatology and Clinical Immunology
der Medizinischen Fakultät Charité – Universitätsmedizin Berlin

DISSERTATION

Molecular characterization of human mesenchymal stem cell differentiation to identify biomarkers for quality assurance in stem cell therapy

zur Erlangung des akademischen Grades
Doctor rerum medicinalium (Dr. rer. medic.)

vorgelegt der Medizinischen Fakultät
Charité – Universitätsmedizin Berlin

von

Mujib Ullah

aus Pakistan

Datum der Promotion: *14-Feburary-2014*

Gutachter/in:

1. Prof. Dr. rer. nat. Michael. Sittinger

2. Prof. Dr. med. R. Arnold

3. Prof. Dr. med. D. Dragun

Date of Doctorate: Dr. rer. Medic: ***14 February 2014***

Table of Contents

1.0. Summary of the Doctoral Research in the Form of Following Graphic Outlines for Publications Based Cumulative Dissertation

1.1. GARPHICAL ABSTRACT

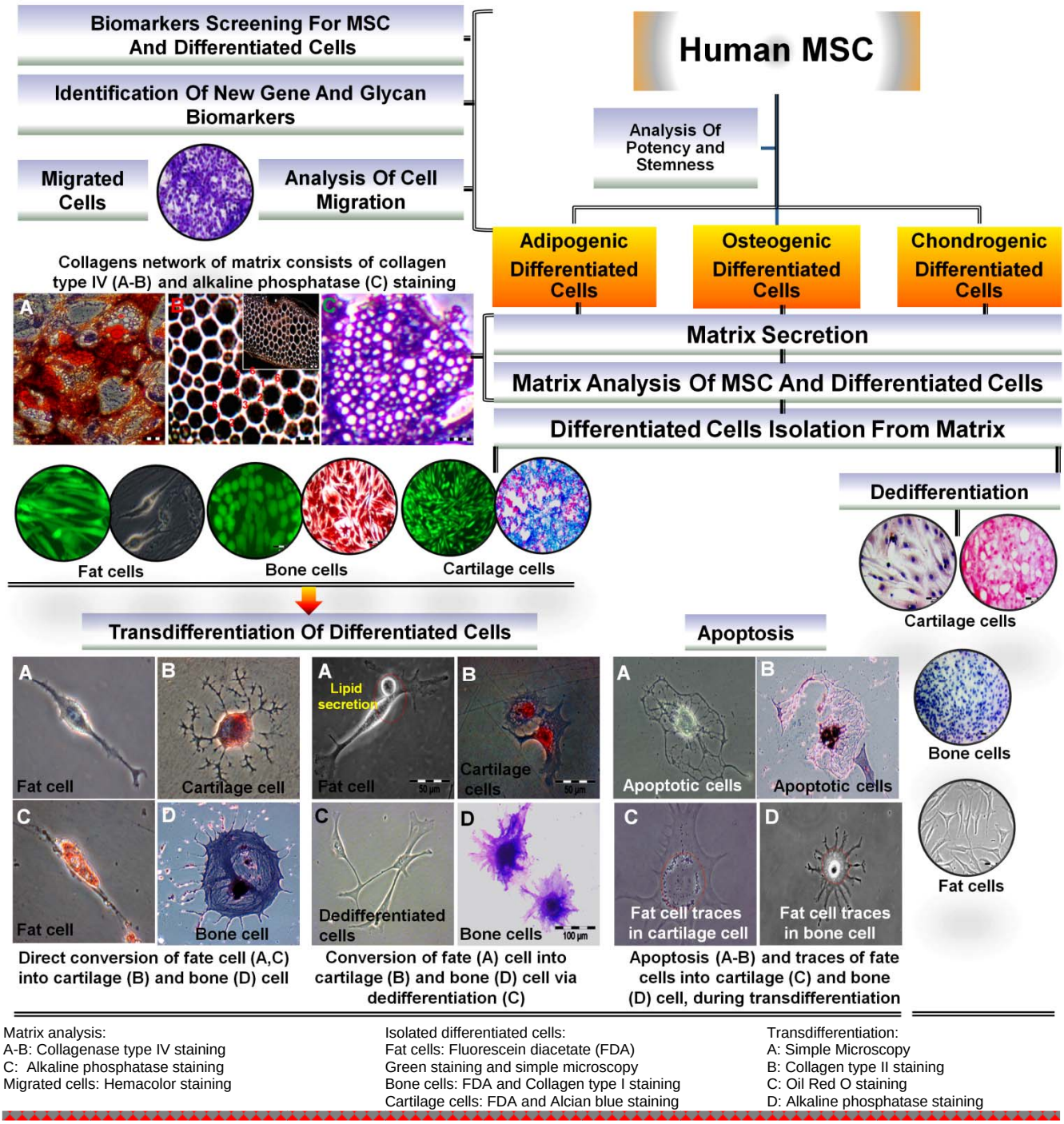

1.2. ABSTRACT

Human mesenchymal stem cells (MSC) are promising candidates for regenerative medicine. Obviously, for practical and regulatory issues, knowledge of transdifferentiation (conversion of one lineage cells into another), new biomarkers characterizing MSC and their differentiated progeny could be crucial. However, after differentiation, whether stem cells increase or decrease their potency and stemness abilities, and whether transdifferentiation proceeds via a direct cell-to-cell conversion or needs dedifferentiation, is not adequately answered. Moreover, little is known about MSC and their adipogenic progeny in terms of lineage specific gene filtration, biomarker selection and matrix analysis. To investigate such issues, MSC were differentiated into adipogenic, osteogenic and chondrogenic lineage cells, and then the vital cells were isolated from their differentiated matrix. Subsequently, in different approaches, the isolated cells were used for the experiments of transdifferentiation, identification of new gene and glycan based biomarkers, matrix analysis, and cellular migration. In this work, it is shown that transdifferentiation was successful via dedifferentiation as confirmed by single cell analysis. On molecular level, a fine tuned association of cell cycle arrest (*DHCR24*, *G0S2*, *MAP2K6*, *SESN3, RB1*) and progression (*CCND1*, *CHEK*, *HGF*, *HMGA2*, *SMAD3*, *CCPG1, RGS2*) genes with transdifferentiation was observed. However, the direct transdifferentiation (without dedifferentiation) of adipogenic lineage cells into osteogenic or chondrogenic resulted in mixed cultures of both lineage cells (adipogenic and new acquiring osteogenic/chondrogenic phenotypes), as confirmed by histology and significantly upregulated gene expression of *PPARG*, *FABP4*, *SPP1*, *RUNX2*, *SOX9,* and *COL2A1*. Beside transdifferentiation, the differentiated cells were screened for the identification of biomarkers. Not only a new method "reverse adipogenesis" for fat marker filtration was established, but also 4 new fat markers *APCDD1*, *CHI3L1*, *RARRES1,* and *SEMA3G* were identified. Apart from this, glycan based biomarkers were discovered (H6N5F1, H7N6F1, and S1H7N6F1 for MSC; highly expressed levels of biantennary fucosylated and sialylated structures for fat cells). Beside biomarker identification, differentiated cells were analyzed for their secreted matrix. Collagen type I, II and IV filaments were found in the adipogenic matrix. The genetic machinery behind the matrix was identified with a significantly regulated expression of C*OL4A1*, *GPC1*, *GPC4*, *ITGA7*, *ICAM3*, *SDC2*, *TIMP4, BGN*, *CLDN11*, *ITGA2*, *ITGB1,* and *LAMA3*. Next, the directional cell migration was investigated, and similar migration rates for both, chondrogenically differentiated cells and MSC towards the stimulus of CCL25 chemokine were found. The presented data of transdifferentiation, gene and glycan based biomarkers for identification and tracking of cells, matrix analysis and directional cell migration could be vital for quality assurance in stem cell therapy.

1.3. ZUSAMMENFASSUNG

Humane mesenchymale Stammzellen sind vielversprechende Kandidaten für Anwendungen in der regenerativen Medizin. Für praktische und regulatorische Fragen ist dabei das Wissen über Transdifferenzierungsprozesse der Zellen (Umwandlung von einer Zelldifferenzierungslinie in ein andere), sowie über neue Biomarker zur Charakterisierung von MSC und deren differenzierten Nachkommen von entscheidender Bedeutung. Jedoch bleibt die Frage, ob Stammzellen ihre Potenz und ihre Stammzellfähigkeiten nach Differenzierungen verlieren oder ob sie diese Merkmale behalten oder sogar verbessern. Weiterhin ist es noch nicht ausreichend beantwortet, ob Transdifferenzierungen über eine direkte Zell-zu-Zell Umwandlung ablaufen oder eine Dedifferenzierung benötigen. Darüber hinaus ist nur wenig über MSC und deren adipogen differenzierte Nachkommen in Bezug auf Linien-spezifische Genfiltration, Biomarker Auswahl und Matrixanalyse bekannt. Um solche Probleme zu untersuchen, wurden MSC in die adipogene, osteogene und chondrogene Richtung differenziert, und anschließend vitale Zellen aus ihrer differenzierten Matrix isoliert. Anschließend wurden die isolierten Zellen in verschiedenen Ansätzen für die Experimente zur Transdifferenzierung, Identifizierung neuer Gen- und Glykan-basierter Biomarker, Matrixanalyse und Zellmigration verwendet. In dieser Arbeit konnte gezeigt werden, dass die Transdifferenzierung über einen Dedifferenzierungsschritt erfolgreich war. Dies konnte durch eine Einzelzellanalyse bestätigt werden. Auf molekularer Ebene konnte eine fein abgestimmte Assoziation der Zellzyklusarrest-spezifischen Gene (DHCR24, *G0S2*, *MAP2K6*, *SESN3* und *RB1*) und der Gene der Progression (CCND1, *CHEK*, HGF, *HMGA2*, *SMAD3*, *CCPG1* und *RGS2*) mit der Transdifferenzierung festgestellt werden. Allerdings führte die direkte Transdifferenzierung (ohne Dedifferenzierung) von adipogen differenzierten Zellen in die osteogene oder chondrogene Richtung zu Mischkulturen beider Zelltypen (adipogener und neu entwickelter osteogener/chondrogener Phänotyp), wie durch histologische Färbungen und die deutlich erhöhten Genexpressionen von *PPARG*, *FABP4*, *SPP1*, *RUNX2* , *SOX9* und *COL2A1* bestätigt werden konnte. Neben der Transdifferenzierung wurden die differenzierten Zellen auch zur Identifizierung neuer Biomarker untersucht. Dabei konnte nicht nur eine neue Methode "reverse Adipogenese" für die Fettmarker Filtration etabliert werden, sondern es wurden auch 4 neue Fettmarker *APCDD1*, *CHI3L1*, *RARRES1* und *SEMA3G* identifiziert. Abgesehen davon wurden Glykan-basierte Biomarker entdeckt (H6N5F1, H7N6F1 und S1H7N6F1 für MSC; stark exprimierte, biantennär fukosylierte und sialylierte Strukturen für Fettzellen). Neben der Identifizierung der Biomarker erfolgte die Untersuchung der sezernierten Matrix von differenzierten Zellen. In der adipogenen Matrix wurden Filamente von Kollagen Typ I, II und IV gefunden. Bei der Indentifizierung der genetischen Maschinerie hinter der Matrix zeigte die Expression von *COL4A1*, *GPC1*, *GPC4*, *ITGA7*, *ICAM3*, *SDC2*, *TIMP4*, *BGN*, *CLDN11*, *ITGA2*, *ITGB1* und *LAMA3* eine signifikante Regulierung. Als nächstes wurde die gerichtete Zellwanderung untersucht und eine ähnliche Migrationsrate für chondrogen differenzierte Zellen und MSC in Richtung des Chemokins CCL25 als Stimulus gefunden. Die gewonnenen Erkenntnisse über die Transdifferenzierung, die Gen- und Glykan-basierten Biomarker zur Identifizierung und Nachverfolgung von Zellen, der Matrix Analyse und der gerichteten Zellwanderung könnten entscheidend für die Qualitätssicherung in der Stammzelltherapie sein.

THIS DOCTORAL RESEARCH IS SUBMITTED AS A CUMULATIVE DISSERTATION (PUBLIKATIONSPROMOTION), WHICH COMPRISED OF 6 PUBLISHED PAPERS (SECTION 10).

2.0. TITLE

Molecular characterization of human mesenchymal stem cell differentiation to identify biomarkers for quality assurance in stem cell therapy

2.1. RESEARCH GOALS

1) To isolate viable cells from differentiated bone marrow-derived mesenchymal stem cell (MSC) cultures (adipogenic, osteogenic and chondrogenic).
2) To evaluate the dedifferentiation, redifferentiation and transdifferentiation capacity of viable cells isolated from differentiated cell cultures into other developmental lineages (adipogenic, osteogenic and chondrogenic).
3) To investigate the direct phenotype switching mechanism of adipogenic differentiated cells into osteogenic or chondrogenic lineage cells.
4) To identify biomarkers for quality assurance in stem cell therapy (MSC and adipogenic lineage cells).
5) To analyze the extracellular matrix (ECM) of MSC and their differentiated progeny of adipogenic and chondrogenic lineage cells.
6) To evaluate the guided and directional cell migration of MSC, chondrogenic differentiated and dedifferentiated cells.

2.2. INTRODUCTION

Human bone marrow mesenchymal stem cells (MSC), also named multipotent mesenchymal stromal cells are easy to isolate, expand and hold great promise for tissue regeneration [1, 2]. For instance, *in vitro* and *in vivo*, they develop into diverse tissues like fat, bone and cartilage [3]. After differentiation, whether stem cells change or preserve their potency and stemness abilities, is not satisfactorily answered. It is generally accepted opinion that after differentiation the stem cells become unipotent and lineage restricted in an irreversible manner. However, the conversion of differentiated cells from one lineage into other lineage cells, a phenomenon called transdifferentiation has been reported [4]. This leads to the questions that how cells transdifferentiate, and whether cells convert from one lineage into another via direct cell-to-cell conversion or dedifferentiation to a progenitor cells and subsequent differentiation, and whether MSC potency decreases or increases during differentiation.

Before diverting this new approach into effective clinical use, transdifferentiation could not be simply overlooked, as it challenges the normal paradigms of biological laws, whereas mature cells not only transdifferentiate within same germ layers, but even across the lineage boundaries [5]. To address such concerns, MSC were adipogenically differentiated followed by direct transdifferentiaton, and subsequently examined by histology, immunohistochemistry, qPCR and single cell analysis.

In regenerative medicine the use of transdifferentiation approach could be more rational as the cells of choice from abundant and easily available sources such as fibroblast and adipose tissue could be converted into cells of demand, to restore the diseased tissues [1, 5]. Although the knowledge of potency and to explore the underlying mechanisms of transdifferentiation is prerequisites, however, not sufficient to clinically characterize the transplants for regenerative approaches. The MSC-based tissue transplants are clinically applied for the restoration of injured and diseased tissues [6]. However, before going into clinical application the tissue forming process requires a proper characterization. In this context, the identification of new biomarkers using new approaches would be a critical step towards the clinics. For instance, during adipogenesis, fat biomarkers are usually selecting on the basis of a single parameter of significant change in gene expression [2]. Generally, this selection is misleading, as adipogenic cocktail not only express adipogenic-specific genes but also express genes for other cellular process. Thus, how to filter only adipogenic-specific genes out of all significantly expressed genes needs an answer. To achieve this, the process of adipogenesis and reverse adipogenesis was combined. In adipogenesis the 991 genes were significantly expressed, however some of the expressed genes not represent the process of adipogenesis. Therefore, to filter only adipogenic-specific genes, the expression of adipogenic genes was undo by reverse adipogenesis and in this way true fat marker genes were selected [2]. Moreover, some new gene and glycan based biomarkers for MSC and adipogenic differentiated cells were identified, which could be beneficial for tracking of cells during regenerative therapy [2, 7].

Apart from transdifferentiation and identification of new biomarkers, the investigation of directional and guided cell migration could be a crucial step in regenerative therapies, as MSC migrate to the sites of injury and participate in the repair process [8, 9]. Stem cell migration not only plays a potential role in cell-colonization inside biomaterial scaffolding, but also takes part in the reorganization of matrix [9]. Thus, guided cell migration was investigated. Similarly, matrix analysis is another step in determining the efficacy of cellular therapies, because matrix not only provides biological shelter but also takes part in diverse cellular activities on functional bases [10]. For instance, matrix plays a critical role in differentiation, proliferation, migration and regeneration of cells [10, 11]. So, these features emphasize the importance of matrix analysis for tissue regeneration.
Therefore, in different approaches, MSC and differentiated cells were used for the combined investigation of transdifferentiation, identification of new gene and glycan based biomarkers, analysis of matrix and to examine the directional and guided cell migration. The collective examination of above parameters could be beneficial to enhance the level of quality assurance in cell based therapies.

3.0. METHODS

3.1. Isolation of MSC from bone marrow and subsequent culturing

Human MSC were isolated from iliac crest bone marrow aspirates as described in our publications [1, 2]. The ethical committee of the Charité-University Medicine Berlin approved the study. Briefly, aspirates were diluted with growth medium. After 48 h of cultivation, non-adherent cells and debris were washed out by the first media exchange. Growth medium was changed three times a week and when reaching 90% confluence, cells were detached and replated at a density of $5x10^3$ cells/cm^2.

3.2. Adipogenic differentiation of human MSC

Adipogenesis was performed as described in our publications [1, 2, 10]. Briefly, cells were incubated for 3 days in induction medium followed by 2 days in maintenance medium in 3 consecutive cycles. The maintenance medium consisted of DME-medium with 10% FBS, 10 µg/ml insulin, 100 U/ml penicillin and 100 µg/ml streptomycin. The induction medium contained, in addition, 1 µM dexamethasone, 0.2 mM indomethacin and 0.5 mM 3-isobutyl-1-methylxanthine. In control cultures, only the maintenance medium was used.

3.3. Isolation and culture expansion of adipogenic differentiated cells

To study the dedifferentiation and transdifferentiation capacity of differentiated cells, adipogenic differentiated cells were selected as a model system, as they are easy to isolate, culture and abundantly available [2, 5]. Adipogenic differentiated vital cells were isolated from their ECM as described in our publications [1]. Afterwards, they were culture expanded (dedifferentiated) for 35 days. Finally, dedifferentiated cells were transdifferentiated.

3.4. Chondrogenic differentiation

For chondrogenic differentiation, $2.5x10^5$ MSC were centrifuged (150g, 5 min) to form high density micromass culture pellets [12]. The chondrogenic differentiation of these pellets were achieved for 28 days with DMEM, ITS supplements, 100 nM dexamethasone, 0.17 mM ascorbic acid-2-phosphate, 1 mM sodium pyruvate, 0.35 mM L-proline and 10 ng/ml transforming growth factor-β3 (TGFβ3). The control pellets were cultured in the same medium in absence of TGFβ3. The media (500 µl) was changed 3 times a week.

3.5. Isolation of, viable, chondrogenic differentiated cells from intact pellets

The pellet culture was washed with PBS. Then, for enzymatic digestion, pellet was digested with 300 U collagenase II, 20 U collagenase P and 2 mM $CaCl_2$ for 90 min incubation at 37°C in presence of 5% CO_2 [12]. This resulted in a mixture of viable, chondrogenic differentiated cells and ECM. Cells were isolated from the pool of 25 pellets (about $2.0x10^5$ cells/pellet) per donor. Subsequently, cells and ECM were separated from each other by mechanically homogenization and centrifugation.

3.6. Isolation of ECM and its enrichment

Mixture of ECM and cellular debris was transferred to a 50 ml tube and centrifuged at 350 g for 6 min and ECM was separated as described in our publications [10, 12]. Briefly, cells and ECM were transferred to culture flasks and incubated at 37°C and 5% CO_2. After 2 h, viable cells were attached to the culture surface while the ECM was not attached. The non-adherent ECM was removed by medium exchange and centrifuged at 350 g for 6 min at 37°C. The process of medium removal and centrifugation was repeated three times to ensure the maximum removal of ECM for its enrichment.

3.7. Flow cytometric analysis

Undifferentiated, differentiated, dedifferentiated, redifferentiated and transdifferentiated cells were analyzed for surface markers with FACSCalibur flow cytometer as described in our publications [1, 9]. Briefly, cells were collected and washed, then centrifuged (250 g, 5 min) and re-suspended in cold PBS/0.5% BSA. Afterwards they were incubated for 15 min on ice with titrated concentrations of R-phycoerythrin labeled mouse anti-human CD14, CD34, CD73, CD166, fluorescein isothiocynate (FITC) labeled mouse anti-human CD44, CD45, CD90, or FITC labeled mouse anti-human CD105. Finally the cells were washed and data were evaluated using CellQuest software.

3.8. Osteogenic lineage differentiation

Osteogenic differentiation was performed as described in our publication [1]. Briefly, confluent growing cell cultures were induced for 28 days in DMEM supplemented with 10% FBS, 20 mM HEPES buffer, 100 U/ml penicillin, 100 µg/ml streptomycin, and as osteogenic cocktail 100 nM dexamethasone, 10 mM β-glycerophosphate, and 0.05 mM L-ascorbic acid 2-phosphate.

3.9. Clonal analysis of adipogenic differentiated cells

For clonal analysis the adipogenic differentiated cells were seeded at 5 to 8 cells/cm^2, the reason for this low cell density was to make the picking process easier for a single cell selection [1, 5]. The detailed procedure of single cell analysis is available in our publications [1, 5].

3.10. Single cell analysis of transdifferentiation

Single adipogenic differentiated cells were confirmed by Oil Red O staining, bloated shape morphology and secretion of lipid droplets, and subsequently were seeded at 5-8 cells/cm^2, as detailed method has been described in our publications [1, 5]. Briefly, a single adipogenic cell was selected and encircled with cloning cylinders, and the remaining cells were removed from the culture dishes. Subsequently, the single adipogenic cell was transdifferentiated for 28 days to osteogenic or chondrogenic lineage cells directly or with including the intermediate step of dedifferentiation.

3.11. Histological and immunohistochemical analysis of differentiated cultures

During adipogenesis, lipid accumulation was examined by Oil Red O staining. Osteogenesis was documented by alkaline phosphatase activity and von Kossa staining. Chondrogenic differentiation was verified by alcian blue and collagen type II staining. The detail procedures of above staining are available in our publications [1, 9, 12].

3.12. Semiquantitative analysis

For semiquantification of histological and immunohistochemical data, images were analyzed by computer assisted software as described in our publications [1, 5]. Briefly, tagged image files were opened with Adobe Photoshop and the staining specific area was determined, calculated and analyzed.

3.13. Isolation of RNA from cell cultures

For all experiments, total RNA was isolated as described in our publications [1, 2, 9]. Briefly, cultures were homogenized with TriReagent, and then 1-bromo-3-chloro-propane was added. Following centrifugation (45 min, 13,000 g) the aqueous phase was collected and mixed with ethanol. After isolation, the total RNA was controlled for integrity and purity with the Bioanalyzer and NanoDrop, respectively.

3.14. Quantitative real-time RT-PCR analysis of cell cultures

TaqMan quantitative real-time RT-PCR for all experiments was performed as described in our publications [1, 2, 10, 12]. Briefly, quantitative gene expression was analyzed for all those marker genes, which were specific to undifferentiated, differentiated, dedifferentiated, redifferentiated, transdifferentiated, adipogenic matrix, new adipogenic genes, CCL25 chemokine and CCR9 receptor. Expression of all these marker genes was normalized to the endogenous *GAPDH* expression level and calculated with the $2^{-\Delta\Delta Ct}$ formula in % *GAPDH* expression [1].

3.15. Gene expression profiling

Gene expression profiling with genome-wide Affymetrix HG-U133 Plus 2.0 olgonucleotide microarrays was performed as described in our publications [1, 2]. Briefly, cDNA was synthesized from 1 µg of total RNA and transcribed into biotin-labeled complementary RNA. 15 µg of the fragmented cRNA were then hybridized to the GeneChips for 16 h at 45°C. GeneChips were washed, stained and scanned with a Genearray scanner controlled by Affymetrix GCOS 1.4 software. DAT, CELL and EXP files were generated with GCOS software and raw data were processed for signal calculation and pairwise chip comparison. Some of the microarray data have already been submitted to Gene Expression Omnibus and accessible via GEO ID: GSE36923. Subsequently, all data files were processed with Filemaker pro database and genes were defined as differentially expressed when fulfilling specific change call and fold change (FC) criteria. As selection criteria, the change call limit was set to 100% and the FC limit was set to ≥2 or ≤-2 for all comparisons.

3.16. Gene ontological analysis

Genes meeting the selection criteria were further analyzed using the gene ontology portal of the FileMaker Pro database software and with the functional annotation clustering tool suite of the online bioinformatics database DAVID and the Kyoto Encyclopedia of Genes and Genomes (KEGG). For reproducibility, we have used DAVID default values and a published step-by-step procedure as described in our publications [1, 2]. With these tools, the most significant biological functions and signalling pathways corresponding to the selected genes were identified.

3.17. Analysis strategy of N-glycans

N-glycome of MSC and adipogenic differentiated cells was analyzed as described in our publication [7]. Briefly, membrane glycoproteins were first isolated, then N-glycans were enzymatically released with endo-β-N-acetylglucosaminidase H, and the glycopeptides were further treated with peptide-N4-(N-acetyl-β-glucosaminyl) asparagine amidase F to release the remaining N-glycans. Permethylation was carried out prior to MALDI-TOF-MS to neutralize the negative charges of sialic acids in order to measure both acidic and neutral glycan structures in the positive ionization mode simultaneously. The identified structures were verified by exoglycosidase digestions and by MALDI-TOF/TOF fragmentation.

3.18. Shedding of lipid droplets and examination of adipogenic ECM

As described in our publications [2, 10], MSC were induced towards adipogenic lineage cells. Cells were washed with PBS and then the medium was switched to cell propagation medium. Whereas the adipogenic differentiated cells were maintained for subsequent 12 days and shedding of lipid droplets and ECM structure were assessed.

3.19. Histology and immunohistochemistry of adipogenic ECM

Network of ECM was stained as described in our publication [10]. Briefly, for direct staining, chamber slides were fixed with 3.7% formaldehyde and incubated for 1 h with primary rabbit anti-human type I, type II and type IV collagen antibodies. Then, they were stained according to the manufacturer's recommendation with the Envision system peroxidase kit, followed by hematoxylin counterstaining. Control samples were treated in a similar manner but without primary antibodies.

3.20. Migration potential of cells

Migration potential of MSC, chondrogenic differentiated and dedifferentiated cells were assessed in response to 10% human allogenic serum or CCL25 chemokine as described in our publication [9]. Briefly, chemotaxis assay was performed with 8 um pore size polycarbonate membranes in 96-multiwell format ChemoTx plates. For migration of cells allogenic serum or selected concentration of CCL25 (500-1000 nM) was applied in triplicates to the lower wells, while cells were seeded in the upper wells for 20 h at 37 °C. Negative controls were performed without chemokine or serum. Migrated cells were fixed in methanol/acetone, stained with hemacolor and counted microscopically with image J software.

3.21. Statistical analysis

In all publications [1, 2, 5, 7, 9, 10, 12, 13], the data were expressed as mean and standard error of mean (SEM). Statistically significant values were calculated and asterisks (*) were assigned in the order of $*P < 0.05$; $**P < 0.01$; $***P < 0.001$. Students` t-test for two groups and one way ANOVA for three groups comparison was performed by using SigmaStat software, while GraphPad Prism4 was used for drawing graphs.

4.0. RESULTS

4.1. Characterization and differentiation of MSC

On characterization, human MSC showed fibroblast like morphology [2, 5]. According to established standards, the MSC culture was uniformly positive for the surface markers CD44, CD73, CD90, CD105 and CD166, and was uniformly negative for CD14, CD34 and CD45 [5, 9]. After confirming the identity of MSC, they were differentiated into adipogenic, osteogenic and chondrogenic lineage cells [5]. To produce MSC and differentiated cells in sufficient quality and quantity was essential to investigate the transdifferentiation ability, migration potential, matrix analysis and to identify some new biomarkers for quality assurance in stem cells therapy.

4.2. Establishment of cell isolation protocols for differentiated cell cultures

To perform dedifferentiation, redifferentiation and transdifferentiation studies, the viable cells were isolated from their fat, bone and cartilage differentiated cell cultures [5, 12]. Here, the novel state of the art techniques for differentiated cells isolation from their matrix was established, and published in peer reviewed journals [1, 5, 10, 12]. The isolation of vital adipogenic, osteogenic and chondrogenic differentiated cells from matrix was a very challenging task, but not only this milestone was achieved, but also developed, optimized and standardized new protocols [10, 12]. The isolated viable cells were characterized for morphology, differentiated state, proliferative rate and growth kinetics [1].

4.3. Isolation of adipogenic differentiated cells from the fat matrix

The adipogenic differentiated cells were isolated from their secreted ECM by incubation with 0.05 trypsin/1 mM EDTA in phosphate-buffered saline (PBS) for 8 min at 37°C [1]. Subsequently the isolated cells were dedifferentiated to study that how a specialized differentiated state converts into an unspecialized primitive state [1]. In addition, such cells were also redifferentiated and transdifferentiated to investigate the cellular conversion from one differentiated state into another state [1, 5]. Moreover, the isolated cells were used for surface and genome-wide screening, to identify new gene and glycan based biomarkers for quality assurance in stem cell therapy [2, 7].

4.4. Isolation of chondrogenic differentiated cells from the cartilage matrix

The cells isolation procedure was extended to cartilage matrix, as the clinical use of chondrogenic differentiated cells could be a promising approach for the regenerative treatment of injured or diseased cartilage [9]. Generally, 3D pellet is the standard culture for chondrogenic differentiation [9]. However, in pellets, the cells are entrapped in the secreted ECM [9, 12]. The viable cell isolation from intact pellets was a challenging task that is why our aim was to develop a reliable protocol for cells isolation. In this context, the pellet digestion for 90 min with 300 U collagenase II, 20 U collagenase P and 2 mM $CaCl_2$ worked quite well and resulted in about $2.5x10^5$ cells/pellet [12]. The protocol was further optimized for the separation of released cells and ECM from each other [12]. Cells were alcian blue and collagen type II positive and expressed *COL2A1* and *SOX9*, verifying a chondrogenic character [12]. Similarly, the ECM was uniformly alcian blue and collagen type II positive [12]. Conclusively, the protocol allows the reliable isolation of a defined number of viable, chondrogenic differentiated cells from high-density pellet cultures. The protocol not only delivered the purified chondrogenic cells, but also the enriched ECM for regenerative therapies [12]. After successful isolation, such cells were used for the experiments of dedifferentiation, transdifferentiation and cell migration.

4.5. Dedifferentiation/transdifferentiation of isolated cells

According to our knowledge, no coherent and mechanistic data about the dedifferentiation and transdifferentiation ability of differentiated MSC into other differentiation lineages exist. Therefore, differentiated cells were isolated from their secreted matrix (adipogenic, osteogenic and chondrogenic lineage matrix). Subsequently cells were characterized, culture expanded and induced them in all three differentiation lineages (fat, bone, cartilage) [1, 5]. Before to analyze, track and identify such processes *in vivo*, the searching of new biomarkers for quality assurance in stem cell therapy would be crucial for regenerative therapies. Therefore, isolated differentiated cells were examined for dedifferentiation, transdifferentiation, and in addition to identify new biomarkers on gene and glycan level [2, 5, 7]. Moreover, directional cell migration and matrix analysis of differentiated cells was investigated from quality assurance perspectives in regenerative therapies [9, 10].

4.6. Transdifferentiation: How cells convert from one differentiated state into another

Transdifferentiation is the conversion process of one differentiated cell types into another and could be a short cut approach in cell based therapies, whereas cell of choice could be converted into cells of demand. Previously, it has been controversially discussed, and most of the questions are still open like, whether transdifferentiation occurs via direct cell-to-cell conversion or dedifferentiation to a progenitor cells and subsequent differentiation, and whether MSC potency decreases or increases during differentiation. After addressing such questions, our study concluded that transdifferentiation is dedifferentiation dependent process for terminally differentiated cells [1, 5, 13]. Interestingly, bioinformatics analysis demonstrated the association of cell cycle genes with the process of transdifferentiation [1]. Concluded, our results indicate that cell fate determination is a reversible process which is regulated by cell cycle genes.

4.7. Direct transdifferentiation

How unipotent differentiated cells reprogram into another, and whether transdifferentiation proceeds directly (without any dedifferentiation). To address such issues direct transdifferentiation was performed. The direct cellular conversion of adipogenic lineage cells into osteogenic or chondrogenic

resulted in mixed culture of both lineage cells (adipogenic and new acquiring osteogenic or chondrogenic phenotype) as confirmed by histology and significantly expressed genes *PPARG*, *FABP4*, *SPP1* and *RUNX2* [5, 13]. Conclusively, only some differentiated cells were transdifferentiated instead of all cells [5, 13]. Single cell analysis also showed and confirmed the mixed culture state [1, 5, 13]. Single cells analysis not supports the direct cell-to-cell conversion, rather highlights the involvement of dedifferentiation and proposing a model of transdifferentiation, consisting of three steps that is differentiation, dedifferentiation and redifferentiation of cells [1, 5].

4.8. Genetic machinery of transdifferentiation

To find out the underlined molecular factors, which take part in the conversion of differentiated cells from one phenotype to another, the association of cell cycle arrest and progression genes was identified [1, 13]. For instance, the 61 differentially expressed genes (*DHCR24*, *G0S2*, *MAP2K6, SESN3, DST*, *KAT2*, *MLL5*, *RB1*, *SMAD3* and *ZAK)* in adipogenic differentiated cells showed an association with cell cycle arrest [1, 13]. While, the other 65 differentially expressed genes (CCND1, CHEK*, HGF, HMGA2, SMAD3, CCPG1*, *RASSF4* and *RGS2)* in dedifferentiated cells revealed an association with cell cycle progression [1, 13]. In context of transdifferentiation, the cell cycle arrest and progression genes play a critical role in phenotype switching from one differentiated state into another.

4.9. Gene filtration method to identify adipogenic specific genes

Apart from transdifferentiation, the adipogenic differentiated cells were used for the gene filtration to identify specific genes for the process of adipogenesis. In regenerative medicine, engineered adipose tissue could be clinically applied for the restoration of soft tissue of burn and cancer patients, and in cosmetic surgery [2, 7]. However, the tissue forming process requires a proper characterization for quality assurance in such therapies. For instance, during MSC conversion into adipocytes, adipogenic-cocktail consisting of insulin, dexamethasone, indomethacin and 3-isobutyl-1-methylxanthine not only induce adipogenic-specific but also other genes for the non-adipogenic process [2]. In MSC-derived adipogenic differentiated cells, fat marker genes are generally selecting on the basis of a single parameter of significantly change in gene expression [2]. Generally this selection is misleading, because adipogenic cocktail not only express adipogenic-specific genes but also express genes for other cellular process. So how to filter only adipogenic-specific genes out of all significantly expressed genes needs an answer. To achieve this, the process of adipogenesis was combined with reverse adipogenesis [2].

In adipogenesis the 991 genes were significantly expressed, and according to our hypothesis some of these genes not represent the process of adipogenesis [2]. Therefore, to filter only adipogenic-specific genes, the expression of adipogenic genes was switch-off by reverse adipogenesis, and in this way true fat marker genes were selected. On the basis of this approach, only 782 genes were filtered, out of total 991 significantly expressed genes [2]. To validate the benefit of this approach, all 991 genes were analyzed bioinformatically for adipogenic specific biological annotations, transcription factors and signaling pathways. Interestingly, only genes from the filtered 782 list of fat markers showed an affiliation to adipogenesis. Even adipogenic most prominent markers like *PPARG*, *FABP4*, *LPL*, *LIPE*, *ADIPOQ*, *PLIN1*, *PLIN4*, *IRS2*, *CEBPA*, *APOE* and *APOL2* were included in the filtered list of genes (782), and favors the importance of our approach [2].

4.10. Biomarkers screening

Biomarkers screening and to identify the suitable signatures for characterizing human MSC could be a valuable approach for the clinical application of stem cells in regenerative therapies [2, 7]. Moreover, such knowledge of biomarkers would be critical for practical and regulatory issues, and the stability of such signature sequences could be of importance for tracking and tracing the appropriate cells type *in vitro* and *in vivo*. Therefore, gene expression profiling assays were performed and a Filemaker database was created for storing, handling and analyzing the huge amount of gene expression data. Subsequently, bioinformatics analysis was performed [2], and a candidate marker gene list was created and finally new biomarkers were identified [1, 2, 10]. The stability and reproducibility of newly identified biomarkers were ensured by qPCR examination and bioinformatics analysis.

4.11. New gene biomarkers

The coupling model system of adipogenesis and reverse adipogenesis, allowed the filtration of 782 adipogenic-specific genes out of total 991 significantly expressed genes [2]. Using the combined approach of adipogenesis and reverse adipogenesis, 4 new potential fat marker genes *APCDD1*, *CHI3L1*, *RARRES1* and *SEMA3G* were identified [2]. These biomarkers could be potentially important for characterization of adipogenesis and monitoring of clinical translation in soft-tissue engineering.

4.12. New glycan biomarkers

Beside gene biomarkers, the identification of glycans biomarkers could be promising targets for the monitoring and tracking of stem cells is regenerative therapies. As glycosylation is a common protein post-translational modification and different cell types express different glycan signatures, thus, glycans represent ideal markers due to their prominent cell surface positions [7]. Therefore, according to our knowledge for the first time the N-glycome of MSC and adipogenic differentiated cells were performed with MALDI-TOF mass spectrometry combined with exoglycosidase digestions. Potentially new and vital glycan based biomarkers for MSC and adipogenic differentiated cells were identified. For instance, the N-glycans like H6N5F1, H7N6F1 and S1H7N6F1 were significantly overexpressed in MSC [7]. For adipogenic differentiated cells, we found an increased amount of biantennary fucosylated structures, and a decreased amount of fucosylated as well as afucosylated tri- and tetraantennary structures, and an increased sialylation [7]. Such N-glycans structures could be potential biomarkers for stem cells and their adipogenic differentiated progeny.

4.13. Cellular Communication between cells and matrix

Next, MSC and their differentiated cells were used for the investigation of matrix. Matrix is the non cellular component of tissues, which takes part in the support and cellular activities of cells [10]. However, little is known about the ECM and especially of stem cells matrix. Therefore, the composition and architecture of the fat ECM was investigated to understand the cellular behavior on functional bases. A series of collagens like type I, II and IV filaments were identified, which were specific to ECM [10]. In addition, alkaline phosphatase activity revealed the ossified nature of such filaments within the framework of matrix. Hexagonal structures were abundant in the matrix and they were interwoven in a crisscross manner [10]. Regarding the genetic machinery, the expression of genes like *ADAMTS9*, *COL4A1*, *GPC1*, *ITGA7*, *ICAM3*, *SDC2* and *TIMP4* was significantly upregulated [10]. While the expression of genes like *ADAMTS5, BGN*, *COL14A, CLDN11*, *ITGA2*, *ITGA4, ITGB1, ITGB8, LAMA3* and *TIMP2* and *TIMP3* was significantly downregulated [10].

Genomic and proteomic based analysis of ECM revealed hexagonal structures in the adipogenic ECM. Hexagonal arrangement having no free space between the structures, and we assume that such structural organization could be responsible for peak accumulation of lipids and fats [10]. The integrin signaling pathway is critical to regulate the mutual interaction of cells and ECM, and also famous for outside-in and inside-out communication on functional bases [10]. Cellular adhesion molecular pathway acts as a central hub in the sensing network of cells and ECM, and activates the mechanistic machinery for biological shelter and cellular decision [10]. Genes belong to the family of collagens, integrins, cadherins, laminins, fibronectins and selectins could play vital role in the cellular decisions for diverse functions [10]. To our knowledge, this is the first report on stem cells originated adipogenic ECM. Therapeutic examination of ECM could be remarkable for soft tissue engineering and to investigate reasons behind obesity. To understand the interactive language between cells and matrix could be valuable for the artificial designing of biomaterials and bioscaffolds.

4.14. Guided cellular migration

Beside transdifferentiation and biomarkers identification, MSC and differentiated cells were also used for guided and directional cell migration, which is a basic approach for appropriate cells homing in regenerative therapies [9]. Similarly, for tissue repair, the use of differentiated cells types is another gold standard probably due to pre-active signaling and biological memory of the differentiated state [9]. CCL25 is well known chemokine for stem cells migration, but little is known about the effects of CCL25 on differentiated cells. Therefore, we have investigated the differentiated cells migration in the presences of serum or CCL25 stimulus as such directional chemotaxis could be beneficial to recruit the differentiated cells to the point of damage. To verify the concept of guided and directional cell migration, we used the standard model of chondrogenic differentiated MSC. In CCL25 mediated directional chemotaxis, the chondrogenic differentiated cells showed almost similar migration ability compared to MSC [9]. CCR9 is a cognate receptor of CCL25, and its expression was higher in chondrogenic differentiated cells, which maybe a possible reason for fast track migration ability in differentiated cells [9]. Summarizingly, CCL25 stimulated the guided cell migration in chondrogenic differentiated cells [9], and such *in vitro* oriented cell migration and homing study could be valuable for regenerative strategies.

In conclusion, the current generated knowledge about transdifferentiation, identification of new biomarkers (genes and glycans based) for characterization of cells, matrix analysis and cell migration could be beneficial for quality assessment in regenerative therapies.

5.0. Discussion

Regarding the route of transdifferentiation, our results indicate that adipogenic differentiated cells transdifferentiate into osteogenic or chondrogenic lineage cells via dedifferentiation and at least in part has an association with cell cycle arrest and progression genes [1]. On molecular level, genome-wide expression profiling validated our concept of transdifferentiation, that differentiated cells restrict their choices due to activation of the cell cycle arresting genes [1, 13]. This statement is in line with previously published reports that differentiated cells narrow down potency, plasticity and cell fate choices [14].

To find those molecular mediators which take part in the cellular conversion from one phenotype into another, we found genes like, *CCND1*, *HGF*, *HMGA2*, *KAT2B* and *SMAD3,* which probably take part in the phenotype conversion [1, 13]. Proliferation associated genes like *ACE*, *CRTAM*, *IFI16*, *NDP*, *TP63* and *UHRF2* probably regulate the respective activation and suppression of cell cycle arrest and progression genes during transdifferentiation [1]. Our results may contribute resolving the conflict of two apparently contradictory concepts, namely lineage and plasticity restriction during differentiation and at the same time lineage and plasticity relaxation during transdifferentiation on the basis of cell cycle arrest and progression genes.

Using the direct route of transdifferentiation (without dedifferentiation), mixed culture (a condition in which only some cells were transdifferentiated instead of all) of cells was found [5, 13]. However, previously it has been shown that differentiated cells transdifferentiate successfully [4], and mixed culture has not been reported so far. Therefore, we propose that in previous reports, maybe committed or semi differentiated cells have been used instead of fully mature differentiated cells. Single cell analysis also confirmed the multiple cells formation during transdifferentiation, indicating that direct conversion of one phenotype into another is somewhat linked to dedifferentiation [5, 13]. It means that differentiated cells enter into dedifferentiation phase before transdifferentiation [1, 5]. During direct phenotype switching, why some cells did not change their phenotypes, we propose that differentiated cells maybe the combination of adipoblasts and adipocytes, whereas only former cell type has the ability to convert instead of later cell type. In addition, the proper characterization of single cells could be valuable to understand the mechanism of transdifferentiation.

Current findings suggest that transdifferentiation is robust and simpler process than normal differentiation [1, 5]. It means that once cells differentiated and memorize the differentiation pathway, then later this memory system, could provide a fast track for a second time redifferentiation. Clinically, transdifferentiation could be a vital approach to treat damaged or diseased tissues. Whereas, *in vivo* conversion of one tissue into another seems possible, as the conversion of endogenous mouse cells into neuron has already been reported [15]. In conclusion, our results support transdifferentiation via dedifferentiation and not favor the statement of direct cellular conversion from one phenotype into another.

Beside transdifferentiation, the characterization of differentiated cells could be crucial before going into clinical trials. In this context, the identification of new biomarkers with new methods could be valuable, as the old methods of biomarkers selection are not significantly fruitful. For instance, the adipogenic marker genes are generally selecting on basis of a single parameter of significant change in gene expression, which is misleading [2]. As, the adipogenic cocktail, not only induces the expression of adipogenic specific but also the expression of other genes for other cellular processes. Thus, significant change in gene expression is not a good parameter for gene selection, and how to filter adipogenic-specific genes out of all significantly expressed genes needs an answer. To filter only adipogenic-specific genes, the process of adipogenesis was reversed. During reverse adipogenesis, the adipogenic specific genes undo their expression and were selected. On the basis of this approach, only 782 genes were filtered, out of total 991 significantly expressed genes [2]. To validate the benefit of this approach, all 991 genes were analyzed bioinformatically, interestingly, only the filtered 782 list of fat markers, showed affiliation to adipogenesis. Such selected genes (782) reflected a real image of adipogenesis [2].

On the basis of coupling approach of adipogenesis and reverse adipogenesis, 4 new possible fat marker genes *APCDD1*, *CHI3L1*, *RARRES1* and *SEMA3G* were selected and bioinformatically verified for the description of adipogenesis [2]. Using the current web-based tools for text mining [1, 10], the 4 potential marker genes showed no direct connection to adipogenesis [2]. Besides adipogenesis, reverse adipogenesis, could be a promising approach for the treatment of obesity and their correlated problems in soft tissue engineering. Next, to indentify the glycan-based biomarkers for MSC and adipogenic differentiated cells, we found that N-glycans H5N1 and H6N1 were abundant in adipogenic differentiated cells [7]. Moreover, we propose that N-glycans like H6N5F1 and H7N6F1 could be specific for MSC and N-glycans like H3N4F1 and H5N4F3 could be possible biomarkers for adipogenic differentiated cells [7]. Identification of such biomarkers could be important for soft tissue engineering, and to monitor/track the cells during tissue regeneration.

Beside biomarkers identification, matrix analysis of differentiated cells could be a promising approach in regenerative medicine. Chondrocytes are well known for cartilage repair, and 3D high-density pellet culture represents a standard culture model for its entrapped chondrocytes [12]. However, inside intact pellet culture, the cells and ECM, enclose and fix each other [12]. It emphasizes the need of a successful protocol for isolation of cells. The combined cue of 300 U collagenase II, 20 U collagenase P and 2mM $CaCl_2$ were added to the pellets and incubated for 90 min for maximum release of viable cells [12]. Further optimization not only results cells isolation, but also separation of ECM [12]. From therapeutic perspective, it has been shown that ECM components play a curative role in cartilage repair [12]. Hyaluronan acid is clinically applied to *in situ* recruit MSC to cartilage defect sites and to promote cartilage differentiation [16]. Thus, our established protocol will play a substantial role in providing purified chondrogenic cells as well as ECM for regenerative application [12].

Next, adipogenic matrix was analysed to identify the interwoven collagen filaments and signalling web of ECM. A hexagonal structural framework of matrix was identified, which was positive for collagen type I, II and IV filaments [10]. After shedding of lipid droplets the collagen staining became negative, indicating the removal or modification of antigenic sites. Previous reports have been confirmed the presence of collagen type V and VI in the adipogenic matrix [17], and we verified the presence of collagen type I, II and IV filaments [10]. Thus, in total, the interwoven network is consisting of collagen type I, II, IV, V and VI filaments. Collagens are the major structural proteins of ECM and takes part in the holding of cells together, to control the active communications between cells and matrix [10]. ECM was mainly consisted of hexagonal structures as such structures are more stable than any other geometrical shapes [10]. Thus, we speculate that hexagonal geometrical shapes in the adipogenic ECM are responsible for peak accumulation of lipids and fats and could be valuable in consideration of obesity treatment. From engineering perspective the hexagonal structural network is the only arrangement having no free space between the structures [10].

To find out the behind genetic machinery of adipogenic matrix, gene chip analysis was performed and then bioinformatics knowledge was used to retrieve matrix associated genes [10]. For instance *TIMP2*, *TIMP3*, *TIMP4*, *COL4A1*were identified, which have been shown to control the formation and maintenance of matrix [11]. Glycoproteins like *CD44*, *GPC1*, *GPC2* and *CHI3L1* belong to the family of proteoglycan and take part in the structural organization of ECM [11]. Similarly, biglycan (*BGN*) is an ECM protein, responsible for matrix assembly, cellular adhesion, proliferation and migration [11]. Fibrillin-1 (*FBN1*) has been shown to regulate the local micro-environment of ECM [11]. Laminins like *LAMA3*, *LAMA4*, *LAMB1*, mediate the sensing for attachment, adhesion, migration and structural

organization of cells inside ECM [11]. Apart from this, signalling pathways of ECM were identified, for instance, integrin signalling pathway is critical to regulate the interaction of cells with matrix [11], and activate other signalling pathways as well. For example, they activate cell adhesion molecules pathway, which act as central hub in the network of cells and ECM and takes part in the biological process of hemostasis, immunogenesis, inflammation, facilitate cell-cell and cell-matrix interactions and differentiation [11]. We suggest that biochemical analysis of native adipogenic ECM could be a crucial guide for artificial-designing of biomaterials.

Guided cellular migration could be a promising approach in regenerative therapies. However, little is known about such directional cell migration, and especially whether differentiated cells move towards chemokine stimulus is not described so far. Thus, cell migration was analyzed, and a significant cell movement of chondrogenic differentiated cells in result of serum or CCL25 mediated chemotaxis was observed. As the differentiated cells migrate, therefore we propose that its use could be valuable for therapeutic repair of cartilage, due to active signaling pathways, chondrogenic character and biological paradigms of the differentiated state. CCL25 is a well-known chemokine for targeted and directional stem cell migration [9]. We noticed a guided cellular trafficking in result of CCL25 mediated chemotaxis [9], and recommend the use of CCL25 as a migratory cue in regenerative applications.

5.1. Conclusions

All milestones/goals (Section 2.1) have been achieved successfully, and published. For instance, differentiated cells isolation from their matrix was a challenging task. However, not only such cells were isolated (Goal 1), but also dedifferentiated and transdifferentiated them, and a correlation between cell cycle genes and phenotype switching was identified (Goal 2). The concept of transdifferentiation was validated on single cell level, and in addition the direct transdifferentiation (without dedifferentiation) was performed (Goal 3), whereas only some differentiated cells changed their phenotype out of all, suggesting further investigation in this direction. Conversion of one cell type (such as fat cells) into another (such as bone cells in case of injuries) could be a short cut and vital approach in cellular replacement therapies.

Beside transdifferentiation, a new method of "adipogenesis and reverse adipogenesis" was established for gene filtration/selection, and 4 new potential fat markers were identified. In addition, some new glycan based biomarkers for MSC and fat cells were discovered (Goal 4). Identification of such biomarkers could be beneficial for monitoring and tracking of cells in regenerative therapies.

Next, matrix of MSC and differentiated cells was analyzed, and collagen filaments were found, which were interwoven in a crisscross manner. A signaling web was also identified, which takes part in the formation of matrix, and can regulate the cellular communication between cells and matrix (Goal 5). The interpretation of interactive language between cells and matrix could be a valuable guide for the designing of biomaterials and bioscaffolds.

Beside this, we found that stem and differentiated cells migrate towards the stimulus of CCL25 chemokine in a well guided fashion (Goal 6). Such guided migration of cells to the point of stimulus could be a vital approach to know the *in vivo* cell migration in case of injuries or damages.

Our investigative study of transdifferentiation, identification of new biomarkers (genes and glycan based) with new methods, matrix analysis and cell migration could boost the field of regenerative medicine towards the best therapeutic solutions for cell based therapies.

6.0. References

1. Ullah, M., et al., *Transdifferentiation of mesenchymal stem cells-derived adipogenic-differentiated cells into osteogenic- or chondrogenic-differentiated cells proceeds via dedifferentiation and have a correlation with cell cycle arresting and driving genes.* Differentiation, 2013. **85**(3): p. 78-90.
2. Ullah, M., et al., *Reverse differentiation as a gene filtering tool in genome expression profiling of adipogenesis for fat marker gene selection and their analysis.* PLoS One, 2013. **8**(7): p. e69754.
3. Pittenger, M.F., et al., *Multilineage potential of adult human mesenchymal stem cells.* Science, 1999. **284**(5411): p. 143-7.
4. Song, L. and R.S. Tuan, *Transdifferentiation potential of human mesenchymal stem cells derived from bone marrow.* FASEB J, 2004. **18**(9): p. 980-2.
5. Ullah, M., M. Sittinger, and J. Ringe, *Transdifferentiation of adipogenically differentiated cells into osteogenically or chondrogenically differentiated cells: Phenotype switching via dedifferentiation.* Int J Biochem Cell Biol, 2013: p. In Press.
6. Wang, S., X. Qu, and R.C. Zhao, *Mesenchymal stem cells hold promise for regenerative medicine.* Front Med, 2011. **5**(4): p. 372-8.
7. Hamouda, H., et al., *N-Glycosylation Profile of Undifferentiated and Adipogenically Differentiated Human Bone Marrow Mesenchymal Stem Cells - Towards a Next Generation of Stem Cell Markers.* Stem Cells Dev, 2013.
8. Kang, S.K., et al., *Journey of mesenchymal stem cells for homing: strategies to enhance efficacy and safety of stem cell therapy.* Stem Cells Int, 2012. **2012**: p. 342968.
9. Ullah, M., et al., *Mesenchymal stem cells and their chondrogenic differentiated and dedifferentiated progeny express chemokine receptor CCR9 and chemotactically migrate towards CCL25 or serum.* Stem Cell Res Ther, 2013. **4**: p. 4:99.
10. Ullah, M., M. Sittinger, and J. Ringe, *Extracellular matrix of adipogenically differentiated mesenchymal stem cells reveals a network of collagen filaments, mostly interwoven by hexagonal structural units.* Matrix Biology, 2013.
11. Kim, S.H., J. Turnbull, and S. Guimond, *Extracellular matrix and cell signalling: the dynamic cooperation of integrin, proteoglycan and growth factor receptor.* Journal of Endocrinology, 2011. **209**(2): p. 139-151.
12. Ullah, M., et al., *A reliable protocol for the isolation of viable, chondrogenically differentiated human mesenchymal stem cells from high-density pellet cultures.* Biores Open Access, 2012. **1**(6): p. 297-305.
13. Ullah, M., et al., *Keynote: In vitro analysis of the transdifferentiation of adipogenic differentiated mesenchymal stem cells towards the osteogenic and chondrogenic lineage via dedifferentiation.* Journal of Tissue Engineering and Regenerative Medicine, 2012. **6**: p. 270-270.
14. Grimaldi, P., et al., *Fate restriction and developmental potential of cerebellar progenitors. Transplantation studies in the developing CNS.* Prog Brain Res, 2005. **148**: p. 57-68.
15. Torper, O., et al., *Generation of induced neurons via direct conversion in vivo.* Proc Natl Acad Sci U S A, 2013.
16. Siclari, A., et al., *A cell-free scaffold-based cartilage repair provides improved function hyaline-like repair at one year.* Clin Orthop Relat Res, 2012. **470**(3): p. 910-9.
17. Stillaert, F.B., et al., *Adipose tissue induction in vivo.* Adv Exp Med Biol, 2006. **585**: p. 403-12.

7.0. Affidavit

I, **Mujib, Ullah** certify under penalty of perjury by my own signature that I have submitted the thesis on the topic "*Molecular characterization of human mesenchymal stem cell differentiation to identify biomarkers for quality assurance in stem cell therapy*".

I wrote this thesis independently and without assistance from third parties, I used no other aids than the listed sources and resources.

All points based literally or in spirit on publications or presentations of other authors are, as such, in proper citations (see "uniform requirements for manuscripts (URM)" the ICMJE www.icmje.org) indicated. The sections on methodology (in particular practical work, laboratory requirements, statistical processing) and results (in particular images, graphics and tables) correspond to the URM (s.o) and are answered by me. My contributions in the selected publications for this dissertation correspond to those that are specified in the following joint declaration with the responsible person and supervisor. All publications resulting from this thesis and which I am author of correspond to the URM (see above) and I am solely responsible.

The importance of this affidavit and the criminal consequences of a false affidavit (section 156,161 of the Criminal Code) are known to me and I understand the rights and responsibilities stated therein.

Mujib Ullah

Date: 02.01.2014 Signature

8.0. Declaration of any eventual publications

Mujib Ullah had the following share in the following 7 published publications:

Publication 1: Ullah M, Stich S, Notter M, Eucker J, Sittinger M, Ringe J. Transdifferentiation of mesenchymal stem cells-derived adipogenic-differentiated cells into osteogenic- or chondrogenic-differentiated cells proceeds via dedifferentiation and have a correlation with cell cycle arresting and driving genes. Differentiation. 2013.
[doi: 10.1016/j.diff.2013.02.001], **Impact Factor: 3.01**.

Ullah M, Contribution: Conceived and designed the experiments, Performed the experiments, Analyzed the data, Wrote and published the paper.

Publication 2: Ullah M, Stich S, Häupl T, Eucker J, Sittinger M, Ringe J. Reverse differentiation as a gene filtering tool in genome expression profiling of adipogenesis for fat marker gene selection and their analysis. PLoS One. 2013.
[doi: 10.1371/journal.pone.0069754], **Impact Factor: 3.24**.

Ullah M, Contribution: Conceived and designed the experiments, Performed the experiments, Analyzed the data, Wrote and published the paper.

Publication 3: Hamouda H, **Ullah M**, Berger M, Sittinger M, Tauber R, Ringe J, Blanchard V. N-Glycosylation Profile of Undifferentiated and Adipogenically Differentiated Human Bone Marrow Mesenchymal Stem Cells - Towards a Next Generation of Stem Cell Markers.
Stem Cells and Development. 2013.
[doi:10.1089/scd.2013.0108], **Impact Factor: 4.67**.
Both, Hamouda H, Ullah M, contributed equally to this paper as mentioned in online version.

Ullah M, Contribution: Co-designed and co-performed the experiments, Co-analyzed the data, jointly wrote and co-published the paper.

Publication 4: Ullah M, Hamouda H, Stich S, Sittinger M, Ringe J. A reliable protocol for the isolation of viable, chondrogenically differentiated human mesenchymal stem cells from high-density pellet cultures. BioResearch Open Access. 2012.
[doi: 10.1089/biores.2012.0279], **Impact Factor: Waiting**.

Ullah M, Contribution: Conceived and designed the experiments, Performed the experiments, Analyzed the data, Wrote and published the paper.

Publication 5: Ullah M, Sittinger M, Ringe J. Extracellular matrix of adipogenically differentiated mesenchymal stem cells reveals a network of collagen filaments, mostly interwoven by hexagonal structural units. Matrix Biology. 2013
[doi: 10.1016/j.matbio.2013.07.001], **Impact Factor: 3.56**.

Ullah M, Contribution: Conceived and designed the experiments, Performed the experiments, Analyzed the data, Wrote and published the paper.

Publication 6: **Ullah M**, Eucker J, Sittinger M, Ringe J. Mesenchymal stem cells and their chondrogenic differentiated and dedifferentiated progeny express chemokine receptor CCR9 and chemotactically migrate towards CCL25 or serum. Stem Cell Research & Therapy. 2013. [doi: 10.1186/scrt310], **Impact Factor: 3.65**.

Ullah M, Contribution: Conceived and designed the experiments, Performed the experiments, Analyzed the data, Wrote and published the paper.

Signature of the doctoral candidate

Mujib Ullah

9.0. Evaluations of Own Publications

Number	Publications	Impact Factor	Journal
1	**Ullah M**, Stich S, Notter M, Eucker J, Sittinger M, Ringe J. Transdifferentiation of mesenchymal stem cells-derived adipogenic-differentiated cells into osteogenic- or chondrogenic-differentiated cells proceeds via dedifferentiation and have a correlation with cell cycle arresting and driving genes.	3.01	Differentiation
2	**Ullah M**, Stich S, Häupl T, Eucker J, Sittinger M, Ringe J. Reverse differentiation as a gene filtering tool in genome expression profiling of adipogenesis for fat marker gene selection and their analysis.	3.24	PLOS ONE
3	Hamouda H, **Ullah M**, Berger M, Sittinger M, Tauber R, Ringe J, Blanchard V. N-Glycosylation Profile of Undifferentiated and Adipogenically Differentiated Human Bone Marrow Mesenchymal Stem Cells - Towards a Next Generation of Stem Cell Markers.	4.67	Stem Cells and Development
4	**Ullah M**, Hamouda H, Stich S, Sittinger M, Ringe J. A reliable protocol for the isolation of viable, chondrogenically differentiated human mesenchymal stem cells from high-density pellet cultures	Waiting 2014	BioResearch Open Access
5	**Ullah M**, Sittinger M, Ringe J. Extracellular matrix of adipogenically differentiated mesenchymal stem cells reveals a network of collagen filaments, mostly interwoven by hexagonal structural units.	3.56	Matrix Biology
6	**Ullah M**, Eucker J, Sittinger M, Ringe J. Mesenchymal stem cells and their chondrogenic differentiated and dedifferentiated progeny express chemokine receptor CCR9 and chemotactically migrate towards CCL25 or serum.	3.65	Stem Cell Research & Therapy

Signature of the doctoral candidate

Mujib Ullah

Differentiation 85 (2013) 78–90

Contents lists available at SciVerse ScienceDirect

Differentiation

journal homepage: www.elsevier.com/locate/diff

Transdifferentiation of mesenchymal stem cells-derived adipogenic-differentiated cells into osteogenic- or chondrogenic-differentiated cells proceeds via dedifferentiation and have a correlation with cell cycle arresting and driving genes

Mujib Ullah [a,1], Stefan Stich [a,2], Michael Notter [b,3], Jan Eucker [c,4], Michael Sittinger [a,5], Jochen Ringe [a,*]

[a] Tissue Engineering Laboratory & Berlin-Brandenburg Center for Regenerative Therapies, Dept. of Rheumatology and Clinical Immunology, Charité-University Medicine Berlin, Charitéplatz 1, 10117 Berlin, Germany
[b] Dept. of Hematology and Oncology, Charité-University Medicine Berlin, Campus Benjamin Franklin, Hindenburgdamm 30, 12200 Berlin, Germany
[c] Dept. of Hematology and Oncology, Charité-University Medicine Berlin, Campus Mitte, Charitéplatz 1, 10117 Berlin, Germany

ARTICLE INFO

Article history:
Received 6 April 2012
Received in revised form
18 December 2012
Accepted 5 February 2013
Available online 3 May 2013

Keywords:
Mesenchymal stem cells
Adipogenesis
Differentiation
Transdifferentiation
Dedifferentiation
Cell cycle

ABSTRACT

It is generally accepted that after differentiation bone marrow mesenchymal stem cells (MSC) become lineage restricted and unipotent in an irreversible manner. However, current results imply that even terminally differentiated cells transdifferentiate across lineage boundaries and therefore act as a progenitor cells for other lineages. This leads to the questions that whether transdifferentiation occurs via direct cell-to-cell conversion or dedifferentiation to a progenitor cells and subsequent differentiation, and whether MSC potency decreases or increases during differentiation. To address these questions, MSC were differentiated into adipogenic lineage cells, followed by dedifferentiation. The process of dedifferentiation was also confirmed by single cell clonal analysis. Finally the dedifferentiated cells were used for adipogenesis, osteogenesis and chondrogenesis. Histology, FACS, qPCR and GeneChip analyses of undifferentiated MSC, adipogenic-differentiated and dedifferentiated cells were performed. Interestingly, gene profiling and bioinformatics demonstrated that upregulation (*DHCR*24, *G0S2*, *MAP2K*6, *SESN*3) and downregulation (*DST*, *KAT*2, *MLL*5, *RB*1, *SMAD*3, *ZAK*) of distinct genes have an association with cell cycle arrest in adipogenic-differentiated cells and perhaps narrow down the lineage potency. However, the upregulation (CCND1, CHEK, *HGF*, *HMGA*2, *SMAD*3) and downregulation (*CCPG*1, *RASSF*4, RG*S*2) of these genes have an association with cell cycle progression and maybe motivate dedifferentiation of adipogenic-differentiated cells. We found that dedifferentiated cells have a multilineage potency comparable to MSC, and also observed the associative role of proliferation genes with cell cycle arrest and progression. Concluded, our results indicate that transdifferentiation of adipogenic-differentiated cells into osteogenic- or chondrogenic-differentiated cells proceeds via dedifferentiation and correlates with cell cycle arresting and deriving genes. Regarding clinical use, the knowledge of potency and underlying mechanisms are prerequisites.

Title: Transdifferentiation of mesenchymal stem cells-derived adipogenic-differentiated cells into osteogenic- or chondrogenic-differentiated cells proceeds via dedifferentiation and have a correlation with cell cycle arresting and driving genes.

Authors: Mujib Ullah[1]*, Stefan Stich[1], Michael Notter[3], Jan Eucker[2], Michael Sittinger[1], Jochen Ringe[1]

Address: [1]Tissue Engineering Laboratory & Berlin-Brandenburg Center for Regenerative Therapies, Dept. of Rheumatology and Clinical Immunology, Charité-University Medicine Berlin, Charitéplatz 1, 10117 Berlin, Germany
[2]Dept. of Hematology and Oncology, Charité-University Medicine Berlin, Campus Mitte, Charitéplatz 1, 10117 Berlin, Germany
[3]Dept. of Hematology and Oncology, Charité-University Medicine Berlin, Campus Benjamin Franklin, Hindenburgdamm 30, 12200 Berlin, Germany

Journal: Differentiation

Volume: 85, **Issue:** 3, February 2013, **Pages:** 78–90

OPEN ACCESS Freely available online

PLOS ONE

Reverse Differentiation as a Gene Filtering Tool in Genome Expression Profiling of Adipogenesis for Fat Marker Gene Selection and Their Analysis

Mujib Ullah[1], Stefan Stich[1], Thomas Häupl[1], Jan Eucker[2], Michael Sittinger[1], Jochen Ringe[1]*

1 Tissue Engineering Laboratory & Berlin-Brandenburg Center for Regenerative Therapies, Department of Rheumatology and Clinical Immunology, Charité-University Medicine Berlin, Berlin, Germany, **2** Department of Hematology and Oncology, Charité-University Medicine Berlin, Berlin, Germany

Abstract

Background: During mesenchymal stem cell (MSC) conversion into adipocytes, the adipogenic cocktail consisting of insulin, dexamethasone, indomethacin and 3-isobutyl-1-methylxanthine not only induces adipogenic-specific but also genes for non-adipogenic processes. Therefore, not all significantly expressed genes represent adipogenic-specific marker genes. So, our aim was to filter only adipogenic-specific out of all expressed genes. We hypothesize that exclusively adipogenic-specific genes change their expression during adipogenesis, and reverse during dedifferentiation. Thus, MSC were adipogenic differentiated and dedifferentiated.

Results: Adipogenesis and reverse adipogenesis was verified by Oil Red O staining and expression of *PPARG* and *FABP4*. Based on GeneChips, 991 genes were differentially expressed during adipogenesis and grouped in 4 clusters. According to bioinformatic analysis the relevance of genes with adipogenic-linked biological annotations, expression sites, molecular functions, signaling pathways and transcription factor binding sites was high in cluster 1, including all prominent adipogenic genes like *ADIPOQ*, *C/EBPA*, *LPL*, *PPARG* and *FABP4*, moderate in clusters 2–3, and negligible in cluster 4. During reversed adipogenesis, only 782 expressed genes (clusters 1–3) were reverted, including 597 genes not reported for adipogenesis before. We identified *APCDD1*, *CHI3L1*, *RARRES1* and *SEMA3G* as potential adipogenic-specific genes.

Conclusion: The model system of adipogenesis linked to reverse adipogenesis allowed the filtration of 782 adipogenic-specific genes out of total 991 significantly expressed genes. Database analysis of adipogenic-specific biological annotations, transcription factors and signaling pathways further validated and valued our concept, because most of the filtered 782 genes showed affiliation to adipogenesis. Based on this approach, the selected and filtered genes would be potentially important for characterization of adipogenesis and monitoring of clinical translation for soft-tissue regeneration. Moreover, we report 4 new marker genes.

Citation: Ullah M, Stich S, Häupl T, Eucker J, Sittinger M, et al. (2013) Reverse Differentiation as a Gene Filtering Tool in Genome Expression Profiling of Adipogenesis for Fat Marker Gene Selection and Their Analysis. PLoS ONE 8(7): e69754. doi:10.1371/journal.pone.0069754

Editor: Stan Gronthos, The University of Adelaide, Australia

Received March 23, 2013; **Accepted** June 11, 2013; **Published** July 26, 2013

Funding: The study was supported by the Investment Bank Berlin (IBB) and European Regional Development Fund (grant no: 10147246), and the Berlin-Brandenburg Center for Regenerative Therapies. The funders had no role in study design, data collection and analysis, decision to publish, or preparation of the manuscript.

Competing Interests: The co-author Michael Sittinger is a shareholder of CellServe Ltd. (Berlin, Germany) and BioRetis Ltd. (Berlin, Germany), and works as consultant for BioTissue Technologies Ltd. (Freiburg, Germany) that develops tissue transplants for the regeneration of bone and cartilage. The product activities of the companies are not related to the scientific topics presented here. This study was partly funded by Investitionsbank Berlin (IBB). There are no patents, products in development or marketed products to declare. This does not alter the authors' adherence to all the PLOS ONE policies on sharing data and materials.

* E-mail: jochen.ringe@charite.de

Introduction

Human bone marrow mesenchymal stem cells, also named as multipotent mesenchymal stromal cells (MSC), are easy to isolate and culture expand, and *in vitro* and *in vivo* develop into mesenchymal tissues such as bone, cartilage and fat [1,2]. In regenerative approaches MSC-based tissue transplants are clinically applied for the restoration of injured and diseased tissues [3]. Before going into clinical application the tissue forming process requires a proper characterization.

Adipose tissue is considered to operate the metabolic regulation, hormonal secretion, energy reservoir and temperature maintenance in a critical manner [4,5,6]. However, excess body fat accumulation results in obesity and associated disorders, while potential shortage leads to skin ulcers, irregular body temperature and glucose deficiency [4,5,6]. Apart from this, adipogenesis, the formation of adipose tissue, has an important impact on different biological aspects of aging, insulin sensitivity, lipid metabolism, stress response and inflammation [5,6]. In regenerative medicine, engineered adipose tissue will be used for instance for the restoration of soft tissue of burn and cancer patients, and in cosmetic surgery [7].

The process of adipogenesis includes the commitment of MSC into the adipogenic lineage and their development to preadipocytes and terminally differentiated adipocytes [8], and is controlled via a series of cellular, chemical, biochemical, nutritional, hormonal and signaling sensing [4,9,10,11]. Moreover, distinct

genes, factors and a whole array of signal cascades play a key role in driving and regulating adipogenesis on the cellular and molecular level [12,13]. In line, factors like fatty acid binding protein-4 (FABP4) and the transcription factor peroxisome proliferator-activated receptor-γ2 (PPARG2) have already been accepted as important markers in the context of adipogenesis [12,13,14]. However, many of these factors need further evaluation to clarify the events during adipogenesis along with new adipogenic markers determination.

Strikingly, many of the molecular markers for adipogenic differentiation were selected on the basis of significantly changed gene expression [12,13,14] after stimulation of mesenchymal stem cells (e.g. primary MSC or C3H10T1/2 cells) or preadipocytes (e.g. 3T3-L1 cells) [15] with an adipogenesis stimulating medium including insulin, dexamethasone, indomethacin and 3-isobutyl-1-methylxanthine (IBMX) [9,16]. The cumulative action of these factors in an appropriate ratio is essential for adipogenic differentiation and adipose tissue maturation [10,16,17]. Here, insulin accelerates lipid storage and lipogenesis but is mostly dispensable for adipogenesis of bone marrow-derived MSC, whereas glucocorticoids or their synthetic agonists like dexamethasone, which stimulate glucocorticoid receptor pathways and activate receptors for adipocyte regulation, are essential [9,12,17,18]. Indomethacin influences adipogenic differentiation and fat maturation [19]. In more detail, indomethacin not only accelerates adipogenesis by increasing *CCAAT/enhancer binding protein-β (C/EBPβ)* and *PPARG* gene expression, but also inhibits *cyclooxygenase 1* and *2* genes (*COX1* and *2*) to probably enhance adipogenesis by an inverse relationship [19]. IBMX acts as a phosphodiesterase inhibitor that stimulates cAMP response element-binding proteins and initiates and drives adipocyte formation via cyclic adenosine monophosphate dependent mechanisms [17,20,21,22].

Clearly, in parallel, the adipogenic supplements take part in cellular processes other than adipogenesis. Thus, since some genes act in non-adipogenic cellular events, the number of genes with significantly changed expression during insulin, dexamethasone, indomethacin and IBMX induced adipogenesis does not reflect the actual number of adipogenic-specific markers. In other words, not all of the marker genes selected on the basis of changed gene expression after stimulation with the essential medium supplements actually represents adipogenic genes. Therefore, they are not sufficient for a proper description of adipogenesis. This emphasized the need of additional studies to narrow down the list of true adipogenic markers with new perspectives to understand adipogenesis.

We hypothesized that the expression of true adipogenic marker genes is significantly up- or downregulated during adipogenesis of MSC and reversed to the level of undifferentiated MSC during dedifferentiation of the adipogenic differentiated cells. Thus, we used the standard approach for adipogenesis of MSC (15 days) and extended them by isolation of the adipogenic differentiated cells from their secreted matrix and subsequent dedifferentiation in expansion medium (35 days). We analyzed the whole processes on the cellular and genome-wide molecular level.

Adipogenic differentiation of human MSC resulted in 991 genes with significantly changed expression values. Based on the expression values during adipogenesis and dedifferentiation, K-means clustering of these genes resulted in 4 clusters. These clusters were individually analyzed. According to its low number of lipid and fat specific biological annotations, expression sites, molecular functions, signaling pathways and transcription factor binding sites, the 209 genes of cluster 4 play a very minor role in adipogenesis. In line with our hypothesis and confirming the benefit of our approach, during dedifferentiation the expression of these genes was not reverted to the undifferentiated state. Therefore, the true marker list could be narrowed down to cluster 1–3 genes. Among those genes, we filtered *adenomatosis polyposis coli down-regulated-1* (*APCDD1*), *chitinase 3-like 1 (cartilage glycoprotein-39)* (*CHI3L1*), *retinoic acid receptor responder (tazarotene induced) 1* (*RARRES1*) and *sema domain, immunoglobulin domain (Ig), short basic domain, secreted, (semaphorin) 3G* (*SEMA3G*) as possible new adipogenic marker genes, which were not mentioned in the context of adipogenesis so far.

Materials and Methods

Ethics statement

All subjects participating in this study provided written informed consent to participate in this study, which was approved by the local ethical committee of the Charité-University Medicine Berlin.

Human MSC isolation, expansion and adipogenic differentiation

Human MSC were isolated from iliac crest bone marrow aspirates of three informed and consenting patients (64, 78 and 78 years old) who were examined to exclude hematopoietic neoplasms and were histologically diagnosed as normal. As already described [23], aspirates were mixed with culture medium consisting of DMEM (Biochrom, Berlin, Germany), 10% fetal bovine serum (FBS; Thermo Scientific Hyclone, Logan, USA), 2 ng/ml basic fibroblast growth factor (PeproTech, Hamburg, Germany), 4 mM L-glutamine, 100 U/ml penicillin and 100 µg/ml streptomycin (all Biochrom), and were seeded at a density of 2×10^5 nucleated cells per cm^2. After 48 h cultivation in monolayer, non-adherent cells were washed out by the first media exchange. During cell expansion up to passage 4 (P4), culture medium was changed three times weekly and after reaching 90% confluence, cells were detached by the addition of 0.05% trypsin/1 mM EDTA (both Biochrom), and re-plated at a density of 5×10^3 cells/cm^2.

For adipogenic differentiation, 2×10^4 MSC (n = 3 patients, P4) were incubated for 3 days in induction medium followed by 2 days in maintenance medium in 3 consecutive cycles. The maintenance medium consisted of DMEM (4.5 g/l glucose; Biochrom) containing 10% FBS, 10 µg/ml insulin (Novo Nordisk, Mainz, Germany), 100 U/ml penicillin and 100 µg/ml streptomycin. The induction medium consisted of maintenance medium supplemented with 1 µM dexamethasone, 0.2 mM indomethacin and 0.5 mM IBMX (all Sigma-Aldrich, Taufkirchen, Germany). For controls only the maintenance medium was used.

Isolation and dedifferentiation of adipogenic differentiated cells

For dedifferentiation or reverse adipogenesis, the adipogenic differentiated cells (n = 3 patients) were isolated from their secreted extracellular matrix by incubation with 0.05 trypsin/1 mM EDTA in phosphate-buffered saline (PBS; Biochrom) for 8 min at 37°C. Then, 5×10^3cells/cm^2 were seeded and culture expanded (dedifferentiated) for 35 days or 4 passages in monolayer culture in MSC culture expansion medium as described above.

Histological evaluation of adipogenic differentiated and dedifferentiated cells

To assess the content of lipid vacuoles in adipogenic differentiated and dedifferentiated cells, Oil Red O staining was performed. Briefly, the cell monolayer was washed with PBS after

removing the medium and then stained with Oil Red O (Roth, Karlsruhe, Germany) for 30 min at room temperature in the dark. Red lipid droplets were evaluated using a light microscope.

RNA extraction from cell cultures

To ensure high quality of RNA, cell cultures were homogenized in TriReagent (Sigma-Aldrich). Subsequently, for protein separation from nucleic acid, 1-bromo-3-chloropropane was added (133 µl/ml TriReagent), incubated for 15 min, and centrifuged. Then, the upper phase being free of proteins was transferred to the same volume of 70% ethanol. The RNA was further purified applying Qiagen's RNeasy Mini Kit (Qiagen, Hilden, Germany) including DNAse digestion. Finally, total RNA was eluted with RNase-free water and their quality and quantity was determined using the Bioanalyzer (Agilent Technologies, Boeblingen, Germany) and NanoDrop (NanoDrop, Wilmington, USA). The total RNA was used for quantitative real-time RT-PCR analysis as well as for microarray gene expression profiling.

Quantitative RT-PCR analysis

First, cDNA was synthesized from the extracted total RNA (2.5 µg) with the iScript cDNA reverse transcription synthesis kit (BioRad, Munich, Germany). Then, the expression of genes of interest was analyzed using TaqMan quantitative real-time RT-PCR (qRT-PCR). The gene expression assays for TaqMan probes and primer sets (Applied Biosystems, Darmstadt, Germany) were performed in triplicates in optical plates on a Mastercycler® ep realplex^2 S system (Eppendorf, Hamburg, Germany). Quantitative gene expression was analyzed for *APCDD1* (assay ID: Hs00537787_m1), *CHI3L1* (Hs01072228_m1), *FABP4* (Hs01086177_m1), *PPARG* (Hs01115513_m1), *RARRES1* (Hs00161204_m1), *SEMA3G* (Hs00220101_m1) and *glyceraldehyde-3-phosphate dehydrogenase* (*GAPDH*; Hs99999905_m1). The expression of genes of interest was normalized to the endogenous *GAPDH* expression level and relative quantification values were calculated in percent of *GAPDH* via using the $2^{-\Delta\Delta Ct}$ formula [24].

Genome-wide gene expression profiling

For genome-wide expression profiling, Affymetrix HG-U133 plus 2 GeneChips (Affymetrix, Santa Clara, USA) were selected and analysis was performed according to Affymetrix recommendations. Briefly, 1 µg total RNA were used to synthesize biotin-labelled cRNA and 15 µg of fragmented cRNA were hybridized to GeneChips for 16 h at 45°C. Washing, staining and scanning of the GeneChips was performed using Affymetrix equipment, expression raw data were processed with Affymetrix GeneChip Operating Software (GCOS) 1.4 for signal calculation, and pairwise chip comparison was performed with GCOS 1.4 software after generating DAT, CEL and EXP files.

Expression profiling was performed for total 12 samples (n = 3 donors), subdivided in 4 time points: 3× (undifferentiated MSC), 3× (adipogenic differentiated cells at day 15), 3× (early state of dedifferentiated cells at day 7) and 3× (late state of dedifferentiated cells at day 35). Parts of the gene expression profiling raw data derived from these cultures have already been used and processed in a study on MSC transdifferentiation in a totally different way and as a result, cell cycle genes that regulate MSC differentiation, dedifferentiation and transdifferentiation were reported [23].

The microarray data sets have been submitted to Gene Expression Omnibus (GEO) database and are accessible via the GEO ID: GSE36923.

Data normalization, selection criteria and analysis strategy

To eliminate experimental or data acquisition variations, gene expression raw data were normalized, log transformed and statistically analyzed with GCOS 1.4 software.

As introduced, first we were interested in genes whose expression was significantly up- or downregulated during the course of adipogenic differentiation. Thus, in the first step, for comparative gene expression analysis each of the 3 GeneChips on day 15 (differentiated state) was compared with each of the 3 GeneChips on day 0 (undifferentiated state). Genes were selected as differentially expressed on the basis of specific change call and fold change (FC) criteria. The change call limit was 100% (9 of 9 possible significant change calls for 3× day 15 versus 3× day 0), and the FC limit >2 or <-2 for the mean FC of nine comparisons. This way, genes that were differentially expressed during adipogenesis could be selected.

Next, we were particularly interested in those of the genes selected in step one, whose expression value during dedifferentiation reverted to the expression value before adipogenic induction (undifferentiated MSC). Therefore, in the second step, we compared the day 0 gene expression values of genes identified in step number one with the corresponding values on day 7 (early dedifferentiated state) and day 35 (late dedifferentiated state).

Classification of genes into clusters and association with biological parameters

In order to classify the selected genes for further evaluation into suitable groups, K-means clustering was performed. Applying the Genesis Expression Similarity Investigation Suite software package 1.7.2 [25], initially Figure of Merit (FOM) analysis was carried out to determine the appropriate number of clusters [26]. Then, based on this information, the K-means clustering tool of the Genesis software was carried out and the selected genes were classified in distinct clusters based on their expression pattern.

The gene list of each individual cluster was uploaded in the Database for Annotation, Visualization and Integrated Discovery (DAVID) 6.7 and analyzed according to the default set of statistical parameters [27,28]. For each cluster we were interested in the gene ontologies, cellular compartmentalization, molecular functions, sites of expression, functional classification and determination of transcription factor binding sites (TFBS). In addition, the gene lists were screened for genes described in the context of adipogenesis relevant signaling pathways. DAVID and the Kyoto Encyclopedia of Genes and Genomes (KEGG) were used [29]. Each relevant gene was evaluated for its expression value along with its statistical relevance during differentiation and dedifferentiation.

Statistical analysis

Statistical analysis was performed with SigmaStat 3.5 (Systat Software, USA), while GraphPad Prism4 (GraphPad Software, USA) was applied for drawing graphs. For two group comparisons simple student t-test was used, and for three or more group comparisons one-way ANOVA. Data sets are reported as means ± SEM and asterisks were assigned to the p-values in the order P***<0.001, P**<0.01 and P*<0.05 for statistical significance. The abbreviation ns was used for statistically non-significant data sets.

Results

Adipogenic differentiation of human MSC

Human mesenchymal stem cells were isolated from iliac crest bone marrow aspirates and culture expanded up to P4. Based on their morphology, surface marker profile and potential to differentiate into fat, bone and cartilage, the MSC character of the cultures has already been shown elsewhere [23].

The MSC were induced towards the adipogenic lineage. On day 5, we observed the formation of Oil Red O stained lipid rich vacuoles (Figure 1A). The quantity and diameter of these vacuoles was continuously increased from day 10 (Figure 1B) to day 15 (Figure 1C). At this stage, we also observed a secretion of lipid droplets into the medium (data not shown). Not stimulated control cultures showed no formation of lipid droplets (Figure 1D). Adipogenesis was also confirmed on the molecular level applying qRT-PCR. Here, the expression of the adipogenic marker genes *PPARG* (Figure 2A) and *FABP4* (Figure 2B) in relation to the expression of the housekeeping gene *GAPDH* was continuously increased during adipogenic culture.

Dedifferentiation of adipogenic differentiated cells

For dedifferentiation, the adipogenic differentiated cells (day 15) were isolated from their secreted fat matrix and cultured for 35 days in culture medium. As shown in detail elsewhere, the adipogenic differentiated cells were converted to dedifferentiated cells with fibroblast-like morphology, no lipid rich vacuoles and the capacity to develop into fat, bone and cartilage [23].

Briefly, as the dedifferentiated cells were derived from adipogenic differentiated cells, dedifferentiation was assessed on the basis of Oil Red O staining. After 7 days, we observed a slightly decreased size and number of lipid rich vacuoles (Figure 1G; early dedifferentiated state). After 5 weeks of dedifferentiation, we found a negative Oil Red O staining (Figure 1H). During dedifferentiation, the adipogenic differentiated cells were switched from bloated to fibroblast-like cell morphology and showed a phenotype (Figure 1F) comparable to undifferentiated MSC (Figure 1E). Likewise adipogenesis, also dedifferentiation was verified on the mRNA level. The expression of *PPARG* (Figure 2C) and *FABP4* (Figure 2D) in relation to

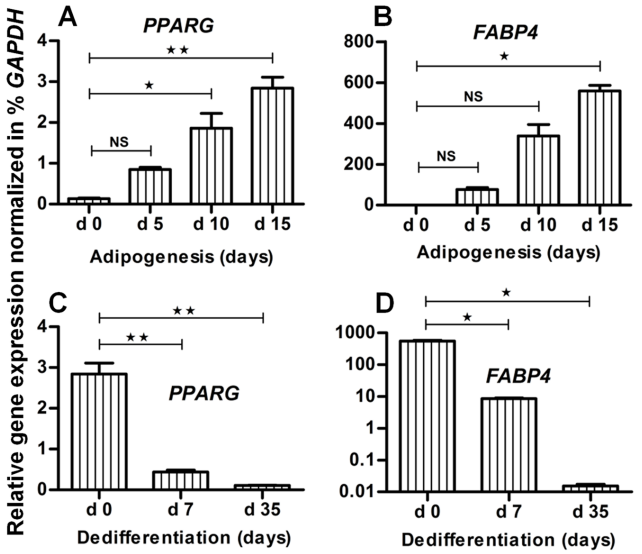

Figure 2. Gene expression profile of fat specific marker genes to assess adipogenesis and reverse adipogenesis. Gene expression analysis was performed using qRT-PCR and the resulted expression data were normalized to *GAPDH* for stepwise assessment of adipogenesis and reverse adipogenesis. Gene expression of adipogenic-specific marker genes (**A**) *PPARG* and (**B**) *FABP4* is given for different stages of adipogenic differentiation i.e. at day 5, day 10 and day 15. Similarly, the gene expression of (**C**) *PPARG* and (**D**) *FABP4* is given for different stages of reverse adipogenesis (dedifferentiation). Error bars, Means ± S.E.M (n = 3); *$P<0.05$; **$P<0.01$; ***$P<0.001$, NS, not significant (student t test performed for statistical analysis).
doi:10.1371/journal.pone.0069754.g002

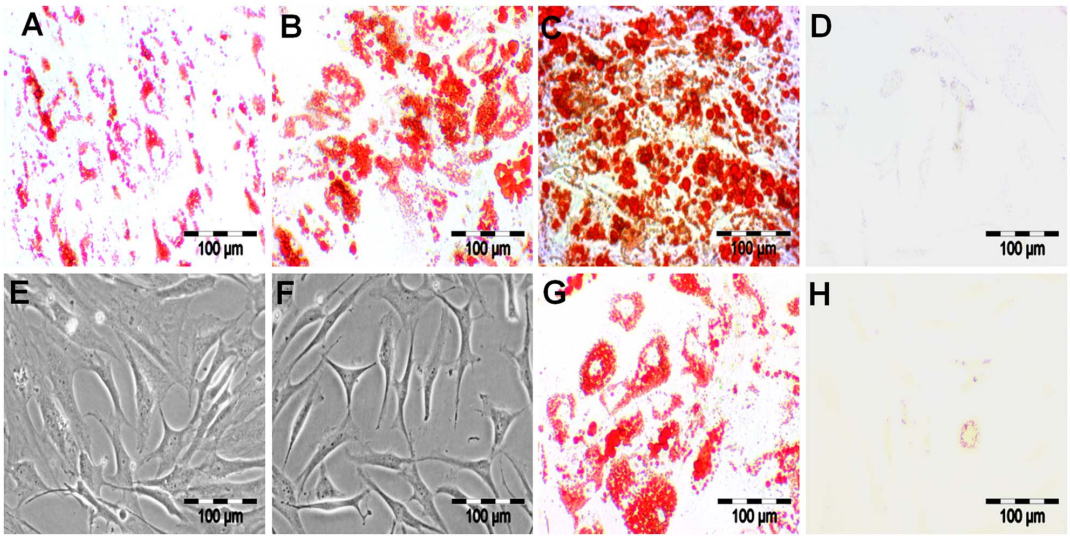

Figure 1. MSC isolation, adipogenic differentiation and dedifferentiation. MSC were induced to adipogenic differentiation for 15 days. (**A**) Oil Red O staining showed the formation of lipid droplets on day 5, (**B**) which increased in size and number, as shown on day 10, and (**C**) reached a peak value on day 15 of adipogenic differentiation. (**D**) Control samples showed no lipid formation even after day 15 of adipogenesis. Oil Red O staining during the conversion of adipogenic differentiated cells into dedifferentiated cells showed (**G**) an intermediate conversion after day 7 and (**H**) complete conversion after day 35 of reverse adipogenesis. Morphology of (**F**) dedifferentiated cells and (**E**) undifferentiated MSC are shown by phase contrast microscopy. Bar: 100 µm.
doi:10.1371/journal.pone.0069754.g001

GAPDH was continuously decreased during dedifferentiation. Taken together, all the results confirmed an advanced state of dedifferentiation.

Expression profiling of undifferentiated MSC, differentiated and dedifferentiated cells

First, to identify the expression profile of undifferentiated MSC, adipogenic differentiated and dedifferentiated cells, we performed a genome-wide GeneChip analysis. The raw data are available in the GEO database (ID: GSE36923). Then, the gene profiles of adipogenic differentiated cells at day 15 (n = 3 patients) were compared to undifferentiated MSC (n = 3 patients). Genes were defined as differentially expressed when the mean FC of 9 comparisons was >2 or <−2 and the change call was 100% (9 of 9 comparisons). This resulted in 1459 probe-sets, which were differentially expressed during adipogenesis. Then, the probe-set list was filtered, sorted and double entries for the same genes as well as entries without any gene title or symbol were removed. This resulted in a list of 991 genes representing possible genes of interest in the context of adipogenesis. Among them, 307 were up- and 684 were downregulated (Suppl. Table S1). Finally, the expression values of these genes were compared with the values after 7 days (n = 3 patients) and 35 days (n = 3 patients) in dedifferentiation culture.

Cluster analysis of the selected genes revealed 4 main groups

In order to break the 991 selected genes into more suitable groups for further evaluation, K-means clustering was performed. The appropriate number of clusters was calculated with the Genesis analytical tool of FOM (Suppl. Figure S3), and the genes were grouped into 4 clusters (Figure 3, Suppl. Table S1). Here, the gray color lines represent the individual gene expression kinetics while the pink color line shows the cumulative average of the specific clusters expression kinetics. The relative temporal gene expression is given on the y-axis while the 4 different time points (day 0: undifferentiated state, day 15: differentiated state, day 7 and 35: early and late dedifferentiated state) are given on the x-axis.

Cluster 1 (Figure 3A) represents a group of 307 genes, such as *PPARG*, *FABP4* and most other prominent markers, whose expression was upregulated during adipogenesis, downregulated in dedifferentiated cells on day 7, became comparable to the value of undifferentiated MSC, and then remained constant until day 35. Therefore, the expression values of cluster 1 genes in dedifferentiated cells reverted to a value nearly equal to those in undifferentiated MSC. The expression of the 198 cluster 2 genes (Figure 3B) like *insulin-like growth factor binding protein-3* (*IGFBP3*) was downregulated during adipogenesis and continuously upregulated during dedifferentiation. On day 35, the expression values of cluster 2 genes in dedifferentiated cells reverted to a value nearly equal to those in undifferentiated MSC. Also the expression of the 277 genes of cluster 3 (Figure 3C), such as *IGFBP*6, was downregulated during adipogenesis but upregulated in dedifferentiated cells on day 7 to the value in undifferentiated MSC, and then remained constant until day 35. Interestingly, cluster 4 (Figure 3D) represents a group of 209 genes, which until day 7 showed the expression time course of cluster 3 genes, but then again were downregulated to the expression value in adipogenic differentiated cells.

In conclusion, the expression of cluster 1–4 genes was significantly up- or downregulated during adipogenesis, but during dedifferentiation only the expression of cluster 1–3 genes was reverted to a value similar to those in undifferentiated MSC; the cells from which they are derived from. Therefore, according to our hypothesis that true markers are differentially expressed during differentiation and that their expression values are reverted to the level of undifferentiated MSC during dedifferentiation, among the 991 genes, first and foremost the 782 (cluster 1–3) genes are relevant. This was the initial result of our approach, extending the standard approach for adipogenesis by isolating the differentiated cells from their secreted matrix and subsequent dedifferentiation. To proof the hypothesis and to get new insights in adipogenesis, in the next steps cluster 1–4 genes were analyzed in the context of biology.

Association of cluster genes with biological parameters

To retrieve more information about the 4 clusters, the gene list of each individual cluster was uploaded in the online database DAVID. Here, first a list of all biological and functional annotations was created for each cluster. These lists were then sorted and filtered on the basis of the statistical relevant enrichment scores (first priority) and the relevance of the entries in context of adipogenesis or adipose tissue (second priority; Table 1). This way, we divided the biological information of each cluster into the 6 categories: biological annotation, cellular compartmentalization, molecular function, signaling pathways, functional classification, and site of expression. As shown in Table 1, the cumulative view of all these parameters indicated that cluster 1 represents a group of genes that has stronger affiliation to adipogenesis than the other clusters. In more detail, for cluster 1 genes, we found the most relevant entries for lipid and fat specific biological annotations, molecular functions, signaling pathways and the other biological events. Following this argumentation, clusters 2 and 3 representing genes have a minor influence on adipogenesis. The entries for cluster 4 have no or minute relation to adipogenesis, thus, indicating a very minor role in adipogenesis.

Our next step was based on the knowledge that transcription factors play a key role in the induction and regulation of adipogenesis. First, we were interested in the number of their binding sites (TFBS). Thus, applying the DAVID tool for TFBS determination, we analyzed the TFBS set and its corresponding transcription factor set of each cluster (Suppl. Table S2). Then, with the help of the National Centre for Biotechnology Information (NCBI) database PubMed and DAVID, all these TFBS and transcription factors were sorted and analysed regarding their possible influencing role in adipogenesis. Here, on the basis of effective relation to adipose tissue development, we selected a panel of adipogenesis related transcription factors like *activator protein-1* (*AP1*), *aryl hydrocarbon receptor nuclear translocator* (*ARNT*), C*CAAT/enhancer binding protein-*α (*C/EBPA*), *hepatocyte nuclear factor-4* (*HNF4*), *kruppel-like factor-12* (*KLF12* or *AP2REP*), *nuclear receptor subfamily-2*, *group F*, *member 2* (*NR2F2* or *COUPTFII*), *PPARA*, *PPARG*, *transcription factor-3* (*TCF3* or *E47*), *sterol regulatory element binding protein-1* (*SREBP1*) and *upstream transcription factor-1* (*USF*) (Suppl. Table S2). As these factors are well known in the context of adipogenesis, we conclude that by TFBS screening and application of the appropriate analytical tools, we have found significant binding sites for several important transcription factors involved in adipogenic development. Strikingly, most of the TFBS for these transcription factors were found in clusters 1–3 but not in cluster 4 (Figure 4). In more detail, only *AP1* and *C/EBPA* have binding sites in all 4 clusters. *ARNT*, *KLF12*, *NR2F2*, *TCF3*, *PPARA*, *PPARG and USF* have binding sites in clusters 1–3, *HNF4* in clusters 1 and 2 and *SREBP1* in clusters 2 and 3.

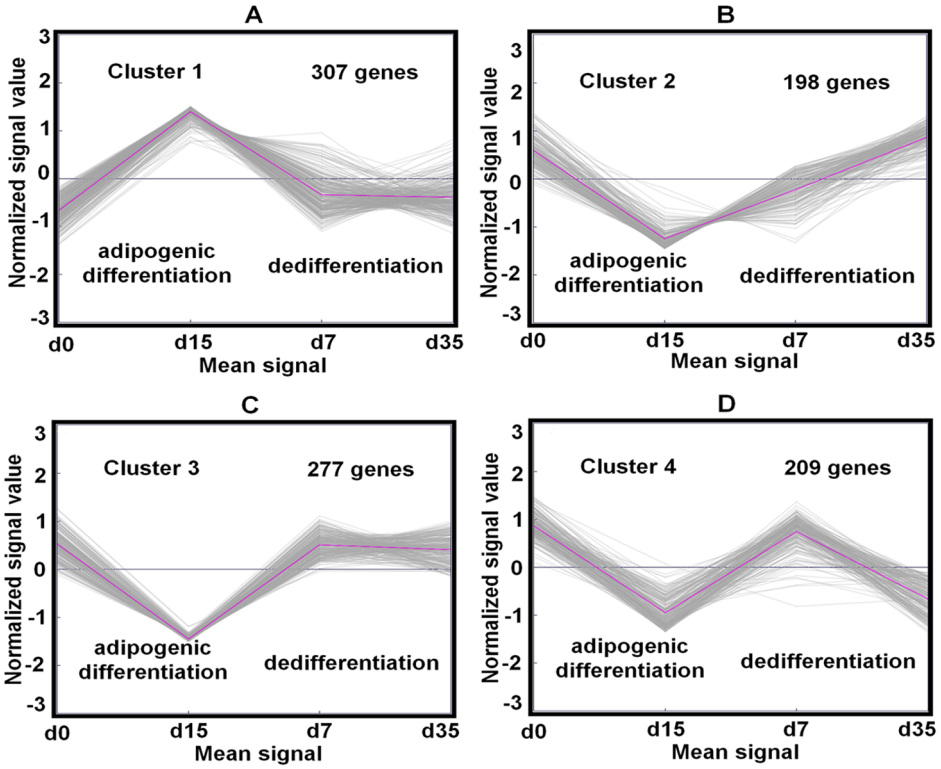

Figure 3. K-means clustering of differentially expressed genes. K-means clustering of 991 genes differentially expressed in adipogenesis resulted in 4 distinct gene groups. (**A–D**) Each group is subdivided into 4 time points, i.e. undifferentiated MSC (day 0), adipogenic differentiated cells (day 15), dedifferentiated cells at early time point (day 7) and dedifferentiated cells at late time point (day 35). (**A**) Genes in cluster 1 are upregulated after 15 days of adipogenic differentiation and downregulated to the level on day 0 during reverse adipogenesis. (**B–D**) Cluster 2–4 genes are downregulated after 15 days of adipogenesis and upregulated to the level on day 0 (**B**) during 35 days or (**C,D**) 7 days of dedifferentiation. Cluster 3 genes maintained this level, cluster 4 genes not. (**A–D**) The gray lines represent the individual gene expression and pink line represents the mean gene expression with respect to each time point in each group. See Suppl. Table S1, for detailed gene lists of each cluster.
doi:10.1371/journal.pone.0069754.g003

Association of cluster genes with adipogenesis relevant signaling pathways

Next, the gene lists of the 4 clusters were screened for genes known in the context of adipogenesis relevant signaling pathways. Here, the KEGG portal of DAVID was used. Many insulin signaling pathway genes were differentially expressed during adipogenesis. On day 15 (differentiated state), the expression of *ACACA*, *ACACB*, *EIF4EBP1*, *FASN*, *FOXO1*, *GYS1*, *IRS1*, *IRS2*, *LIPE*, *MKNK2*, *PCK1*, *PDE3B*, *PRKAR2B* and *SORBS1* was up-, and of *NRAS*, *PPP1R3B*, *PRKCI* and *SOCS3* was downregulated (Figure 5A; Suppl. Table S1 for detailed data). During dedifferentiation, on day 7 (early state) and day 35 (late state) the expression value of all these genes was almost reversed to the level on day 0 (undifferentiated state). In addition, many genes of the *PPARG* signaling pathway were differentially expressed during adipogenesis. From day 0 to day 15, the expression of *ACSL1*, *ADIPOQ*, *DBI*, *FABP4*, *FABP5*, *LPL*, *ME1*, *NR1H3*, *PCK1*, *PLIN1*, *PPARG*, *SCD* and *SORBS1* was up-, and in the time course of dedifferentiation downregulated to about the level on day 0 (Figure 5B). *ACACA*, *ACACB* and *FASN* are members of the fatty acid biosynthesis signaling pathway, whose expression was significantly upregulated during adipogenesis and reverted to the level in undifferentiated MSC during dedifferentiation (Figure 5C). *ACACB*, *ACSL1*, *ADIPOQ*, *IRS1*, *IRS2*, *NFKBIA*, *PCK1* and *SOCS3* belong to the adipocytokine signaling pathway and were differentially expressed between day 0 and day 15 (Figure 5D). Clearly, during dedifferentiation their expression values were changed in such a way that they almost become similar to the level of undifferentiated MSC. Also genes of the fatty acid elongation pathway, such as *ACADS*, *ECHS1*, *HADH*, *HADHA* and *ACAA2* (Figure 5E), and of the pathway for biosynthesis of unsaturated fatty acids, like *ELOVL5*, *FADS1*, *FADS3*, *HADHA*, *PECR*, *SCD* and *TECR* (Figure 5F), were differentially expressed (upregulated) during adipogenesis. During dedifferentiation, their expression was downregulated and nearly reached the level on day 0. Similarly, the gene expression of *ACAA2*, *ACADS*, *ACSL1*, *ALDH2*, *ECHS1* and *GCDH*, members of the fatty acid metabolic pathway, was upregulated in adipogenic differentiated cells (Figure 5G), and during dedifferentiation almost comes back to the expression level of undifferentiated MSC; the cells they are derived from.

Interestingly, about all of the genes reported here in the context of adipogenic signaling pathways belong to clusters 1–3 but not cluster 4. In summary, it can be stated that based on Table 1 data, transcription factors and its TFBS (Figure 4, Suppl. Table S2), and on participation in signaling pathways (Figure 5), clusters 1–3 are the relevant ones in context of adipogenesis. Thus, in line with our hypothesis and confirming the benefit of our approach of extended adipogenesis, possible true adipogenic marker genes belong to clusters, in which the expression during dedifferentiation was reverted to the undifferentiated state. Fat marker selection only on the basis of significantly changed gene expression as a result of induction with insulin, dexamethasone, indomethacin and IBMX would be misleading. Finally, cluster 1 included about all prominent adipogenic and fat markers, and according to the

Table 1. Evaluation of different biological parameters for each cluster.

Cluster 1

Gene ontologies	Cellular compartmentalization	Molecular function	KEGG signaling pathways	Functional categories	Expression site
GO:0008610~lipid biosynthetic process (24)	GO:0005739~mitochondrion (59)	GO:0048037~cofactor binding (32)	hsa03320:PPAR signaling pathway (13)	phosphoprotein (129)	Placenta (75)
GO:0006631~fatty acid metabolic process (23)	GO:0031090~organelle membrane (49)	GO:0008289~lipid binding (22)	hsa04910:Insulin signaling pathway (13)	acetylation (71)	Liver (72)
GO:0032868~response to insulin stimulus (13)	GO:0000267~cell fraction (48)	GO:0031406~carboxylic acid binding (19)	hsa00071:Fatty acid metabolism (8)	oxidoreductase (43)	Skin (48)
GO:0010876~lipid localization (8)	GO:0005829~cytosol (48)	GO:0000287~magnesium ion binding (15)	hsa01040:Biosynthesis of unsaturated fatty acids (6)	transferase (32)	Adipose tissue (17)
GO:0055088~lipid homeostasis (7)	GO:0005783~endoplasmic reticulum (44)	GO:0019842~vitamin binding (14)	hsa04920:Adipocytokine signaling pathway (6)	lipoprotein (16)	Fetal liver (11)
GO:0006869~lipid transport (7)	GO:0031975~envelope (31)	GO:0009055~electron carrier activity (11)	hsa00564:Glycerophospholipid metabolism (6)	Apoptosis (14)	Fetal brain cortex (11)
GO:0030258~lipid modification (6)	GO:0005794~Golgi apparatus (30)	GO:0005504~fatty acid binding (9)	hsa00062:Fatty acid elongation in mitochondria (4)	Acyltransferase (7)	Adipocyte (8)
GO:0034440~lipid oxidation (5)	GO:0005615~extracellular space (22)	GO:0004091~carboxylesterase activity (7)	hsa00061:Fatty acid biosynthesis (3)	diabetes mellitus (6)	
GO:0045444~fat cell differentiation (5)	GO:0005792~microsome (16)	GO:0016229~steroid dehydrogenase activity (5)			
GO:0010883~regulation of lipid storage (4)	GO:0009986~cell surface (12)				

Cluster 2

Gene ontologies	Cellular compartmentalization	Molecular function	KEGG signaling pathways	Functional categories	Expression site
GO:0007155~cell adhesion (14)	GO:0005886~plasma membrane (63)	GO:0005509~calcium ion binding (21)	hsa04060:Cytokine-cytokine receptor interaction (10)	glycoprotein (93)	Placenta (44)
GO:0008283~cell proliferation (13)	GO:0005576~extracellular region (39)	GO:0030246~carbohydrate binding (13)	hsa05200:Pathways in cancer (9)	phosphoprotein (90)	Liver (32)
GO:0007267~cell-cell signaling (13)	GO:0009986~cell surface (9)	GO:0019838~growth factor binding (9)	hsa04612:Antigen processing and presentation (7)	disulfide bond (63)	Uterus (26)
GO:0048545~response to steroid hormone stimulus (8)	GO:0043235~receptor complex (5)	GO:0005125~cytokine activity (7)	hsa04020:Calcium signaling pathway (6)	transmembrane protein (21)	Skin (26)
GO:0001775~cell activation (8)		GO:0005543~phospholipid binding (6)	hsa04940:Type I diabetes mellitus (5)	lipoprotein (15)	Kidney (23)
GO:0006935~chemotaxis (7)		GO:0005539~glycosaminoglycan binding (5)	hsa04115:p53 signaling pathway (4)	cytokine (7)	Pancreas (16)
GO:0000165~MAPKKK cascade (6)				Lectin (6)	Endothelial cell (4)
GO:0043627~response to estrogen stimulus (5)				membrane protein (4)	Myometrium (2)
GO:0031960~response to corticosteroid stimulus (4)					

Table 1. Cont.

Cluster 3					
Gene ontologies	**Cellular compartmentalization**	**Molecular function**	**KEGG signaling pathways**	**Functional categories**	**Expression site**
GO:0045449~regulation of transcription (52)	GO:0005886~plasma membrane (77)	GO:0008270~zinc ion binding (46)	hsa04514:Cell adhesion molecules (CAMs) (12)	alternative splicing (145)	Brain (133)
GO:0042127~regulation of cell proliferation (26)	GO:0005576~extracellular region (45)	GO:0030528~transcription regulator activity (35)	hsa05200:Pathways in cancer (12)	phosphoprotein (143)	Placenta (64)
GO:0007155~cell adhesion (23)	GO:0000267~cell fraction (25)	GO:0003723~RNA binding (18)	hsa04510:Focal adhesion (9)	glycoprotein (90)	Liver (55)
GO:0007049~cell cycle (19)	GO:0044451~nucleoplasm part (15)	GO:0008233~peptidase activity (15)	hsa04612:Antigen processing and presentation (7)	disulfide bond (68)	Epithelium (51)
GO:0006928~cell motion (18)	GO:0009986~cell surface (13)	GO:0003682~chromatin binding (7)	hsa04144:Endocytosis (7)	acetylation (48)	Skin (35)
GO:0051276~chromosome organization (16)	GO:0000785~chromatin (8)	GO:0005518~collagen binding (5)	hsa04940:Type I diabetes mellitus (6)	transcription regulation (41)	Uterus (34)
GO:0016477~cell migration (13)	GO:0005773~vacuole (8)	GO:0003690~double-stranded DNA binding (5)	hsa04512:ECM-receptor interaction (5)	chromosomal r earrangement (15)	Bone marrow (20)
GO:0051674~localization of cell (13)	GO:0000228~nuclear chromosome (6)	GO:0008266~poly(U) RNA binding (2)		DNA damage (7)	Plasma (11)
GO:0040008~regulation of growth (12)				growth regulation (4)	Fetal kidney (9)
Cluster 4					
Gene ontologies	**Cellular compartmentalization**	**Molecular function**	**KEGG signaling pathways**	**Functional categories**	**Expression site**
GO:0006350~transcription (39)	GO:0043228~non-membrane-bounded organelle (41)	GO:0003677~DNA binding (43)	hsa05200:Pathways in cancer (7)	phosphoprotein (148)	Brain (111)
GO:0007242~intracellular signaling cascade (23)	GO:0005856~cytoskeleton (24)	GO:0030528~transcription regulator activity (25)	hsa04530:Tight junction (5)	alternative splicing (115)	Epithelium (76)
GO:0007049~cell cycle (20)	GO:0031981~nuclear lumen (20)	GO:0003779~actin binding (8)	hsa04370:VEGF signaling pathway (3)	acetylation (45)	Testis (72)
GO:0051276~chromosome organization (12)	GO:0005654~nucleoplasm (14)	GO:0032403~protein complex binding (6)	hsa04630:Jak-STAT signaling pathway (3)	transcription regulation (39)	Placenta (66)
GO:0016568~chromatin modification (8)	GO:0005694~chromosome (11)	GO:0046332~SMAD binding (3)	hsa04010:MAPK signaling pathway (3)	dna-binding (33)	Uterus (35)
GO:0043549~regulation of kinase activity (8)	GO:0005813~centrosome (8)			cell cycle (11)	Fetal brain (16)
GO:0007050~cell cycle arrest (5)	GO:0031012~extracellular matrix (8)			chromatin regulator (8)	Fetal kidney (11)
GO:0000075~cell cycle checkpoint (4)	GO:0005874~microtubule (7)			methylation (8)	Fibroblast (5)

The genes of each cluster were uploaded individually to online databases (DAVID and KEGG) and analyzed for their link to different biological parameters like gene ontology, cellular compartmentalization, molecular function, signaling pathway and site of expression. The parameters were selected on the basis of the enrichment score and relevance for adipogenesis. The numbers given in brackets are the numbers of genes associated to the corresponding GO term and signaling pathways.

doi:10.1371/journal.pone.0069754.t001

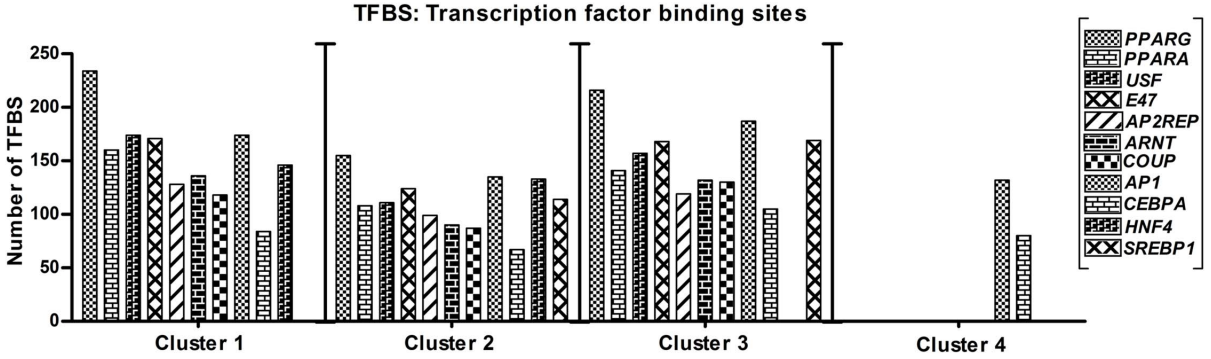

Figure 4. Transcription factor binding sites (TFBS) analysis. Analysis of transcription factor binding sites (TFBS) was performed and the selected adipogenic-specific TFBS showed most of the binding sites in cluster 1–3 genes and only a few significant sites in cluster 4 genes.
doi:10.1371/journal.pone.0069754.g004

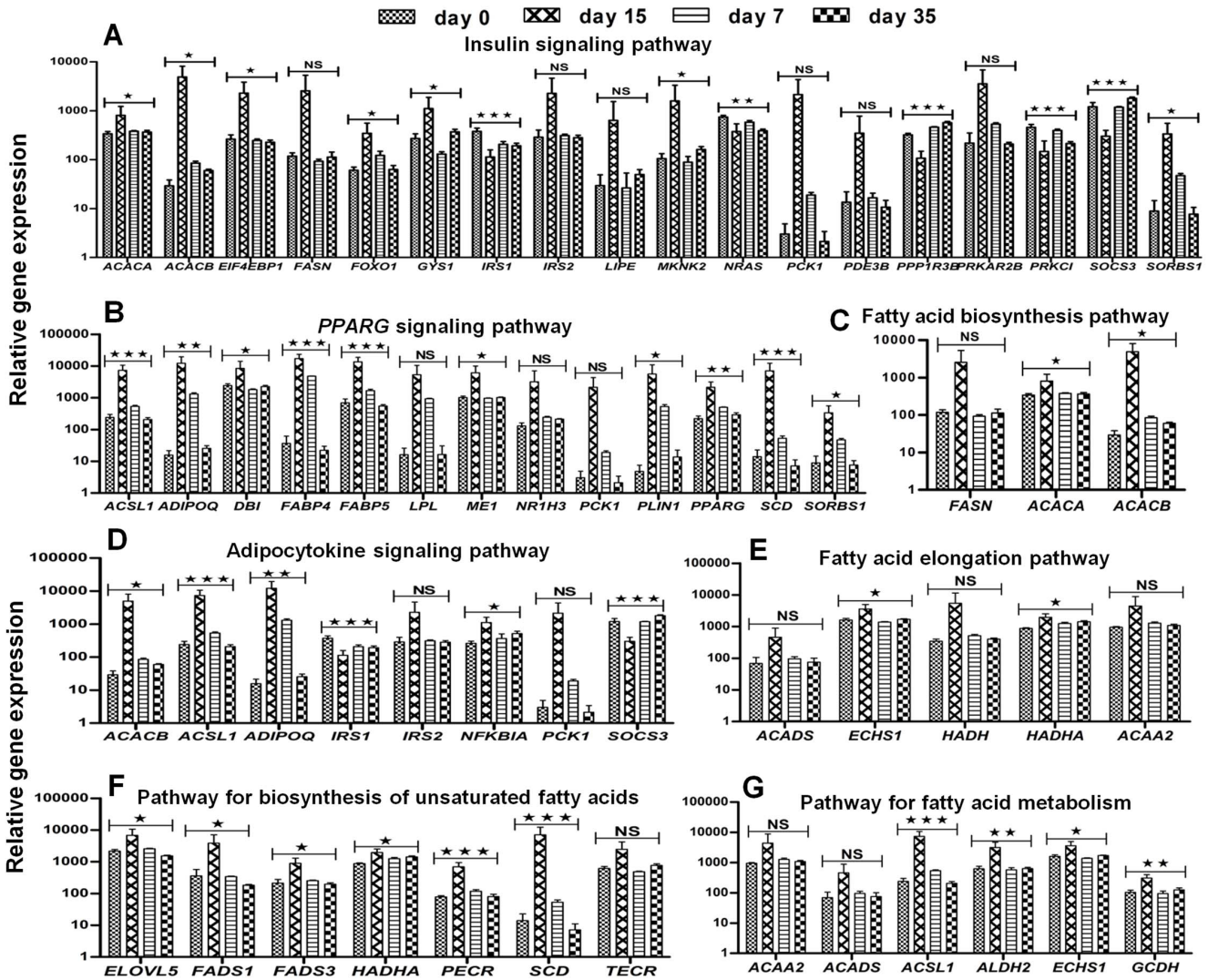

Figure 5. Analysis of adipogenic-specific signaling pathways. The 991 genes that were differentially expressed during adipogenesis were uploaded to the KEGG database to determine their involvement in adipogenic signaling pathways. We found different signaling cascades for adipogenesis like the (**A**) insulin signaling pathway, (**B**) *PPARG* signaling pathway, (**C**) fatty acid biosynthesis pathway, (**D**) adipocytokine signaling pathway, (**E**) fatty acid elongation pathway, (**F**) pathway for biosynthesis of unsaturated fatty acids and (**G**) pathway for fatty acid metabolism. Error bars, Means ± S.E.M.; $*P<0.05$; $**P<0.01$; $***P<0.001$, NS, not significant (One way ANOVA, performed for statistical analysis).
doi:10.1371/journal.pone.0069754.g005

results had more association with adipogenesis relevant terms and features than clusters 2 and 3.

Selection and analysis of new marker genes for adipogenesis

991 genes were differentially expressed during adipogenic differentiation of human MSC and therefore, presented possible marker genes to describe adipogenesis (Suppl. Table S1). These genes were subdivided into 4 groups or K-means clusters (Figure 3A–D) with 307 (cluster 1), 198 (cluster 2), 277 (cluster 3) and 209 genes (cluster 4). As shown, the expression of cluster 4 genes was not reverted to the undifferentiated state during dedifferentiation. On the contrary, after 35 days in dedifferentiation culture they had the expression values of adipogenic differentiated cells. So, according to our approach, we excluded the 209 cluster 4 genes and therefore, the marker list could be narrowed down to the 782 cluster 1–3 genes. For the determination of already known and new markers, this list was analyzed applying different bioinformatics tools of the online databases DAVID, Information Hyperlinked Over Proteins (iHOP) [30], KEGG, PubMed and WikiGenes [31].

Genes were considered as already known markers, if according to these databases they are directly associated with terms like adipogenesis, lipid or fat. As a result, we obtained a list of 185 possible marker genes, which have already been published in the context of adipogenic development and adipose tissue (Suppl. Table S1). Since we were interested in new marker genes, we excluded these 185 genes. This resulted in 597 genes (Suppl. Table S1), which were sorted according to their main fold change value in adipogenesis (first priority), and searched gene by gene for an indirect association with adipogenesis (exclusion criterion).

As a result, we selected the 4 genes *APCDD1*, *CHI3L1*, *RARRES1* and *SEMA3G* as possible new marker genes for the verification and description of adipogenesis (Suppl. Figure S1). Then, their usability was validated applying qRT-PCR. Nine adipogenic cultures (15 days) were analyzed and showed a consistent and reproducible expression of all 4 markers genes (Suppl. Figure S2). Finally, the adipogenesis and dedifferentiation cultures, which were used for GeneChip experiments, were qRT-PCR analyzed. For the fat markers *PPARG* and *FABP4* the results were already presented in Figure 2. Regarding the new markers, during adipogenesis of human MSC the expression of *APCDD1* (Figure 6A) and *SEMA3G* (Figure 6B) in relation to the expression of the housekeeping gene *GAPDH* was continuously up-, and of *CHI3L1* (Figure 6C) and *RARRES1* (Figure 6D) downregulated from day 0 until day 15. During dedifferentiation of adipogenic differentiated cells, the expression of all 4 new markers was reverted. The expression of *APCDD1* (Figure 6E) and *SEMA3G* (Figure 6F) in relation to *GAPDH* was significantly down-, and of *CHI3L1* (Figure 6G) and *RARRES1* (Figure 6H) upregulated from day 0 (start of dedifferentiation culture) to day 35. In conclusion, we found and validated 4 new possible marker genes, which so far have not been published in the context of adipogenesis.

Discussion

The aim of this study was to analyze the adipogenic differentiation of MSC and to discover potential new adipogenic-specific marker genes. For the first time, this aim should be achieved not only by cell differentiation but also by reversing this process by dedifferentiation. In this regard, MSC were isolated [2,23], differentiated into adipogenic lineage cells [23] and finally were dedifferentiated (reverse adipogenesis). Here, bone marrow-derived MSC were used instead of fat tissue-derived MSC with similar properties. The most important reason was that fat tissue-derived MSC potentially are already primed into the adipogenic lineage and express genes relevant for adipogenesis without adding an adipogenic cocktail. Another reason was that bone marrow-derived MSC have already been used in several studies in the context of genome-wide expression profiling and regenerative medicine [2,12,13]. Both adipogenesis and reverse adipogenesis were confirmed on histological level by Oil Red O staining and on molecular level by qRT-PCR of the adipogenic marker genes *PPARG* and *FABP4*. Furthermore, genome-wide microarrays were performed to evaluate our hypothesis that by reversing adipogenesis (dedifferentiation) the adipogenic-specific genes alter their expression and resume to a level comparable to undifferentiated MSC. Such genes may reflect a real image of adipogenesis. In this context, we selected 991 genes with significantly changed expression during the course of adipogenesis. Then, we compared the expression of these genes with their expression during dedifferentiation. Subsequently, the list of 991 genes was divided into 4 clusters by K-means clustering on the basis of their expression values to facilitate the evaluation process for a profound insight into adipogenesis.

Overall, cluster 1 showed the highest relevance for adipogenesis, followed by clusters 2 and 3, while cluster 4 showed no or very minute associations with this differentiation lineage. Cluster 1 genes were upregulated during adipogenesis and downregulated during dedifferentiation. Applying web-based tools for text mining revealed an influence of many genes like *PPARG*, *FABP4*, *LPL*, *LIPE*, *ADIPOQ*, *PLIN1*, *PLIN4*, *IRS2*, *C/EBPA*, *APOE* and *APOL2* on diverse adipogenic events [11,29,30], which supports our conclusion that cluster 1 genes have major relevance to adipogenesis. For instance, *PPARG* is a well known adipogenic target and acts as a central hub among different signaling cascades to regulate and fine tune the adipogenic differentiation of MSC [11]. *FABP4* takes part in the predisposition of cardiac fats in obese persons [32], and *ADIPOQ* upregulation is the main cause of type 2 diabetes and obesity [33]. Cluster 2 and 3 genes were downregulated during differentiation and upregulated during dedifferentiation to their level in undifferentiated cells (cluster 2 at day 35, cluster 3 at day 7). Some genes like *PARP4* and *SOCS3* found in these clusters were already known to have relevance for adipogenesis. The downregulated expression of *PARP4* and *SOCS3* makes it inhibitory targets for adipogenesis, and also negatively regulates the process of adipogenesis [34,35]. Moreover, application of web-based tools for text mining showed both a positive and negative correlation of cluster 2 and 3 genes to fat formation, regulation and metabolism [30,36,37,38], and therefore indicates the association of above cluster genes to adipogenesis. Finally, again using web-based tools for text mining, for cluster 4 genes like *RB1*, *STAG1*, *DST*, *NPAT*, *CGGBP1*, *SMAD5*, *ARID4B*, *NCOA7* and *NR3C1*, we found high enrichment scores for biological annotations like cell cycle, transcription and chromosomal reorganization [27,30,39]. For instance, *STAG1* is a cell cycle regulator and its overexpression is reported for breast cancer and cellular proliferation [40], while the methylation of *RB1* by *SMYD2* enhances cell cycle progression [39]. The expression of cluster 4 genes was not assignable to a typical differentiation or dedifferentiation lineage. Expression values were downregulated during differentiation, upregulated to the undifferentiated expression level at day 7 of dedifferentiation and again changed at day 35 to a level of the differentiated cells. Therefore, the option arises that genes in cluster 4 are not regulated due to an adipogenic induction but according to an independent regulation mechanism. Genes like *RB1*, *STAG2*, *HAUS6*, *MSH2*, *TLK1*, *AEBP2* and *CAND1* may be involved in the reorganization and inter-

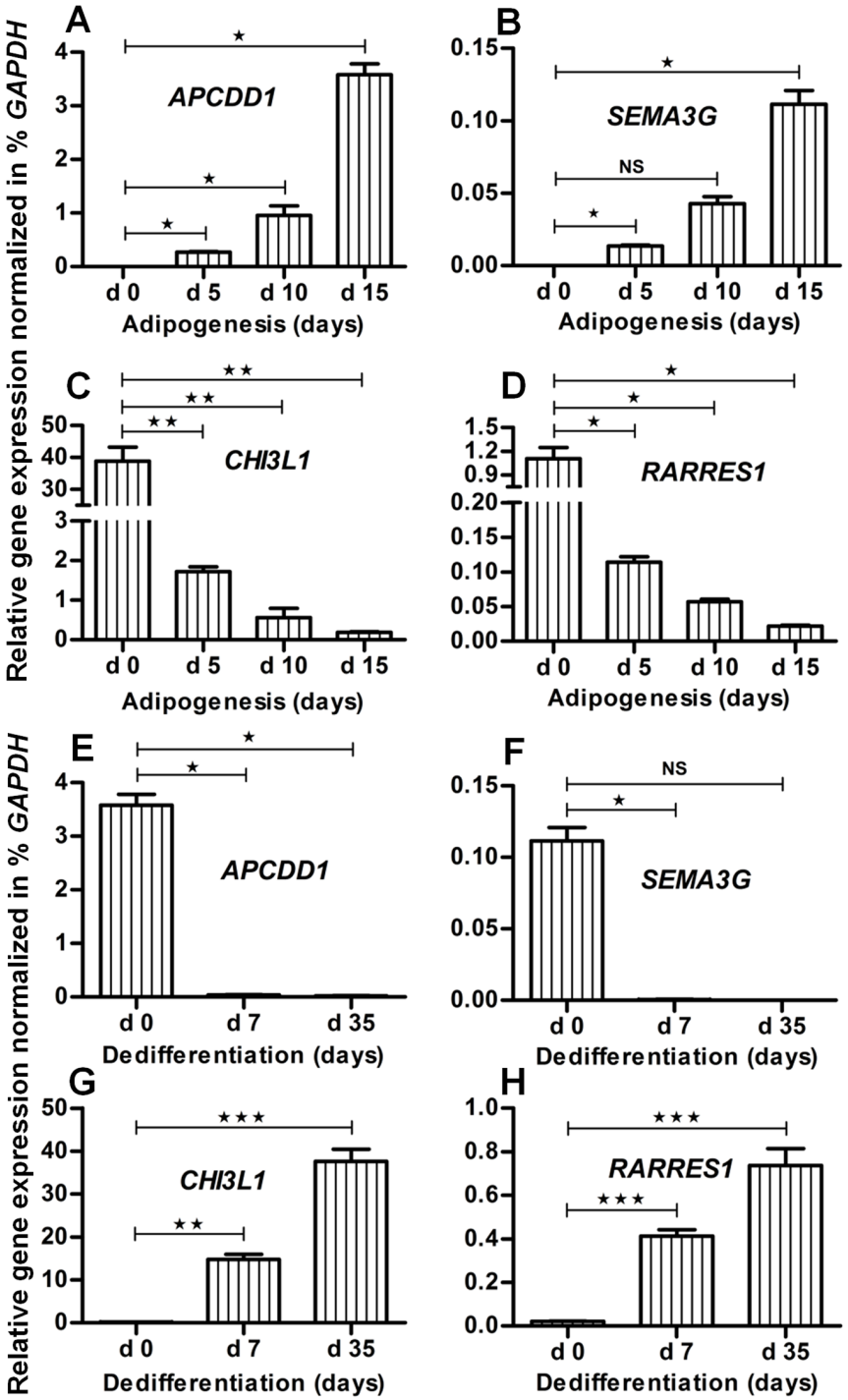

Figure 6. New potential fat marker genes, selected based on the coupling model of adipogenesis and reverse adipogenesis. Gene expression analysis was performed using qRT-PCR and the expression values were normalized to *GAPDH* for stepwise assessment of adipogenesis and reverse adipogenesis (dedifferentiation). Gene expression of new potential fat marker genes (**A**) *APCDD1*, (**B**) *SEMA3G*, (**C**) *CHI3L1* and (**D**) *RARRES1* is given for different stages of adipogenesis, i.e. at day 5, day 10 and day 15. Similarly, the expression of (**E**) *APCDD1*, (**F**) *SEMA3G*, (**G**) *CHI3L1* and (**H**) *RARRES1* is given for different stages of dedifferentiation (reverse adipogenesis). Here the gene expression of adipogenic differentiated cells is represented by day 0 as a reference for dedifferentiation. Error bars, Means ± S.E.M (n = 3); *$P<0.05$; **$P<0.01$; ***$P<0.001$, NS, not significant (student t test, performed for statistical analysis).
doi:10.1371/journal.pone.0069754.g006

conversion of the different states of cells. Text mining revealed a biological association of chromosomal reorganization with cluster 4 genes [27,30,37], and thus strengthen our speculative interpretation. Another possible explanation is that also these genes are important for adipogenesis but are downregulated to maintain the undifferentiated state of the reverse differentiated adipocytes. Alternatively, it also seems possible that some of them may reflect

a state of replicative senescence, as *RB1*, *STAG2* and *CAND1* are well known cell cycle regulators [39,40,41].

Transcription factors are considered to be crucial for adipogenesis [42]. These factors control the flow of genetic information and regulate most cellular processes by binding to specific sequences of DNA [43,44]. Thus applying different bioinformatic tools [27,30,45], we showed the expression of several prominent adipogenic transcription factors like *PPARG*, *PPARA*, *USF*, *E47*, *AP2REP*, *ARNT* and *COUP*. By analysis of their binding sites, we showed TFBS in clusters 1–3, and no sites in cluster 4 genes. Similarly, *HNF4* showed TFBS in clusters 1 and 2 while the TFBS of *SREBP1* were present in clusters 2 and 3 instead of cluster 1 genes. In addition, the transcription factors *AP1* and *C/EBPA* showed binding sites not only in clusters 1–3 but also in cluster 4, even though *C/EBPA* having affiliation with adipogenesis [46]. However, *C/EBPA* needs *PPARG* sites for its functional activation [46]. Due to the fact that we found no *PPARG* binding sites in cluster 4 genes, it further emphasizes that these genes have only a very minor or no role in adipogenesis. TFBS analysis provides a prompt overview about any cellular process [43,44,45], therefore based on it, clusters 1–3 include more genes involved in adipogenesis compared to cluster 4.

Normally, signaling pathways are considered to interplay a vital role during any cellular process via significant alteration in their gene expression [47]. For adipogenesis, signaling pathways facilitate a controlling and regulating mechanism to fine tune the overall process [11,47]. We analyzed and interpreted our results using the online analytical tool of the KEGG database [29,48]. The expressed transcripts showed a profound crosstalking among different signaling pathways and represented a relevance to adipogenesis. In this regard, the insulin signaling pathway is critical to regulate the carbohydrate metabolism in response to body's demand of energy. Furthermore, its ability for glucose uptake, consumption and distribution makes it one of the crucial signaling events for diabetics [10,49] and adipogenesis [50]. The *PPARG* signaling pathway plays an essential and comparatively more influencing role than any other known signaling pathways in the context of adipogenesis [51]. It controls and operates the overall cellular process of fat formation and also plays a unique role in fine tuning the process of adipogenesis [11]. In addition to these pathways, we also found many genes involved in the fatty acid biosynthesis pathway, the adipocytokine signaling pathway, the fatty acid elongation pathway, the pathway for biosynthesis of unsaturated fatty acids and pathway for fatty acid metabolism. Most of the genes found in these signaling pathways were highly expressed during adipogenesis and decreased their expression to a level similar to undifferentiated MSC. In this way, we could broadly verify the differentiation of MSC towards the adipogenic lineage and their subsequent dedifferentiation.

To study a cellular process by a reverse approach is not new in the scientific community [52]. Using this reverse approach for adipogenesis for the first time we generated a more detailed image of adipogenic differentiation and found that the selection of adipogenic-specific genes only on the basis of significant expression during adipogenesis is not sufficient and could be misleading. Therefore, as a consequence of our approach that coupled the processes of adipogenesis and reverse adipogenesis, cluster 4 genes were excluded because of their minute or almost no association with adipogenesis. We identified only 782 genes out of total 991 significantly expressed genes, which reflect a real image of adipogenesis.

Our study supports most of the genes from previously published studies that describe significantly changed expressions during adipogenesis [12,13,47]. Nevertheless, the selection method for so far selected fat markers, which are just based on significant changes during gene expression, is not sufficient. On the basis of our approach, we selected 4 new possible fat marker genes (*APCDD1*, *CHI3L1*, *RARRES1* and *SEMA3G*) for the verification and description of adipogenesis that show high changes in gene expression but are so far known not yet to be involved in adipogenesis. Overexpression of *APCDD1* is reported in context of colorectal carcinogenesis [53], and also known for its inhibitory effect on the WNT signaling pathway [54]. This pathway takes part in the regulation, development and metabolism of adipose tissue [55]. In addition, WNT signaling is an essential requirement for the conversion of MSC into preadipocytes [56]. Thus, *APCDD1* is indirectly related with adipogenesis or is a negative regulator of adipogenic differentiation. *SEMA3G* is another potential marker for adipogenesis, has an inhibitory effect on tumor progression [57], and takes part in controlling the function of endothelial cells and smooth muscle cells [58]. *CHI3L1* encodes a glycoprotein that takes part in macrophage differentiation [59] and has an association with chondrocytes but no association with rheumatoid arthritis [60]. *RARRES1* is a retinoic acid receptor that acts as a vital tumor suppressor gene [61]. Its downregulation is reported for cancer by interacting with *ATP/GTP binding protein-like 2* (*AGBL2*) [62]. Apart from this, it also takes part in proliferation processes and in nasopharyngeal carcinoma [63]. Retinoic acid is known for suppressing adipogenesis and obesity by promoting energy consumption [64]. By using the current web-based tools for text mining [27,30,65], the 4 potential marker genes showed no direct connection to adipogenesis. Based on their expression pattern as well as on the coupling approach of adipogenesis and reverse adipogenesis, *APCDD1*, *CHI3L1*, *RARRES1* and *SEMA3G* are potential marker genes for the analysis of adipogenic processes.

Besides this, the reversion of adipogenesis, dedifferentiation, could be a promising approach for the treatment of obesity and their correlated problems. This reversing approach of adipogenesis also advocates soft tissue engineering with a new therapeutic angle, and will also open new doors for further studies in this direction.

Conclusions

Adipogenic marker genes are generally selected on the basis of a significant change in their expression during adipogenic differentiation. Generally this selection is misleading, because the adipogenesis inducing cocktail not only induces the expression of adipogenic-specific genes but also the expression of genes for involved in other cellular processes. So, how to filter adipogenic-specific genes out of all differentially expressed genes needs an answer. To achieve this, we combined the process of adipogenesis with reverse adipogenesis. During adipogenesis, 991 genes were significantly expressed, and according to our hypothesis some of these genes not represent the process of adipogenesis. Therefore, to filter adipogenic-specific genes, we reversed the expression of adipogenic genes by reverse adipogenesis and in this way, we selected more relevant fat marker genes. On the basis of this approach, we filtered 782 genes out of total 991 significantly expressed genes. To validate the benefit of our approach, we analyzed all 991 genes for adipogenic-linked biological annotations, adipogenic transcription factors and adipogenic signaling pathway. Interestingly, genes from our filtered 782 fat markers, such as the most prominent adipogenic marker genes *PPARG*, *FABP4*, *LPL*, *LIPE*, *ADIPOQ*, *PLIN1*, *PLIN4*, *IRS2*, *C/EBPA*, *APOE* and *APOL2*, showed a much stronger affiliation to adipogenesis than the other 209 genes. Clearly, this shows the usefulness and importance of our approach. Furthermore, we identified *APCDD1*, *CHI3L1*, *RARRES1* and *SEMA3G* as potential adipogenic-specific

marker genes by using the model of adipogenesis and reverse adipogenesis.

Supporting Information

Figure S1 Microarray gene expression profile of potential new fat marker genes during adipogenesis and reverse adipogenesis. Microarray gene expression analysis was performed for potential new fat marker genes (n = 3 donors) during adipogenesis and reverse adipogenesis (dedifferentiation). Relative gene expression of new introductory fat marker genes of (**A**) *APCDD1*, (**B**) *SEMA3G*, (**C**) *CHI3L1* and (**D**) *RARRES1* is given for different donors (n = 3). Error bars, Means ± S.E.M (n = 3).
(TIF)

Figure S2 Gene expression profile validation of new fat marker genes via qRT-PCR for different individual donors (n = 9). Gene expression analysis of potential new fat marker genes was performed using qRT-PCR for individual donors (n = 9). Gene expression of new introductory fat marker genes of (**A**) *APCDD1*, (**B**) *SEMA3G*, (**C**) *CHI3L1* and (**D**) *RARRES1* is given for 9 different donors. The gene expression was normalized to % *GAPDH* expression.
(TIF)

Figure S3 Figure Of Merit (FOM) analysis. The 991 selected genes, which were significantly expressed during adipogenesis as compared to undifferentiated MSC, were divided into 4 clusters on the basis of FOM. FOM classification of genes confirmed that only 4 cluster are significant, because as shown, any increase in cluster number didn't result in any significant cluster.
(TIF)

Table S1 The selected 991 genes, differentially expressed during adipogenesis. 991 candidate genes were selected on the basis of differentially expression in adipogenesis. Their mean signal expression values are given for different time points, i.e. undifferentiated MSC (day 0), adipogenic differentiated cells (day 15), early time point of dedifferentiated cells (day 7) and late time point of dedifferentiated cells (day 35). 991 genes were grouped into 4 clusters on the basis of K means classification. The genes in each cluster were organized according to ascending alphabetical order on the basis of gene symbol. ± std: standard deviation, MFC: mean fold change, In cluster 1–3 the gene symbol with ***asterix*** (*) representing published fat markers, while other without asterix are unpublished fat marker genes.
(DOCX)

Table S2 Transcription factor binding sites (TFBS) included in each cluster. The numbers of transcription factor binding sites (TFBS) are given in this table, and are organized according to ascending alphabetical order. The number in brackets represents the number of transcription factor binding sites (TFBS), and these TFBS are specific to each cluster gene as given in the Suppl. Table S1. For more detail of gene titles and expression values of the respective cluster genes, see Suppl. Table S1.
(DOCX)

Acknowledgments

We gratefully thank Barbara Walewska and Anja Wachtel for excellent technical assistance.

Author Contributions

Conceived and designed the experiments: MU SS JR MS. Performed the experiments: MU SS. Analyzed the data: MU SS JR TH JE MS. Contributed reagents/materials/analysis tools: JE TH JR. Wrote the paper: MU SS JR MS.

References

1. Dominici M, Le Blanc K, Mueller I, Slaper-Cortenbach I, Marini F, et al. (2006) Minimal criteria for defining multipotent mesenchymal stromal cells. The International Society for Cellular Therapy position statement. Cytotherapy 8: 315–317.
2. Pittenger MF, Mackay AM, Beck SC, Jaiswal RK, Douglas R, et al. (1999) Multilineage potential of adult human mesenchymal stem cells. Science 284: 143–147.
3. Wang S, Qu X, Zhao RC (2011) Mesenchymal stem cells hold promise for regenerative medicine. Front Med 5: 372–378.
4. Greenberg AS, Obin MS (2006) Obesity and the role of adipose tissue in inflammation and metabolism. Am J Clin Nutr 83: 461S–465S.
5. Trayhurn P, Beattie JH (2001) Physiological role of adipose tissue: white adipose tissue as an endocrine and secretory organ. Proc Nutr Soc 60: 329–339.
6. Waki H, Tontonoz P (2007) Endocrine functions of adipose tissue. Annu Rev Pathol 2: 31–56.
7. Philips BJ, Marra KG, Rubin JP (2012) Adipose stem cell-based soft tissue regeneration. Expert Opin Biol Ther 12: 155–163.
8. Feve B (2005) Adipogenesis: cellular and molecular aspects. Best Pract Res Clin Endocrinol Metab 19: 483–499.
9. Balachandran A, Guan H, Sellan M, van Uum S, Yang K (2008) Insulin and dexamethasone dynamically regulate adipocyte 11beta-hydroxysteroid dehydrogenase type 1. Endocrinology 149: 4069–4079.
10. Lizcano JM, Alessi DR (2002) The insulin signalling pathway. Curr Biol 12: R236–238.
11. Takada I, Kouzmenko AP, Kato S (2010) PPAR-gamma Signaling Crosstalk in Mesenchymal Stem Cells. PPAR Res 2010.
12. Menssen A, Haupl T, Sittinger M, Delorme B, Charbord P, et al. (2011) Differential gene expression profiling of human bone marrow-derived mesenchymal stem cells during adipogenic development. BMC Genomics 12: 461.
13. Schilling T, Kuffner R, Klein-Hitpass L, Zimmer R, Jakob F, et al. (2008) Microarray analyses of transdifferentiated mesenchymal stem cells. J Cell Biochem 103: 413–433.
14. Monaco E, Bionaz M, Rodriguez-Zas S, Hurley WL, Wheeler MB (2012) Transcriptomics comparison between porcine adipose and bone marrow mesenchymal stem cells during in vitro osteogenic and adipogenic differentiation. PLoS One 7: e32481.
15. Armani A, Mammi C, Marzolla V, Calanchini M, Antelmi A, et al. (2010) Cellular models for understanding adipogenesis, adipose dysfunction, and obesity. J Cell Biochem 110: 564–572.
16. Scott MA, Nguyen VT, Levi B, James AW (2011) Current methods of adipogenic differentiation of mesenchymal stem cells. Stem Cells Dev 20: 1793–1804.
17. Vater C, Kasten P, Stiehler M (2011) Culture media for the differentiation of mesenchymal stromal cells. Acta Biomater 7: 463–477.
18. Grimaldi PA (2001) The roles of PPARs in adipocyte differentiation. Prog Lipid Res 40: 269–281.
19. Styner M, Sen B, Xie Z, Case N, Rubin J (2010) Indomethacin promotes adipogenesis of mesenchymal stem cells through a cyclooxygenase independent mechanism. J Cell Biochem 111: 1042–1050.
20. Yang DC, Tsay HJ, Lin SY, Chiou SH, Li MJ, et al. (2008) cAMP/PKA regulates osteogenesis, adipogenesis and ratio of RANKL/OPG mRNA expression in mesenchymal stem cells by suppressing leptin. PLoS One 3: e1540.
21. Weinberger-Ohana P, Goldschmit D, Mizrachi L, Orly J (1984) Cyclic nucleotide phosphodiesterase inhibitor, 3-isobutyl-1-methylxanthine, induces cytodifferentiation of follicular granulosa cells cultured in serum-free medium. Endocrinology 115: 2160–2169.
22. Brzozowski T, Konturek PC, Pajdo R, Kwiecien SN, Konturek S, et al. (2005) Agonist of peroxisome proliferator-activated receptor gamma (PPAR-gamma): a new compound with potent gastroprotective and ulcer healing properties. Inflammopharmacology 13: 317–330.
23. Ullah M, Stich S, Notter M, Eucker J, Sittinger M, et al. (2013) Transdifferentiation of mesenchymal stem cells-derived adipogenic-differentiated cells into osteogenic- or chondrogenic-differentiated cells proceeds via dedifferentiation and have a correlation with cell cycle arresting and driving genes. Differentiation 85: 78–90.
24. Pfaffl MW (2001) A new mathematical model for relative quantification in real-time RT-PCR. Nucleic Acids Res 29: e45.
25. Sturn A, Quackenbush J, Trajanoski Z (2002) Genesis: cluster analysis of microarray data. Bioinformatics 18: 207–208.

26. Eisen MB, Spellman PT, Brown PO, Botstein D (1998) Cluster analysis and display of genome-wide expression patterns. Proc Natl Acad Sci U S A 95: 14863–14868.
27. Dennis G, Jr., Sherman BT, Hosack DA, Yang J, Gao W, et al. (2003) DAVID: Database for Annotation, Visualization, and Integrated Discovery. Genome Biol 4: P3.
28. Huang da W, Sherman BT, Lempicki RA (2009) Systematic and integrative analysis of large gene lists using DAVID bioinformatics resources. Nat Protoc 4: 44–57.
29. Kanehisa M, Araki M, Goto S, Hattori M, Hirakawa M, et al. (2008) KEGG for linking genomes to life and the environment. Nucleic Acids Res 36: D480–484.
30. Hoffmann R, Valencia A (2004) A gene network for navigating the literature. Nat Genet 36: 664.
31. Hoffmann R (2008) A wiki for the life sciences where authorship matters. Nat Genet 40: 1047–1051.
32. Engeli S, Utz W, Haufe S, Lamounier-Zepter V, Pofahl M, et al. (2013) Fatty acid binding protein 4 predicts left ventricular mass and longitudinal function in overweight and obese women. Heart.
33. Siitonen N, Pulkkinen L, Lindstrom J, Kolehmainen M, Eriksson JG, et al. (2011) Association of ADIPOQ gene variants with body weight, type 2 diabetes and serum adiponectin concentrations: the Finnish Diabetes Prevention Study. BMC Med Genet 12: 5.
34. Rouleau M, Patel A, Hendzel MJ, Kaufmann SH, Poirier GG (2010) PARP inhibition: PARP1 and beyond. Nat Rev Cancer 10: 293–301.
35. Shi H, Tzameli I, Bjorbaek C, Flier JS (2004) Suppressor of cytokine signaling 3 is a physiological regulator of adipocyte insulin signaling. J Biol Chem 279: 34733–34740.
36. Hoffmann R, Valencia A (2005) Implementing the iHOP concept for navigation of biomedical literature. Bioinformatics 21 Suppl 2: ii252–258.
37. Hoffmann R, Krallinger M, Andres E, Tamames J, Blaschke C, et al. (2005) Text mining for metabolic pathways, signaling cascades, and protein networks. Sci STKE 2005: pe21.
38. Hoffmann R (2007) Using the iHOP information resource to mine the biomedical literature on genes, proteins, and chemical compounds. Curr Protoc Bioinformatics Chapter 1: Unit1 16.
39. Cho HS, Hayami S, Toyokawa G, Maejima K, Yamane Y, et al. (2012) RB1 Methylation by SMYD2 Enhances Cell Cycle Progression through an Increase of RB1 Phosphorylation. Neoplasia 14: 476–486.
40. Giannini G, Ambrosini MI, Di Marcotullio L, Cerignoli F, Zani M, et al. (2003) EGF- and cell-cycle-regulated STAG1/PMEPA1/ERG1.2 belongs to a conserved gene family and is overexpressed and amplified in breast and ovarian cancer. Mol Carcinog 38: 188–200.
41. Chua YS, Boh BK, Ponyeam W, Hagen T (2011) Regulation of cullin RING E3 ubiquitin ligases by CAND1 in vivo. PLoS One 6: e16071.
42. Rosen ED, Walkey CJ, Puigserver P, Spiegelman BM (2000) Transcriptional regulation of adipogenesis. Genes Dev 14: 1293–1307.
43. Latchman DS (1997) Transcription factors: an overview. Int J Biochem Cell Biol 29: 1305–1312.
44. van Nimwegen E (2003) Scaling laws in the functional content of genomes. Trends Genet 19: 479–484.
45. Matys V, Kel-Margoulis OV, Fricke E, Liebich I, Land S, et al. (2006) TRANSFAC and its module TRANSCompel: transcriptional gene regulation in eukaryotes. Nucleic Acids Res 34: D108–110.
46. Schmidt SF, Jorgensen M, Chen Y, Nielsen R, Sandelin A, et al. (2011) Cross species comparison of C/EBPalpha and PPARgamma profiles in mouse and human adipocytes reveals interdependent retention of binding sites. BMC Genomics 12: 152.
47. Ito T, Tsuruta S, Tomita K, Kikuchi K, Yokoi T, et al. (2011) Genes that integrate multiple adipogenic signaling pathways in human mesenchymal stem cells. Biochem Biophys Res Commun 409: 786–791.
48. Zhang JD, Wiemann S (2009) KEGGgraph: a graph approach to KEGG PATHWAY in R and bioconductor. Bioinformatics 25: 1470–1471.
49. Liu Y, Liu F, Grundke-Iqbal I, Iqbal K, Gong CX (2011) Deficient brain insulin signalling pathway in Alzheimer's disease and diabetes. J Pathol 225: 54–62.
50. Zhang HH, Huang JX, Duvel K, Boback B, Wu SL, et al. (2009) Insulin Stimulates Adipogenesis through the Akt-TSC2-mTORC1 Pathway. PLoS One 4.
51. Takada I, Kouzmenko AP, Kato S (2010) PPAR-gamma Signaling Crosstalk in Mesenchymal Stem Cells. Ppar Research.
52. Tomlin CJ, Axelrod JD (2005) Understanding biology by reverse engineering the control. Proc Natl Acad Sci U S A 102: 4219–4220.
53. Takahashi M, Fujita M, Furukawa Y, Hamamoto R, Shimokawa T, et al. (2002) Isolation of a novel human gene, APCDD1, as a direct target of the beta-catenin/T-cell factor 4 complex with probable involvement in colorectal carcinogenesis. Cancer Research 62: 5651–5656.
54. Shimomura Y, Agalliu D, Vonica A, Luria V, Wajid M, et al. (2010) APCDD1 is a novel Wnt inhibitor mutated in hereditary hypotrichosis simplex. Nature 464: 1043–1047.
55. Christodoulides C, Lagathu C, Sethi JK, Vidal-Puig A (2009) Adipogenesis and WNT signalling. Trends in Endocrinology and Metabolism 20: 16–24.
56. Laudes M (2011) Role of WNT signalling in the determination of human mesenchymal stem cells into preadipocytes. J Mol Endocrinol 46: R65–72.
57. Kigel B, Varshavsky A, Kessler O, Neufeld G (2008) Successful inhibition of tumor development by specific class-3 semaphorins is associated with expression of appropriate semaphorin receptors by tumor cells. PLoS One 3: e3287.
58. Kutschera S, Weber H, Weick A, De Smet F, Genove G, et al. (2011) Differential endothelial transcriptomics identifies semaphorin 3G as a vascular class 3 semaphorin. Arterioscler Thromb Vasc Biol 31: 151–159.
59. Rehli M, Krause SW, Andreesen R (1997) Molecular characterization of the gene for human cartilage gp-39 (CHI3L1), a member of the chitinase protein family and marker for late stages of macrophage differentiation. Genomics 43: 221–225.
60. Srivastava SK, Antal P, Gal J, Hullam G, Semsei AF, et al. (2011) Lack of evidence for association of two functional SNPs of CHI3L1 gene (HC-gp39) with rheumatoid arthritis. Rheumatol Int 31: 1003–1007.
61. Sahab ZJ, Hall MD, Zhang L, Cheema AK, Byers SW (2010) Tumor Suppressor RARRES1 Regulates DLG2, PP2A, VCP, EB1, and Ankrd26. J Cancer 1: 14–22.
62. Sahab ZJ, Hall MD, Me Sung Y, Dakshanamurthy S, Ji Y, et al. (2011) Tumor suppressor RARRES1 interacts with cytoplasmic carboxypeptidase AGBL2 to regulate the alpha-tubulin tyrosination cycle. Cancer Res 71: 1219–1228.
63. Kwok WK, Pang JC, Lo KW, Ng HK (2009) Role of the RARRES1 gene in nasopharyngeal carcinoma. Cancer Genet Cytogenet 194: 58–64.
64. Berry DC, DeSantis D, Soltanian H, Croniger CM, Noy N (2012) Retinoic acid upregulates preadipocyte genes to block adipogenesis and suppress diet-induced obesity. Diabetes 61: 1112–1121.
65. Harel A, Inger A, Stelzer G, Strichman-Almashanu L, Dalah I, et al. (2009) GIFtS: annotation landscape analysis with GeneCards. BMC Bioinformatics 10: 348.

STEM CELLS AND DEVELOPMENT
Volume 22, Number 23, 2013

DOI: 10.1089/scd.2013.0108

ORIGINAL RESEARCH REPORT

N-Glycosylation Profile of Undifferentiated and Adipogenically Differentiated Human Bone Marrow Mesenchymal Stem Cells: Towards a Next Generation of Stem Cell Markers

Houda Hamouda,[1,2,*] Mujib Ullah,[3,*] Markus Berger,[1] Michael Sittinger,[3] Rudolf Tauber,[1] Jochen Ringe,[3] and Véronique Blanchard[1]

Mesenchymal stem cells (MSCs) are multipotent cells that are easy to isolate and expand, develop into several tissues, including fat, migrate to diseased organs, have immunosuppressive properties and secrete regenerative factors. This makes MSCs ideal for regenerative medicine. For application and regulatory purposes, knowledge of (bio)markers characterizing MSCs and their development stages is of paramount importance. The cell surface is coated with glycans that possess lineage-specific nature, which makes glycans to be promising candidate markers. In the context of soft tissue generation, we aimed to identify glycans that could be markers for MSCs and their adipogenically differentiated progeny. MSCs were isolated from human bone marrow, adipogenically stimulated for 15 days and adipogenesis was verified by staining the lipid droplets and quantitative real time polymerase chain reaction of the marker genes peroxisome proliferator-activated receptor gamma (*PPARG*) and fatty acid binding protein-4 (*FABP4*). Using matrix-assisted laser desorption-ionization-time of flight mass spectrometry combined with exoglycosidase digestions, we report for the first time the N-glycome of MSCs during adipogenic differentiation. We were able to detect more than 100 different N-glycans, including high-mannose, hybrid, and complex N-glycans, as well as poly-*N*-acetyllactosamine chains. Adipogenesis was accompanied by an increased amount of biantennary fucosylated structures, decreased amount of fucosylated, afucosylated tri- and tetraantennary structures and increased sialylation. N-glycans H6N5F1 and H7N6F1 were significantly overexpressed in undifferentiated MSCs while H3N4F1 and H5N4F3 were upregulated in adipogenically differentiated MSCs. These glycan structures are promising candidate markers to detect and distinguish MSCs and their adipogenic progeny.

Title: N-glycosylation profile of undifferentiated and adipogenically differentiated human bone marrow mesenchymal stem cells: towards a next generation of stem cell markers.

Authors: Houda Hamouda[2]*, Mujib Ullah[1]*, Markus Berger[2], Michael Sittinger[1], Rudolf Tauber[2], Jochen Ringe[1], and Véronique Blanchard[2]

Address: [1]Tissue Engineering Laboratory & Berlin-Brandenburg Center for Regenerative Therapies, Dept. of Rheumatology and Clinical Immunology, Charité-University Medicine Berlin, Charitéplatz 1, 10117 Berlin, Germany
[2]Institute of Laboratory Medicine, Clinical Chemistry and Pathobiochemistry, Charité-Universitätsmedizin Berlin, Berlin, Germany

Journal: Stem Cells and Development

Volume: 22, **Issue**: 23, November 25, 2013, **Pages:** 01–14

BioResearch Open Access
Volume 1, Number 6, December 2012

DOI: 10.1089/biores.2012.0279

A Reliable Protocol for the Isolation of Viable, Chondrogenically Differentiated Human Mesenchymal Stem Cells from High-Density Pellet Cultures

Mujib Ullah,[1] Houda Hamouda,[2] Stefan Stich,[1] Michael Sittinger,[1] and Jochen Ringe[1]

Abstract

Administration of chondrogenically differentiated mesenchymal stem cells (MSC) is discussed as a promising approach for the regenerative treatment of injured or diseased cartilage. The high-density pellet culture is the standard culture for chondrogenic differentiation, but cells in pellets secrete extracellular matrix (ECM) that they become entrapped in. Protocols for cell isolation from pellets often result in cell damage and dedifferentiation towards less differentiated MSC. Therefore, our aim was to develop a reliable protocol for the isolation of viable, chondrogenically differentiated MSC from high-density pellet cultures. Human bone marrow MSC were chondrogenically stimulated with transforming growth factor-β3, and the cartilaginous structure of the pellets was verified by alcian blue staining of cartilage proteoglycans, antibody staining of cartilage collagen type II, and quantitative real-time reverse-transcription polymerase chain reaction of the marker genes *COL2A1* and *SOX9.* Trypsin and collagenases II and P were tested alone or in combination, and for different concentrations and times, to find a protocol for optimized pellet digestion. Whereas trypsin was not able to release viable cells, 90-min digestion with 300 U of collagenase II, 20 U of collagenase P, and 2 mM $CaCl_2$ worked quite well and resulted in about 2.5×10^5 cells/pellet. The protocol was further optimized for the separation of released cells and ECM from each other. Cells were alcian blue and collagen type II positive and expressed *COL2A1* and *SOX9*, verifying a chondrogenic character. However, they had different morphological shapes. The ECM was also uniformly alcian blue and collagen type II positive but showed different organizational and structural forms. To conclude, our protocol allows the reliable isolation of a defined number of viable, chondrogenically differentiated MSC from high-density pellet cultures. Such cells, as well as the ECM components, are of interest as research tools and for cartilage tissue engineering.

Key words: cell isolation; chondrogenic differentiation; enzymatic pellet digestion; extracellular matrix

Introduction

Hyaline cartilage not only plays an integral role in the skeletal framework of the body but also coats the surfaces of bones in joints to facilitate bone gliding and to prevent bone abrasion.[1,2] In general, cartilage consists of chondrocytes and extracellular matrix (ECM), and both components work in an interdependent manner to maintain structure and function.[3,4] Cartilage disorders due to injury or disease not only disturb this structural organization but also affect the functional ability of this tissue.[5,6] It is known that cartilage has a limited ability for self-repair due to its lack of vascular supply, lymphatic drainage, and innervations. Moreover, chondrocytes are entrapped in their ECM and thus have no physical contact with each other and restricted migration potential to defect sites.[2,3,7] For these reasons, cartilage disorders often result in destruction of hyaline joints and require joint arthroplasty.

Today, for the regenerative treatment of cartilage lesions, autologous chondrocytes are routinely clinically applied as a cell suspension (ACI), a high-density pellet of cells and ECM, or in combination with matrices (MACI).[8–10] However, problems arise when chondrocytes are cultured because the propagation to achieve sufficient cell numbers is accompanied by chondrocyte senescence[11,12] and dedifferentiation of round cells to fibroblast-like cells with decreased cartilage formation capacity.[13,14] Three-dimensional (3D) culture reduces but does not overcome the problem. In general, chondrocyte-

[1]Tissue Engineering Laboratory and Berlin-Brandenburg Center for Regenerative Therapies, Department of Rheumatology and Clinical Immunology; [2]AG Glycodesign and Glycoanalytics, Institute of Laboratory Medicine, Clinical Chemistry, and Pathobiochemistry; Charité-Universitätsmedizin Berlin, Berlin, Germany.

based techniques do not result in native cartilage but rather pain relief, formation of hyaline and/or inferior fibrocartilage, and a delay of joint destruction.

Mesenchymal stem cells (MSC), or multipotent mesenchymal stromal cells, are discussed as an alternative cell source.[13–16] Because they are easy to isolate and to expand and can differentiate into cartilage, migrate to diseased organs, and secrete molecules enabling their allogeneic use as a kind of controlled factor delivery system, MSC are promising cells for cartilage tissue engineering.[10,17] Today, for the regenerative treatment of injured or diseased cartilage, bone marrow–stimulating techniques like microfracture, combined with supporting matrices, are routinely applied *in situ* to recruit MSC to cartilage defect sites.[18,19] Results are similar to ACI and MACI. However, no cell product based on administration of differentiated or undifferentiated MSC exists.

The 3D high-density pellet culture is the standard assay for chondrogenesis *in vitro*.[15,20] Here, a loose, spherical MSC pellet is chondrogenically induced by the addition of the standard stimulus, transforming growth factor (TGF)β, leading to a firm, spherical MSC pellet resembling hyaline cartilage and consisting of differentiated MSC and their ECM. The ECM mostly consists of different proteoglycans and collagens, which are usually cross-linked and provide a protective cage in which the TGFβ-stimulated MSC are entrapped.[21–23] So, the isolation of these cells from their ECM is a challenging task, but is the prerequisite to deliver viable, chondrogenically differentiated MSC. To our knowledge, no successful procedure for the isolation of such cells from pellets has been published.

Herein, we present a protocol for isolation of viable, chondrogenically differentiated human MSC from high-density pellet cultures for research and regenerative applications.[24,25] This reliable and easy-to-use protocol, based on an enzymatic cocktail of collagenase II, collagenase P, and $CaCl_2$, results in about 2.5×10^5 cells per pellet and maintains the chondrogenically differentiated state of these cells. This is shown with cell-culture techniques, histological and immunohistochemical staining and quantitative real-time reverse-transcription polymerase chain reaction (qPCR). As a by-product, cartilage ECM components, often discussed as growth and differentiation factors, are enriched and can be used in research.

Material and Methods

Isolation and culture propagation of human MSC

Human MSC were isolated from bone marrow aspirates of the iliac crest of three informed, consenting donors ($n=3$, average age: 68 ± 4.6 years) who were examined to exclude hematopoietic neoplasms; samples were found to be histologically normal. The local ethical committee of the Charité-Universitätsmedizin Berlin approved the study. Nucleated cells in the aspirates were counted and suspended in culture medium consisting of Dulbecco's modified Eagle's medium (DMEM; Biochrom), 10% fetal bovine serum (Thermo Scientific Hyclone), 2 ng/mL basic fibroblast growth factor (FGF; PeproTech), 10 mM HEPES buffer, 4 mM L-glutamine, 100 U/mL penicillin, and 100 μg/mL streptomycin (all Biochrom). Cells were seeded at a density of 2×10^5 cells/cm^2. After 72 h, nonadherent cells and debris were washed out by the first media exchange. Then, medium was exchanged three times a week and cells were detached after 90% confluence with 0.05% trypsin/1 mM EDTA (both Biochrom), subcultured (seeding density: 5×10^3 cells/cm^2), and expanded until passage 3 (P3).

Flow cytometric analysis of human MSC

To verify their presentation of MSC marker, P3 MSC of all donors were analyzed using a FACSCalibur flow cytometer (Becton Dickinson). Briefly, cells were collected and suspensions of 2.5×10^5 cells were washed with phosphate-buffered saline (PBS)/0.5% bovine serum albumin (BSA; both Biochrom). For direct staining, cells were centrifuged (250 *g*, 5 min) and resuspended in cold PBS/0.5% BSA. Afterwards they were incubated for 15 min on ice with titrated concentrations of R-phycoerythrin–labeled mouse anti-human CD14, CD34, CD73, CD166, fluorescein isothiocynate (FITC)-labeled mouse anti-human CD44, CD45, CD90 (all BD Pharmingen), or FITC-labeled mouse anti-human CD105 (Acris Antibodies). Finally the cells were washed in cold PBS/0.5% BSA and resuspended in the same buffer before flow cytometric analysis. Propidium iodide (100 μg/mL; Sigma-Aldrich) staining was applied to exclude dead cells and debris, while unstained cells were used as a negative control. Data were evaluated using CellQuest software (Becton Dickinson).

Chondrogenic differentiation of human MSC

For chondrogenic differentiation in high-density pellet cultures ($n=6$ donors, P3), 2.5×10^5 MSC were centrifuged (150 *g*, 5 min) in a 15-mL polypropylene tube (Becton Dickinson) to form a pellet. The pellets were treated for 28 days with defined serum-free chondrogenic medium, which consisted of DMEM (4.5 g/L glucose; Biochrom), ITS+1 supplement, 100 nM dexamethasone, 0.17 mM L-ascorbic acid-2-phosphate, 1 mM sodium pyruvate, 0.35 mM L-prolin (all Sigma-Aldrich), and 10 ng/mL TGFβ3 (R&D Systems). Control pellets were cultured in the same medium without TGFβ3. Medium was changed three times a week.

Establishment of an appropriate protocol for cell isolation from pellet cultures

To isolate viable, chondrogenically differentiated MSC from entrapped ECM, we established a step-by-step protocol. High-density pellets were digested by using six different approaches. In the first approach, pellets were incubated with 0.05% trypsin/1 mM EDTA for 10, 20, and 30 min at 37°C and 5% CO_2. In the second approach, they were cut into small pieces with a sharp blade and then incubated with 0.05% trypsin/1 mM EDTA for 10, 20, and 30 min. In the third approach, they were incubated for 60 and 120 min with 100, 200, and 300 U of collagenase II (Biochrom), and in the fourth approach for the same time with 10, 20, and 30 U of collagenase P (Roche). In the fifth approach, 300 U of collagenase II and 20 U of collagenase P were mixed and the mixture was incubated for 30, 60, 90, and 120 min. Finally, in the sixth approach, 2 mM $CaCl_2$ was added to the fifth approach mixture, which was then incubated for 90 and 120 min at 37°C and 5% CO_2 to digest pellet cultures. As presented in the *Results*, the last approach (90 min) was best.

Isolation of viable, chondrogenically differentiated human MSC from pellet cultures

The newly established protocol was applied in all further studies. Initially, medium was removed and the pellet culture was washed with PBS. Then, for enzymatic digestion, the pellet was digested with 300 U of collagenase II, 20 U of collagenase P, and 2 mM $CaCl_2$ for 90 min at 37°C and 5% CO_2. This resulted in a mixture of viable, chondrogenically differentiated cells, ECM, semidigested pellets, enzymes, and debris. Based on our targeted cell number, mixtures were isolated from 25 pellets (about 2.0×10^5 cells/pellet) per donor ($n=3$), pooled, and then mechanically homogenized by gentle pipetting to dislodge and release the cells from ECM.

Isolation of ECM and its enrichment

To isolate ECM, the whole digested extract consisting of cells, ECM, enzymes, and debris was transferred to a 50-mL tube and centrifuged at 350 *g* for 6 min. Then supernatant was discarded, and the precipitate was resuspended in culture medium supplemented with TGFβ3. We added this chondrogenic stimulus to maintain the differentiated state of chondrogenically differentiated cells and to exclude cell dedifferentiation. Subsequently, cells along with ECM and other debris were transferred to a culture flask and incubated at 37°C and 5% CO_2. After 2 h, viable, chondrogenic cells were attached to the culture surface, while the ECM, dead cells, and cellular debris remained unattached. The nonadherent substances were removed by medium exchange and centrifuged at 350 *g* for 6 min at 37°C. The process of medium removal and centrifugation was repeated three times to ensure the maximum removal of ECM for its enrichment. Cells and ECM were used separately for histological, immunohistochemical, and gene expression analysis.

Histological and immunohistochemical analysis

To demonstrate chondrogenesis, high-density pellet cultures were embedded in Tissue-Tek O.C.T. compound (Sakura Finetek), frozen in liquid nitrogen and cryosectioned (6 μm thickness). To analyze the secretion of cartilage proteoglycans, sections were stained with alcian blue 8GS (Roth) and counterstained with nuclear fast red (Sigma-Aldrich). For immunohistochemical analysis of collagen type II formation, sections were incubated for 1 h with a primary rabbit anti-human collagen type II antibody (Acris Antibodies), processed with the EnVision system peroxidase kit (DAKO), and counterstained with hematoxylin (Merck).

For histological and immunohistochemical analysis of viable, chondrogenic cells, four-well chamber slides were used (Thermo Scientific). For alcian blue and collagen type II staining, 2.0×10^5 chondrogenically differentiated cells were transferred to each well. Slides were then incubated at 37°C and 5% CO_2 for 4 days. Then, for direct staining the medium was removed, and cells were washed with PBS and fixed for 5 min in cooled 3.7% formaldehyde in PBS. Finally, cells were stained according to the protocols already described for cryosections.

Isolation of RNA from high-density pellet cultures and qPCR

For qPCR analysis of high-density pellet cultures and viable, chondrogenically differentiated cells, total RNA was harvested. For pellet RNA extraction, pellets were pooled for each individual donor ($n=3$, 14 pellets for each donor), mixed with TriReagent (Sigma-Aldrich), and mechanically homogenized with an Ultra-Turrax (IKA). For RNA extraction from monolayer cells ($n=3$ donors), mechanical homogenization was not necessary; 1-bromo-3-chloro-propane (Sigma-Aldrich) was added followed by centrifugation (13,000 *g*, 45 min). The aqueous phase was collected and mixed with an equal amount of ethanol. Further steps were performed applying the RNeasy Mini Kit (Qiagen). Finally, RNA quality and quantity were measured with the NanoDrop (NanoDrop products).

For qPCR, cDNA was synthesized from total RNA (2.5 μg) with the iScript cDNA synthesis kit (BioRad). Then, TaqMan qPCR was performed in triplicate in 96-well optical plates on a Mastercycler® ep realplex2 S system (Eppendorf) with gene expression assays for TaqMan probes and primer sets (Applied Biosystems). Quantitative gene expression was analyzed for the chondrogenic marker genes collagen type 2 A1 (*COL2A1*; assay ID: Hs00264051_m1) and SRY (sex determining region Y)-box-9 (*SOX9*; Hs00165814_m1) and for the housekeeping gene glyceraldehyde-3-phosphate dehydrogenase (*GAPDH*; Hs99999905_m1). *COL2A1* and *SOX9* expression was normalized to the endogenous *GAPDH* expression level and calculated with the $2^{-\Delta\Delta Ct}$ formula as percentage of *GAPDH* expression.[26]

Statistical analysis

Statistical analysis was performed using SigmaStat 3.5 (Systat), while GraphPad Prism4 (GraphPad) was applied to draw graphs. Students' *t*-test was applied for nonparametric quantitative data sets analysis and one tailed *p*-values were calculated; $p<0.05$ and $p<0.001$ were considered to be statistically significant. Error bars in all figures represent the standard error of the mean (SEM).

Results

Isolation and culture of human MSC

MSC were isolated from human bone marrow aspirates of three donors and subsequently culture expanded up to P3. In P0, cells showed the typical fibroblast-like morphology of primary MSC (Fig. 1A). During culture propagation up to P3, cells were slightly flattened but still showed a homogeneous fibroblast-like morphology (Fig. 1B). In P3, flow cytometric analysis was performed to verify if the cells had the standard MSC surface marker profile. As expected, MSC were uniformly positive for CD44, CD73, CD90, CD105, and CD166 and negative for the hematopoietic markers CD14, CD34, and CD45 (Fig. 1C). We and others have shown the multilineage differentiation potential of such cells in many studies; here we were only interested in their chondrogenic differentiation potential.

Chondrogenic differentiation of MSC in high-density pellet cultures

MSC were chondrogenically stimulated with TGFβ3 in the standard pellet culture assay. After initial centrifugation in 15-mL polypropylene tubes, MSC settled and formed loose, spherical pellets. During the first week, pellets started to increase in size and had a thinner central zone as compared

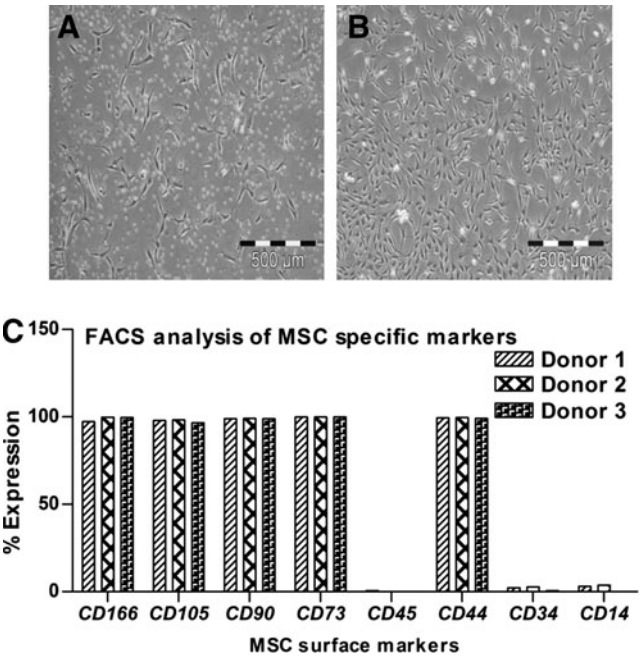

FIG. 1. **(A)** During isolation, human bone marrow mesenchymal stem cells (MSCs) appeared as single cells in passage 0 (P0), **(B)** then they showed uniform growth and fibroblast like morphology in P3. **(C)** On FACS analysis the cells were positive for typical MSC antigens like CD166, CD105, CD90, CD73, and CD44, while negative for hematopoietic lineage-specific antigens like CD45, CD34, and CD14. Bar: 500 μm.

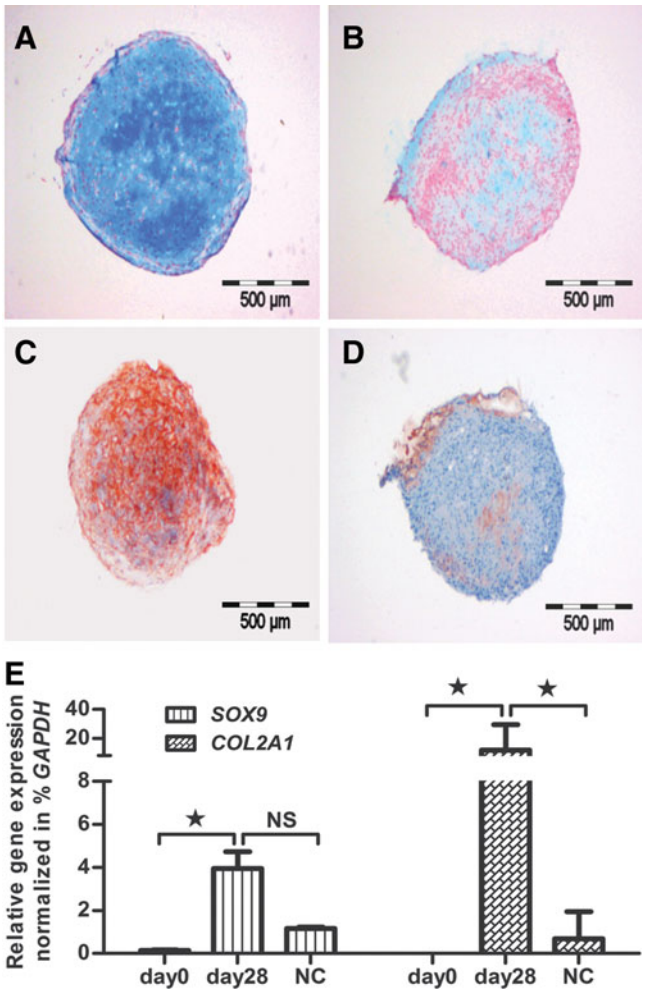

FIG. 2. MSC were induced to chondrogenic lineage cells. Their chondrogenic ability was assessed via **(A)** alcian blue and **(C)** collagen type II staining, while the controls were negative for both **(B)** alcian blue and **(D)** collagen type II staining. **(E)** After 28 days of induction, the chondrogenic MSC showed significant expression of cartilage-specific genes *SOX9* and *COL2A1* as compared to negative controls (NC) and undifferentiated MSC, day 0. Bar: 500 μm.

to a thicker circumferential border. After 28 days, pellets were converted into firm, mechanically strong cultures (Fig. 2). At that point, alcian blue staining of cartilage proteoglycans (Fig. 2A) and antibody staining of cartilage-specific collagen type II (Fig. 2C) revealed the formation of a cartilaginous ECM. Both alcian blue (Fig. 2B) and collagen type II (Fig. 2D) staining were negative in unstimulated pellet cultures. On the gene expression level, chondrogenesis was measured by significantly increased expression of the cartilage marker genes *SOX9* and *COL2A1* from day 0 to day 28 (Fig. 2E). Both genes were also much more highly expressed in stimulated cultures than in unstimulated cultures (Fig. 2E).

Establishment of a protocol to isolate viable, chondrogenically differentiated MSC

The isolation of viable, chondrogenically differentiated cells from high-density pellet cultures was a challenging task because they were entrapped in the firm, mechanically strong ECM, and no appropriate protocol was known. Testing different approaches, we established a step-by-step procedure for the enzymatic release of cells from such cultures. The first approach was based on the knowledge that trypsin is the standard enzyme to release viable cells from a broad spectrum of tissues. So, pellets were incubated under standard cell culture conditions with 0.05% trypsin/1 mM EDTA for 10, 20, and 30 min. However, according to trypan blue staining of cells and subsequent counting by hemocytometer, no viable or dead cells were released (Fig. 3A). We assumed that due to the presence of a protective ECM layer on the pellet surface, trypsin was not able to release any cells. Therefore, in the second approach, each pellet was cut into small pieces with a sharp blade; incubated with 0.05% trypsin/1 mM EDTA for 10, 20, and 30 min; and then mechanically dislodged to release the cells by pipetting. Obviously, some viable cells were released (Fig. 3B) but compared to the number of dead cells, after 10-min (Fig. 3C, D), 20-min (Fig. 3E, F), and 30-min (Fig. 3G, H) incubation, their number was very low. Moreover, the majority of the few viable cells were unable to proliferate and most of them died after 1 day in subsequent cell culture (data not shown). Based on these results, trypsin was excluded from our study. In the third approach, 100, 200, and 300 U of collagenase II (Fig. 4A) and in the fourth approach, 10, 20, and 30 U of collagenase P (Fig. 4B) were used in 60- and 120-min incubations under standard cell culture conditions. This was based on the knowledge that the ECM contains diverse collagens, among which collagen type II is

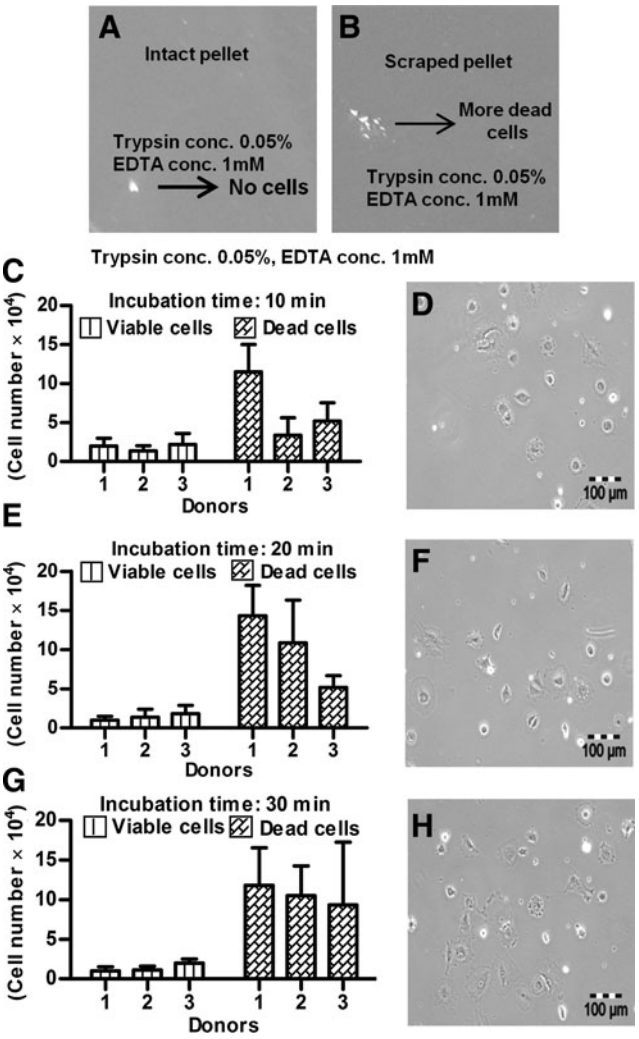

FIG. 3. **(A)** Incubation of intact pellets with trypsin did not release any cells, **(B)** while incubation with trypsin of pieces scraped from pellets released cells, the majority of which were dead. The numbers of released cells from the scraped pieces are shown after 10 min **(C)** with corresponding morphology **(D)**; after 20 min **(E)** with corresponding morphology **(F)**; and after 30 min **(G)** with corresponding morphology **(H)**. Bar: 100 μm.

prominent. After 60 and 120 min, 300 U of collagenase II resulted in the highest number of viable, released cells (Fig. 4A). For collagenase P, results were ambiguous (Fig. 4B) and the amount of released cells was lower than in the collagenase II approach. In the fifth approach, 300 U of collagenase II and 20 U of collagenase P were combined together for 30- to 120-min incubations. The resultant semidigested pellets were mechanical dislodged by gentle pipetting. After the 30-min incubation, roughly 1.5×10^4 viable cells per pellet were released (Fig. 4C) and showed normal morphology (Fig. 4E). However, the number of nonviable cell was relatively high, and some cells remained as small clumps in the ECM (Fig. 4C,E). After 60 min, the number of released, viable cells was increased, and the other characteristics were constant (Fig. 4D, F). Thirty minutes later, the number of viable cells was further increased (roughly 2.8×10^4 cells/pellet; Fig. 4G), the morphology was slightly flattened, and the number of clumps was decreased (Fig. 4I). After 120 min, with about 3.0×10^4 cells/pellet, the highest number of viable cells was released from the pellet cultures (Fig. 4H), but most of them died in subsequent culture, and the remaining cells became more flattened and showed almost no proliferation (Fig. 4J). We assumed that cell damage was correlated with an increased incubation time in the enzymatic cocktail; therefore, to reduce this time, we added $CaCl_2$ in the last approach. Calcium chloride is considered to be a stabilizing agent for diverse collagenases and increases their activity.[27,28] Pellets were incubated in 300 U of collagenase II, 20 U of collagenase P, and 2 mM $CaCl_2$ at 37°C and 5% CO_2 for 90 and 120 min. As expected, at 90 min, $CaCl_2$ supplementation resulted in a very high number of released cells (about 3.9×10^4 cells/pellet) (Fig. 5A). These cells were morphologically normal and proliferated in subsequent culture (Fig. 5C). After 120 min, we did not observe any further increase in the amount of released, viable cells (Fig. 5B), and there were more dead cells (Fig. 5D). In conclusion, 300 U of collagenase II, 20 U of collagenase P, and 2 mM $CaCl_2$ were used in our protocol for 90 min at 37°C and 5% CO_2. The protocol was then further optimized for the separation of released cells and ECM from each other (*Materials and Methods*) and resulted in about 2.5×10^5 cells per pellet.

Morphology and chondrogenic character of isolated cells

The culture appearance of viable, chondrogenically differentiated cells was inhomogeneous. We observed groups of cells that were different in size from small (Fig. 6A) to large (Fig. 6B), in shape from spherical (Fig. 6A) to polygonal (Fig. 6B), and in appearance from individual (Fig. 6A) to grouped (Fig. 6B). Some had flatted ends compared to others (Fig. 6C), with distinct nucleus and abundant cytoplasm (Fig. 6C,D). Clearly, most had a tri- or multi-angular morphology (Fig. 6D). However, during isolation cells retained their chondrogenic character, as shown by positive alcian blue (Fig. 7A) and collagen type II (Fig. 7C) staining. Cells isolated from unstimulated negative control pellets were alcian blue (Fig. 7B) and collagen type II negative (Fig. 7D). Cells were also cross-checked on the gene level for expression of *SOX9* and *COL2A1*. The expression of both marker genes in percent expression of *GAPDH* in cultures with cells released from chondrogenically stimulated pellets was significantly higher than in cultures with cells released from unstimulated control pellets (Fig. 7E).

Extracellular matrix

After separation of released cells and ECM from each other, we further analyzed the ECM-enriched fraction, which contained some debris, that did not attach to the culture surface during separation. In morphological evaluation, we observed two main structures (Fig. 8), a small particle-like structure (Fig. 8A) and an almost uniform, small membrane-like structure (Fig. 8B). The chondrogenic characteristic of these two ECM structures was examined by alcian blue and collagen type II staining. Alcian blue staining confirmed the presence of cartilage proteoglycans in both morphological structures (Fig. 8C, D). However, the intensity was higher in the group with particle-like structures (Fig. 8C). Counterstaining with nuclear fast red was negative, indicating that no cells were in the ECM fraction. Both structures were

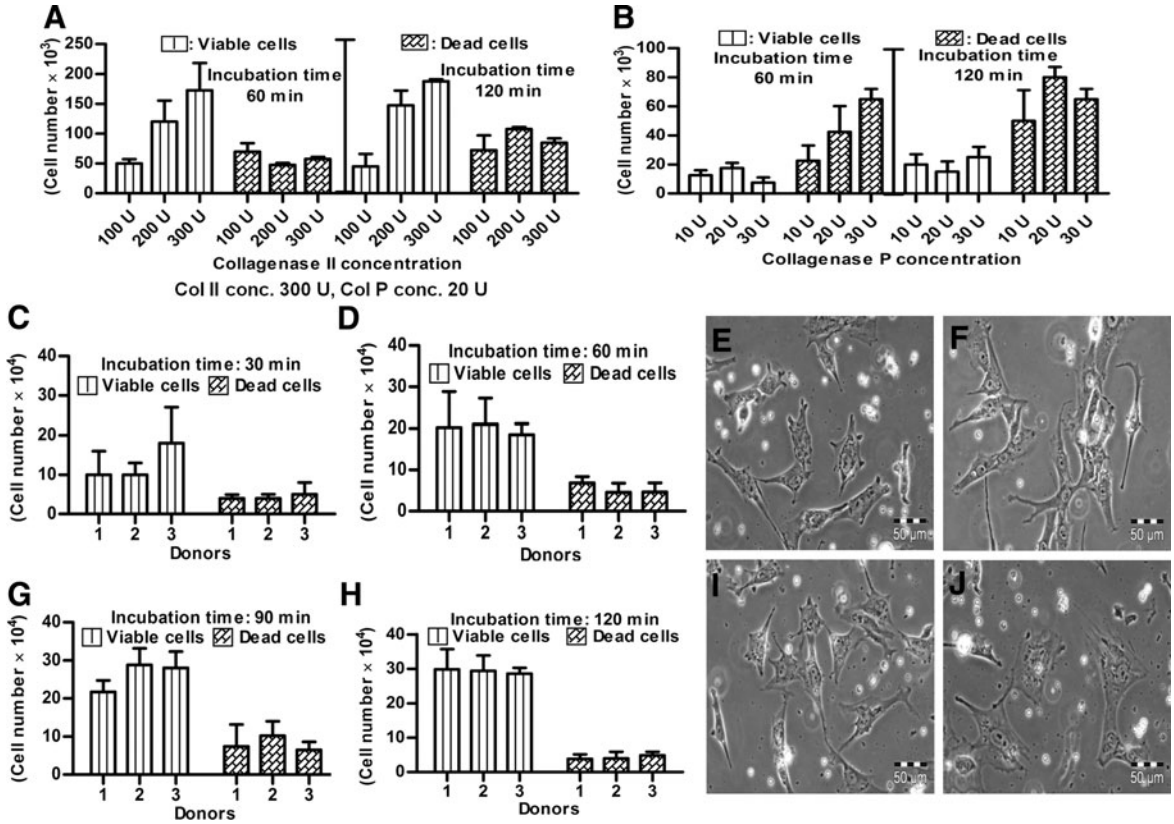

FIG. 4. The chondrogenic intact pellets were digested with **(A)** collagenase II and **(B)** collagenase P for different time points on individual bases. Then 300 U of collagenase II and 20 U of collagenase P were combined together and added to the intact pellets. The cell numbers released upon digestion are shown after **(C)** 30 min, **(D)** 60 min, **(G)** 90 min, and **(H)** 120 min incubation time point. Their corresponding morphology is given after enzymatic digestion of **(E)** 30 min, **(F)** 60 min, **(I)** 90 min and **(J)** 120 min. Bar: 50 μm.

collagen type II positive (Fig. 8E, F), with a higher intensity in the membranous-like structure. As shown exemplarily in Fig. 8D and 8F, ECM from unstimulated control pellets was both alcian blue and collagen type II negative.

Discussion

For the regenerative treatment of injured or damaged articular cartilage, chondrogenically differentiated MSC, isolated from diverse tissues with or without matrices, are considered a promising alternative for autologous chondrocytes transplantation.[13,25,29] In this context the high-density pellet culture represents a model system to provide a large amount of chondrogenic MSC,[15,20] especially when such cells should be applied as a suspension for regenerative application. However, inside intact pellet culture, the cells and their secreted ECM components enclose and fix each other,[1–3] hindering the release of chondrogenic MSC. This emphasizes the need for a successful protocol to isolate cells from pellets, despite an array of published protocols for chondrocyte isolation from native cartilage.[30,31] Unfortunately, such protocols are not applicable to isolating viable cells from pellets, and we believed that appropriate pellet digestion represented the key step to achieve this. We thus examined the parameters of enzyme selection, concentration, and incubation time to establish uniform standards for the reproducible release of viable cells from high-density pellet cultures.

First, MSC were chondrogenically stimulated with TGFβ3 for 28 days to generate high-density pellet cultures. The chondrogenic nature of these pellets was verified by histochemical examination of cartilage proteoglycan, antibody staining of cartilage collagen type II, and qPCR of *COL2A1* and *SOX9*.

Then, to start pellet digestion, trypsin was applied because it is broadly accepted as the enzyme for release of cells from culture surfaces and diverse native tissues. Initially trypsin did not release any cells from intact whole pellets, and very few cells were released from small pieces of knife-scraped pellets. In line with these results, trypsin was previously found to be insufficient to isolate chondrocytes from cartilage.[30] Since cartilage and chondrogenic pellet cultures contain a huge amount of collagen, collagenases are important digestion enzymes. We and others have used a mixture of collagenase II and collagenase P to isolate chondrocytes from normal and osteoarthritic cartilage.[30,32,33] Therefore, we next tested these two enzymes alone or in combination, and found a mixture of 300 U of collagenase II and 20 U of collagenase P optimum at 90 and 120 min of incubation for maximum release of viable cells. But most cells either died on subsequent culturing or otherwise showed low proliferation rate. Since digestion of native cartilage with these enzymes is often performed overnight, we did not expect such a negative influence with our incubation times,[30,32,33] especially with our selected enzyme concentration being in the standard range. This implies differences between the structure of native

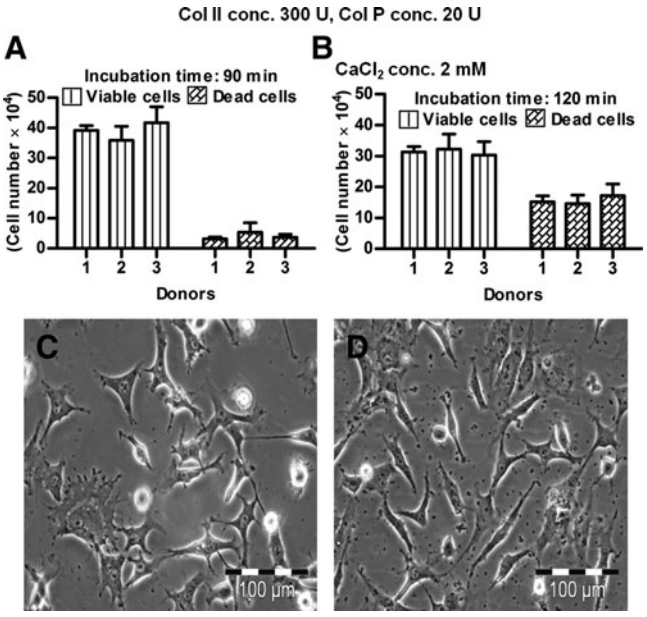

FIG. 5. The chondrogenic intact pellets were digested with collagenase II (Col II) and collagenase P (Col P) in presence of $CaCl_2$ for different time points. The released cell numbers are shown after **(A)** 90-min and **(B)** 120-min incubation. Similarly their morphology is given after **(C)** 90-min and **(D)** 120-min enzymatic digestion. Bar: 100 μm.

cartilage and pellet culture cartilage. Since it is known that $CaCl_2$ stabilizes several collagenases and increases their activity, thus accelerating the digestion process, we added it to our enzymatic cocktail.[27,28] After 90 min, with about 3.9×10^4 cells/pellet, this addition resulted in a highly increased number of released cells. Cells were morphologically normal and proliferated in subculture. Since 120-min incubation did not result in more released cells, 90 min was selected as the appropriate incubation time.

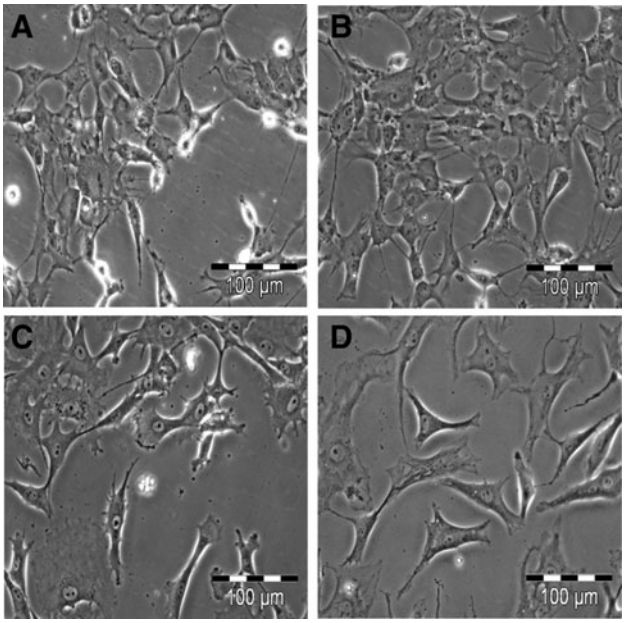

FIG. 6. The released cells were purified from the components of ECM, which showed different morphology such as being **(A)** small in size and spherical in shape, **(B)** large in size and polygonal in shape, **(C)** large in size and longitudinal in shape with one flattened end, and **(D)** large in size and triangular in shape. Bar: 100 μm.

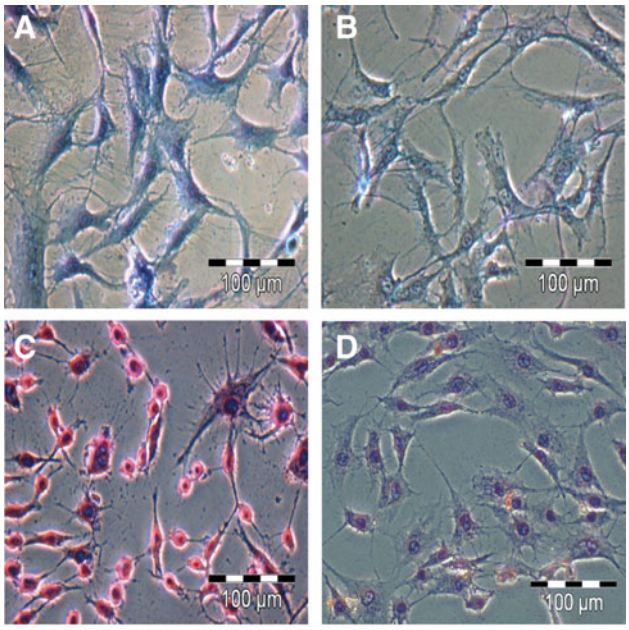

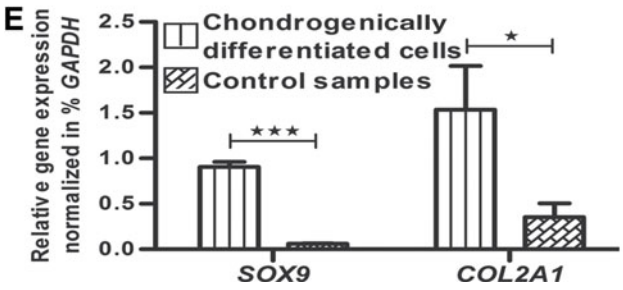

FIG. 7. The released cells from chondrogenically induced pellets were positive for **(A)** alcian blue and **(C)** collagen type II staining, while the control samples were negative for **(B)** alcian blue and **(D)** collagen type II staining. **(E)** On the gene level, they showed significant expression for chondrogenic-specific makers like *SOX9* and *COL2A1* as compared to control samples. Bar: 100 μm.

After further optimization of the protocol (centrifugation steps, cell attachment times) for the separation of released cells and ECM from each other, about 2.5×10^5 viable cells/pellet were released. The next question was whether the enzymatic cocktail affected cell physiology. It has been reported that $CaCl_2$, at least in serum-free media, maintains the chondrogenic phenotype in monolayer and keeps the cells in suspension culture.[34] However, the viable, chondrogenic cells showed different morphologies. One reason may be a non-uniform nutrient supply to single cells or cell aggregates inside high-density pellet cultures. In this context, we also did not ignore the variable rate of diffusion for TGFβ3 and enzymes for chondrogenesis and pellet digestion, respectively. It also seems possible that the chondrogenic capacity of the primary MSC varied. Anyway, based on cartilage proteoglycan and collagen type II presentation and gene

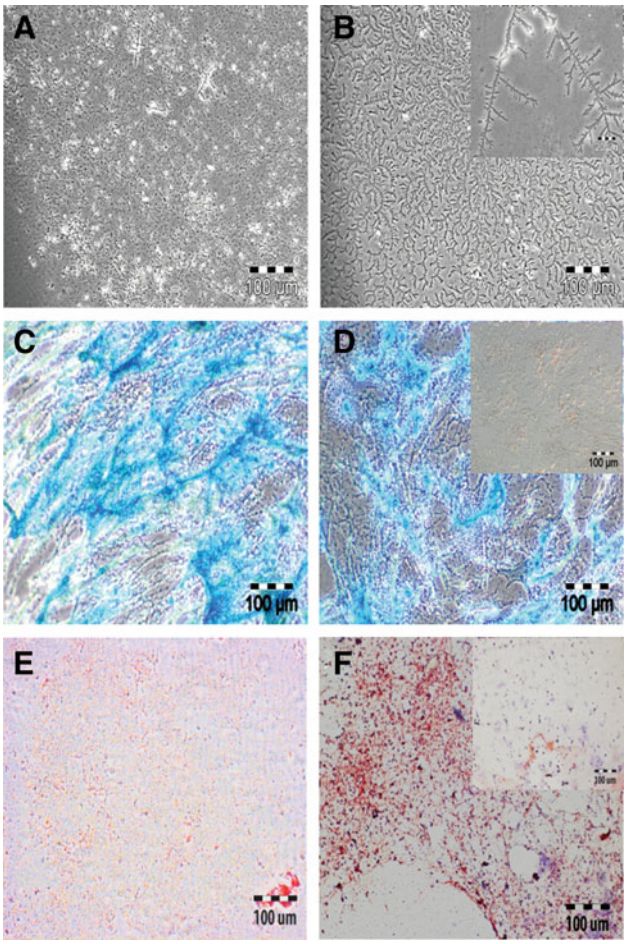

FIG. 8. On morphological evaluation, ECM showed two prominent forms, **(A)** particle-like appearance and **(B)** small membrane-like structures (*inset* is a higher resolution image, bar: 20 μm). The particle-like structures of ECM were **(C)** positive for alcian blue and **(E)** marginally positive for collagen type II staining. The membrane-like structures of ECM were equally positive for both **(D)** alcian blue and **(F)** collagen type II staining. *Insets* **(D, F)**: ECM from control samples. Bar: 100 μm.

expression of *COL2A1* and *SOX9*, released cells had a chondrogenic phenotype.[35] Not showing here, we observed an extensive proliferation with beginning dedifferentiation towards a less differentiated phenotype, when seeding the cells in MSC culture medium. Therefore, we added the chondrogenic stimulus TGFβ3 to the culture medium to maintain the chondrogenic phenotype and noticed that most of the cells did not lose their morphological specificity.

Besides the cell fraction, the ECM fraction was isolated, enriched, and preliminarily investigated. Purified ECM not only plays a stimulating role in chondrogenic cell aggregation,[36] but it is also interesting for therapeutic approaches. For instance, it has been shown that the components of ECM play a curative role in cartilage repair.[37–39] Additionally, their roles as growth and differentiation factors and cell-recruiting molecules are known and constitute an important research topic. Hyaluronan acid is clinically applied *in situ* to recruit MSC to cartilage defect sites and to promote cartilage differentiation.[10,19] This established protocol will play a substantial role in providing purified chondrogenic cells and ECM for future regenerative application.

Conclusion

The 3D high-density pellet culture is considered a standard culture model for its entrapped chondrogenically differentiated cells. We present a protocol for the reproducible isolation of a defined number of viable, chondrogenically differentiated MSC from this culture. Simple steps, including enzymatic digestion, mechanical homogenization, selective adherence of viable cells, and removal of the ECM-enriched supernatants, result in two fractions consisting of purified chondrogenically differentiated cells and enriched cartilage ECM components. Perhaps this may not seem highly important on the first view. However, for the very high number of groups working on MSC, chondrogenic differentiation, and cartilage repair, our protocol delivers purified chondrogenic MSC and enriched ECM not only for research and development, but also for regenerative therapies. The protocol may also provide a basis for MSC isolation from other matrix-free or matrix-based chondrogenic 3D cartilage cultures.

Acknowledgments

We gratefully thank Barbara Walewska (Tissue Engineering Laboratory, Charité-Universitätsmedizin Berlin) for excellent technical assistance. The study was supported by the Investment Bank Berlin (IBB) and European Regional Development Fund (grant 10147246), and the Bundesministerium für Bildung und Forschung (grant BCRT 0315848A).

Author Disclosure Statement

M.S. is a shareholder of CellServe Ltd. (Berlin, Germany) and BioRetis Ltd. (Berlin, Germany) and works as a consultant for BioTissue Technologies Ltd. (Freiburg, Germany), which develops tissue transplants for the regeneration of bone and cartilage. The product activities of the companies are not related to the scientific topics presented here. M.U., H.H., S.S., and J.R. indicate no potential conflicts of interest. All authors disclose any financial and personal relationship with people or organizations that could inappropriately influence this scientifically oriented *in vitro* study. Therefore, no competing financial interests exist.

References

1. Pearle AD, Warren RF, Rodeo SA. Basic science of articular cartilage and osteoarthritis. Clin Sports Med. 2005;24:1–12.
2. Tetteh ES, Bajaj S, Ghodadra NS. Basic science and surgical treatment options for articular cartilage injuries of the knee. J Orthop Sports Phys Ther. 2012;42:243–253.
3. Bhosale AM, Richardson JB. Articular cartilage: structure, injuries and review of management. Br Med Bull. 2008;87: 77–95.
4. Temenoff JS, Mikos AG. Review: tissue engineering for regeneration of articular cartilage. Biomaterials. 2000;21: 431–440.
5. Seed SM, Dunican KC, Lynch AM. Osteoarthritis: a review of treatment options. Geriatrics. 2009;64:20–29.
6. Swift A. Osteoarthritis 1: physiology, risk factors and causes of pain. Nurs Times. 2012;108:12–15.
7. Chiang H, Jiang CC. Repair of articular cartilage defects: review and perspectives. J Formos Med Assoc. 2009;108:87–101.

8. Brittberg M, Lindahl A, Nilsson A, et al. Treatment of deep cartilage defects in the knee with autologous chondrocyte transplantation. N Engl J Med. 1994;331:889–895.
9. Meyer U, Wiesmann HP, Libera J, et al. Cartilage defect regeneration by ex vivo engineered autologous microtissue—preliminary results. In Vivo. 2012;26:251–257.
10. Ringe J, Burmester GR, Sittinger M. Regenerative medicine in rheumatic disease—progress in tissue engineering. Nat Rev Rheumatol. 2012;8:493–498.
11. Loeser RF. Aging and osteoarthritis: the role of chondrocyte senescence and aging changes in the cartilage matrix. Osteoarthritis Cartilage. 2009;17:971–979.
12. Martin JA, Brown T, Heiner A, Buckwalter JA. Post-traumatic osteoarthritis: the role of accelerated chondrocyte senescence. Biorheology. 2004;41:479–491.
13. Tang QO, Carasco CF, Gamie Z, et al. Preclinical and clinical data for the use of mesenchymal stem cells in articular cartilage tissue engineering. Expert Opin Biol Ther. 2012;12: 1361–1382.
14. Barbero A, Ploegert S, Heberer M, Martin I. Plasticity of clonal populations of dedifferentiated adult human articular chondrocytes. Arthritis Rheum. 2003;48:1315–1325.
15. Pittenger MF, Mackay AM, Beck SC, et al. Multilineage potential of adult human mesenchymal stem cells. Science. 1999;284:143–147.
16. Dominici M, Le Blanc K, Mueller I, et al. Minimal criteria for defining multipotent mesenchymal stromal cells. The International Society for Cellular Therapy position statement. Cytotherapy. 2006;8:315–317.
17. Jorgensen C, Noel D. Mesenchymal stem cells in osteoarticular diseases. Regen Med. 2011;6:44–51.
18. Benthien JP, Behrens P. The treatment of chondral and osteochondral defects of the knee with autologous matrix-induced chondrogenesis (AMIC): method description and recent developments. Knee Surg Sports Traumatol Arthrosc. 2011;19: 1316–1319.
19. Siclari A, Mascaro G, Gentili C, et al. A cell-free scaffold-based cartilage repair provides improved function hyaline-like repair at one year. Clin Orthop Relat Res. 2012;470: 910–919.
20. Johnstone B, Hering TM, Caplan AI, et al. In vitro chondrogenesis of bone marrow-derived mesenchymal progenitor cells. Exp Cell Res. 1998;238:265–272.
21. Eyre DR, Weis MA, Wu JJ. Articular cartilage collagen: an irreplaceable framework? Eur Cell Mater. 2006;12:57–63.
22. Qi WN, Scully SP. Type II collagen modulates the composition of extracellular matrix synthesized by articular chondrocytes. J Orthop Res. 2003;21:282–289.
23. Roughley PJ. The structure and function of cartilage proteoglycans. Eur Cell Mater. 2006;12:92–101.
24. Mrugala D, Dossat N, Ringe J, et al. Gene expression profile of multipotent mesenchymal stromal cells: identification of pathways common to TGFbeta3/BMP2-induced chondrogenesis. Cloning Stem Cells. 2009;11:61–76.
25. Ringe J, Sittinger M. Tissue engineering in the rheumatic diseases. Arthritis Res Ther. 2009;11:211.
26. Pfaffl MW. A new mathematical model for relative quantification in real-time RT-PCR. Nucleic Acids Res. 2001;29:e45.
27. Wu Q, Li C, Li C, et al. Purification and characterization of a novel collagenase from *Bacillus pumilus* Col-J. Appl Biochem Biotechnol. 2010;160:129–139.
28. Petrova D, Derekova A, Vlahov S. Purification and properties of individual collagenases from *Streptomyces* sp. strain 3B. Folia Microbiol (Praha). 2006;51:93–98.
29. Mohal JS, Tailor HD, Khan WS. Sources of adult mesenchymal stem cells and their applicability for musculoskeletal applications. Curr Stem Cell Res Ther. 2012;7:103–109.
30. Hayman DM, Blumberg TJ, Scott CC, Athanasiou KA. The effects of isolation on chondrocyte gene expression. Tissue Eng. 2006;12:2573–2581.
31. Wolf F, Candrian C, Wendt D, et al. Cartilage tissue engineering using pre-aggregated human articular chondrocytes. Eur Cell Mater. 2008;16:92–99.
32. Dehne T, Karlsson C, Ringe J, et al. Chondrogenic differentiation potential of osteoarthritic chondrocytes and their possible use in matrix-associated autologous chondrocyte transplantation. Arthritis Res Ther. 2009;11:R133.
33. Endres M, Neumann K, Schroder SE, et al. Human polymer-based cartilage grafts for the regeneration of articular cartilage defects. Tissue Cell. 2007;39:293–301.
34. Gigout A, Jolicoeur M, Buschmann MD. Low calcium levels in serum-free media maintain chondrocyte phenotype in monolayer culture and reduce chondrocyte aggregation in suspension culture. Osteoarthritis Cartilage. 2005;13: 1012–1024.
35. Lefebvre V, Smits P. Transcriptional control of chondrocyte fate and differentiation. Birth Defects Res C Embryo Today. 2005;75:200–212.
36. Gigout A, Jolicoeur M, Nelea M, et al. Chondrocyte aggregation in suspension culture is GFOGER-GPP- and beta1 integrin-dependent. J Biol Chem. 2008;283:31522–31530.
37. Henson FM, Getgood AM, Caborn DM, et al. Effect of a solution of hyaluronic acid-chondroitin sulfate-N-acetyl glucosamine on the repair response of cartilage to single-impact load damage. Am J Vet Res. 2012;73:306–312.
38. Marti-Bonmati L, Sanz-Requena R, Rodrigo JL, et al. Glucosamine sulfate effect on the degenerated patellar cartilage: preliminary findings by pharmacokinetic magnetic resonance modeling. Eur Radiol. 2009;19:1512–1518.
39. Taniguchi S, Ryu J, Seki M, et al. Long-term oral administration of glucosamine or chondroitin sulfate reduces destruction of cartilage and up-regulation of MMP-3 mRNA in a model of spontaneous osteoarthritis in Hartley guinea pigs. J Orthop Res. 2012;30:673–678.

Address correspondence to:
Jochen Ringe, PhD
Tissue Engineering Laboratory
Department of Rheumatology
Charité-Universitätsmedizin Berlin
Charitéplatz 1
10117 Berlin
Germany

E-mail: jochen.ringe@charite.de

Matrix Biology 32 (2013) 452–465

Contents lists available at ScienceDirect

Matrix Biology

journal homepage: www.elsevier.com/locate/matbio

Extracellular matrix of adipogenically differentiated mesenchymal stem cells reveals a network of collagen filaments, mostly interwoven by hexagonal structural units

Mujib Ullah *, Michael Sittinger [1], Jochen Ringe [2]

Tissue Engineering Laboratory & Berlin-Brandenburg Center for Regenerative Therapies, Dept. of Rheumatology and Clinical Immunology, Charité-University Medicine Berlin, Charitéplatz 1, 10117 Berlin, Germany

ARTICLE INFO

Article history:
Received 13 May 2013
Received in revised form 2 July 2013
Accepted 4 July 2013

Keywords:
ECM
Integrins
Cadherins
Selectins
Lipid droplets
Matrix signaling

ABSTRACT

Extracellular matrix (ECM) is the non-cellular component of tissues, which not only provides biological shelter but also takes part in the cellular decisions for diverse functions. Every tissue has an ECM with unique composition and topology that governs the process of determination, differentiation, proliferation, migration and regeneration of cells. Little is known about the structural organization of matrix especially of MSC-derived adipogenic ECM. Here, we particularly focus on the composition and architecture of the fat ECM to understand the cellular behavior on functional bases. Thus, mesenchymal stem cells (MSC) were adipogenically differentiated, then, were transferred to adipogenic propagation medium, whereas they started the release of lipid droplets leaving bare network of ECM. Microarray analysis was performed, to indentify the molecular machinery of matrix. Adipogenesis was verified by Oil Red O staining of lipid droplets and by qPCR of adipogenic marker genes *PPARG* and *FABP4*. Antibody staining demonstrated the presence of collagen type I, II and IV filaments, while alkaline phosphatase activity verified the ossified nature of these filaments. In the adipogenic matrix, the hexagonal structures were abundant followed by octagonal structures, whereas they interwoven in a crisscross manner. Regarding molecular machinery of adipogenic ECM, the bioinformatics analysis revealed the upregulated expression of *COL4A1*, *ITGA7*, *ITGA7*, *SDC2*, *ICAM3*, *ADAMTS9*, *TIMP4*, *GPC1*, *GPC4* and downregulated expression of *COL14A1*, *ADAMTS5*, *TIMP2*, *TIMP3*, *BGN*, *LAMA3*, *ITGA2*, *ITGA4*, *ITGB1*, *ITGB8*, *CLDN11*. Moreover, genes associated with integrins, glycoproteins, laminins, fibronectins, cadherins, selectins and linked signaling pathways were found. Knowledge of the interactive-language between cells and matrix could be beneficial for the artificial designing of biomaterials and bioscaffolds.

Title: Extracellular matrix of adipogenically differentiated mesenchymal stem cells reveals a network of collagen filaments, mostly interwoven by hexagonal structural units.

Authors: Mujib Ullah*, Michael Sittinger, Jochen Ringe

Address: Tissue Engineering Laboratory & Berlin-Brandenburg Center for Regenerative Therapies, Dept. of Rheumatology and Clinical Immunology, Charité-University Medicine Berlin, Charitéplatz 1, 10117 Berlin, Germany

Journal: Matrix Biology

Volume: 32, **Issues:** 7–8, October–November 2013, **Pages:** 452–465

stem cell research&therapy

RESEARCH Open Access

Mesenchymal stem cells and their chondrogenic differentiated and dedifferentiated progeny express chemokine receptor CCR9 and chemotactically migrate toward CCL25 or serum

Mujib Ullah[1*], Jan Eucker[2], Michael Sittinger[1] and Jochen Ringe[1]

Abstract

Introduction: Guided migration of chondrogenically differentiated cells has not been well studied, even though it may be critical for growth, repair, and regenerative processes. The chemokine CCL25 is believed to play a critical role in the directional migration of leukocytes and stem cells. To investigate the motility effect of serum- or CCL25-mediated chemotaxis on chondrogenically differentiated cells, mesenchymal stem cells (MSCs) were induced to chondrogenic lineage cells.

Methods: MSC-derived chondrogenically differentiated cells were characterized for morphology, histology, immunohistochemistry, quantitative polymerase chain reaction (qPCR), surface profile, and serum- or CCL25-mediated cell migration. Additionally, the chemokine receptor, CCR9, was examined in different states of MSCs.

Results: The chondrogenic differentiated state of MSCs was positive for collagen type II and Alcian blue staining, and showed significantly upregulated expression of *COL2A1*and *SOX9*, and downregulated expression of CD44, CD73, CD90, CD105 and CD166, in contrast to the undifferentiated and dedifferentiated states of MSCs. For the chondrogenic differentiated, undifferentiated, and dedifferentiated states of MSCs, the serum-mediated chemotaxis was in a percentage ratio of 33%:84%:85%, and CCL25-mediated chemotaxis was in percentage ratio of 12%:14%:13%, respectively. On the protein level, CCR9, receptor of CCL25, was expressed in the form of extracellular and intracellular domains. On the gene level, qPCR confirmed the expression of *CCR9* in different states of MSCs.

Conclusions: CCL25 is an effective cue to guide migration in a directional way. In CCL25-mediated chemotaxis, the cell-migration rate was almost the same for different states of MSCs. In serum-mediated chemotaxis, the cell-migration rate of chondrogenically differentiated cells was significantly lower than that in undifferentiated or dedifferentiated cells. Current knowledge of the surface CD profile and cell migration could be beneficial for regenerative cellular therapies.

Keywords: Chondrogenically differentiated cells, Stem cells, Cell migration, Chemotaxis, CCL25, CCR9

* Correspondence: mujib.ullah@charite.de
[1]Tissue Engineering Laboratory & Berlin-Brandenburg Center for Regenerative Therapies, Department of Rheumatology and Clinical Immunology, Charité-Universitätsmedizin Berlin, Charitéplatz 1, 10117 Berlin, Germany
Full list of author information is available at the end of the article

Introduction

Human mesenchymal stem cells (MSCs) hold great promise for tissue regeneration. During tissue repair, MSCs migrate to the sites of injury and participate in the repair process [1,2]. Stem cell migration not only plays a potential role in cell colonization inside biomaterial scaffolding [3], but also takes part in the reorganization of matrix [4]. Moreover, the guided migration of MSCs creates a therapeutic environment for bone regeneration [5]. These features emphasize the importance of targeted stem cell migration in tissue-engineering approaches.

Stem cell migration improves the curative ability of diseased tissues via appropriate homing inside injured sites [1,2,6]. Previously, it was reported that cell migration and subsequent suitable colonization of progenitor stem cells within injured sites accelerate myocardial regeneration [7,8], reduce heart damage [9,10], aid in recovery from spinal-cord injuries [11], cure nerve damage [12], and repair cartilage [13,14]. The MSCs have the potential to migrate through bone marrow endothelium, by using the regulatory mediators of matrix metalloproteinase-2 and tissue-inhibitor metalloproteinase-3 [15]. The administration of allogenic MSCs, whether derived from bone marrow or from adipose tissue, was reported for cellular proliferation, neurogenesis, and takes part in the functional recovery of brain after ischemic stroke [16]. Moreover, clinical trials of using human MSCs for bone fractures, bone defects, and cartilage disorders have been performed [17-19]. The investigation of targeted stem cell migration could be beneficial for tissue regeneration, especially for cartilage restoration. Chondrocytes in the articular cartilage lack innervations and vascularization and have low mitotic potential. Moreover, the chondrocytes have no physical contact to each other and entrapped into extracellular matrix [20-22]. These features make cartilage restoration is a hot issue in case of regeneration.

Autologous chondrocyte transplantation is an established technique for cartilage repair [23-25], which consists of chondrocyte isolation, *in vitro* dedifferentiation, and transplantation [25-27]. It is established that dedifferentiation is necessary to achieve a high cell number, and it is considered a curative step in such technologies [28-30]. However, massive dedifferentiation of chondrocytes results in loss of the chondrogenic phenotype and formation of primitive multipotent cell types [28-31]. To overcome such shortcomings, chondrogenic maintenance cues such as cytokines, chemokines, and growth factors are required to regulate and control the process of chondrocyte transplantation. The theoretic assumption is that this would increase remedial time and therapeutic cost because of *in vivo* posttransplantational procedures for chondrogenic differentiation and maintenance. It necessitates the use of such culture techniques and cell types, which not only maintain a chondrogenic-specific phenotype, from the beginning of transplantation, but also proliferate to increase the number of cells.

Therefore, the direct mobilization of endogenous cells and subsequent migration to the point of injury could be a promising approach for cartilage regeneration. In this context, the motility and migratory features of chondrocytes have been characterized [32]. To investigate the migratory effect of serum- or CCL25-mediated chemotaxis on chondrogenic cells, we isolated differentiated cells from compact pellets, after 28 days of chondrogenic differentiation. They maintained the chondrogenic nature for about 14 days in the culture and were able to proliferate. After chondrogenic confirmation, their surface profile and cell-migration ability were examined for serum- or CCL25-mediated chemotaxis.

Present strategies of stem cells transplantation advocate the use of MSCs [23,33-35], for diverse regenerative application, including cartilage repair [23,26]. In some cases, the clinical use of MSCs is considered more valuable than autologous chondrocytes transplantation [36,37], as it requires one less knee surgery, is easy to isolate, has a high proliferative rate, reduces cost, and provides better regenerative efficiency [28,35,36]. For instance, the use of magnetized MSCs is the best choice for articular cartilage repair [38]. In such cases, one controversial and basic question needs an answer: which cell type would be more suitable for cartilage regeneration, undifferentiated MSCs or their chondrogenic differentiated progeny? Therefore, we investigated the cell-migration profile of chondrogenically differentiated cells compared with the undifferentiated and dedifferentiated states of MSCs, according to already described formulation and concentration of allogenic serum [39].

However, allogenic serum has a complex composition [40-42], which is unknown and undefined for some molecular functions. It emphasizes the need for a defined and targeted chemokine, to make the present regenerative strategies more valuable and beneficial for appropriate cell homing. Moreover, chemokines are recognized as an essential factors for diverse cellular process including activation of the central hub of cellular migration via direct or indirect mechanisms and signaling events [39,43-45], and stimulation of the therapeutic efficiency of regeneration.

Chemotaxis is defined as directional movement of cells toward concentration gradients or chemoattractants, whereas chemokinesis is random cell movement without any chemoattractants [46]. Directional migration of MSCs to the site of injury is controlled by several factors, such as hypoxia and the Rho family of GTPases

[47,48]. Generally, tissue regeneration requires a coordinating and well-regulating cell migration for its restoration in response to different cues like cytokines and growth factors [43,49]. Apart from this, chemokines play a vital role in a biologic plethora of migration and are considered guided cues for directional and targeted stem cell trafficking [39,43,49]. Chemokines enable the activity of migratory processes in hematopoietic and nonhematopoietic cells [50], navigate the cellular trafficking between tissue compartments, and play a potential role in cell activation, differentiation, survival, and recruitment of leukocytes [51]. In addition, they play a decisive role in mobilization of T lymphocytes during allergenic reactions [52] and contribute to the complex pathophysiology of asthma by using the coordinating network of cellular activation and signaling web [53].

Chemokine-based recruitment of MSCs to the point of injury is a promising approach, whereas chemokine (C-C motif) ligand 25 (CCL25) could play a vital role in cell migration [44,54]. After nerve damage or myocardial infarction, the mutual interactions of chemokines and their receptors mediate the migration of MSCs to injured sites [55]. Obviously, to understand the underlying mechanism would be of interest. In this context, CCL25 has been suggested as a potential chemoattractant for the directional movement of MSCs [56], and C-C chemokine receptor type 9 (CCR9) is known as a cognate receptor of CCL25 [57,58]. To check whether the chondrogenic differentiated state of MSCs affects the cell-migration rate, we performed the chemotaxis assay for undifferentiated, chondrogenic differentiated and dedifferentiated cells, by using the chemokine CCL25 [54]. Furthermore, the receptor CCR9 was examined in different states of MSCs, as CCR9 is an established known receptor of CCL25 and plays a decisive role in the targeted migration of stem cells [43,44,54].

To cope with the challenges of the growing tissue-engineering industry, we need an appropriate cell source and suitable cell types, which are able not only to migrate to the site of injuries or damage in a well-guided way, but also to facilitate quick regeneration. Our introduced cell types could be valuable and beneficial in this regard.

Materials and methods

Ethics statement and MSC isolation

The study was approved by the institutional ethical committee of the Charité-University Medicine Berlin. Written informed consent was obtained from all participants, as a requirement of the ethical review board. The human MSCs were isolated from iliac crest bone marrow aspirates ($n = 3$; two men, one women; average age, 52.3 ± 1.5 years) of the healthy donors, who were examined to exclude hematopoietic neoplasms and were histologically diagnosed as normal. The 1-ml aspirate was seeded per T175 cm^2 of culture flasks (Becton Dickinson, Heidelberg, Germany). After 72 hours, nonadherent cells and cellular debris were washed out by media exchange, and cultures were further expanded in Dulbecco Modified Eagle Medium (DMEM; Biochrom, Berlin, Germany), supplemented with 10% fetal bovine serum (FBS; Hyclone, Cramlington, UK), 20 m*M* Hepes buffer (Biochrom), 2 m*M* L-glutamine (Biochrom), 2 ng/ml human basic-fibroblast growth factor (bFGF; Pepro Tech, London, UK) 100 units/ml penicillin and 100 μg/ml streptomycin (Biochrom), under established conditions. After expansion and subsequent confluences, the cells were detached with trypsin (0.05% 1 m*M* EDTA), and replated until passage 3.

Chondrogenic differentiation

For chondrogenic differentiation, 2.5×10^5 MSCs were centrifuged (150 *g*, 5 minutes) to form high-density micromass culture pellets. The chondrogenic differentiation of these pellets was achieved for 28 days with DMEM (4.5 g/L glucose; Biochrom), ITS supplements, 100 n*M* dexamethasone, 0.17 m*M* ascorbic acid-2-phosphate, 1 m*M* sodium pyruvate, 0.35 m*M* L-proline (all Sigma-Aldrich) and 10 ng/ml transforming growth factor-β3 (TGF-β3; PeproTeck, Hamburg, Germany). The control pellets were cultured in the same medium in the absence of TGF-β3. The medium (500 μl) was changed 3 times per week.

Cell isolation from chondrogenic pellets and dedifferentiation

After chondrogenic differentiation of the pellets for 28 days, cells were isolated with 300 U of collagenase II, 20 U of collagenase P, and 2 m*M* $CaCl_2$ for 90 minutes at 37°C [59]. Subsequently, some cells were cultured in a monolayer for 14 days in the presence of the chondrogenic differentiation-specific stimulus of TGF-β3, to maintain their chondrogenic nature. Conversely, the chondrogenically differentiated cells were cultured for five passages in the normal MSC expansion medium to accelerate proliferation and to generate dedifferentiated progenitor cells.

Flow-cytometric analysis for cell-surface screening

Fluorescence-activated cell sorting (FACS) analysis was performed not only to characterize the MSCs for their typical specific surface antigens, but also to determine the expression of these antigens in chondrogenic differentiated and dedifferentiated cells. For all experimental cell types, the cells ($n = 3$) were prepared in the form of a single-cell suspension, then washed with PBS/0.5% bovine serum albumin (BSA; both Biochrom), and centrifuged for 5 minutes at 250 *g*. The resuspended cells in the cold PBS/0.5% BSA were incubated for 15 minutes

on ice with R-phycoerythrin-labeled mouse anti-human CD14, CD34, CD73, CD166, and fluorescein isothiocyanate (FITC)-labeled mouse anti-human CD44, CD45, CD90, and CD105 antibodies. All antibodies were purchased from BD-Pharmingen (Heidelberg, Germany) except CD105, which was purchased from Acris Antibodies (Hiddenhausen, Germany).

After incubation, the cells were centrifuged (250 *g*, 5 minutes), washed with cold PBS/0.5% BSA, and re-suspended in the same buffer before cytometric analysis. To examine the extracellular domain of CCR9 receptor, staining was performed as described earlier but with PE-labeled mouse anti-human CCR9 (R&D Systems, Wiesbaden, Germany). For measurement of the intracellular domain of the CCR9 receptor, one additional step of permeabilization was added. After fixation with 4% paraformaldehyde (Sigma, Germany) for 15 minutes, cells were permeabilized for 10 minutes with FACS permeabilizing solution-2 (Becton Dickinson, Germany) and then processed as described earlier. The propidium iodide (100 μg/ml; Sigma-Aldrich) staining was applied for the exclusion of dead cells and cellular debris, whereas unstained cells were used as a negative control. The single-cell suspension was analyzed with flow cytometry, and CellQuest software (Becton Dickinson) was used for the interpretation and analysis of results.

Migration potential of cells

Migration potential of MSCs, chondrogenic differentiated cells, and dedifferentiated cells were assessed in response to 10% human allogenic serum or CCL25 chemokine (PeproTech, Germany). An already established chemotaxis assay by our group [33,54,60], was performed for all cell types with 8-μm pore size polycarbonate membranes in 96-multiwell format ChemoTx plates (Neuroprobe, Gaithersburg, USA). For migration of cells, either 10% allogenic serum or a selected concentration of CCL25 (500 nm, 750 nm, and 1,000 nm) [54] was applied in triplicate to the lower wells. The 4×10^4 cells for serum and 3×10^4 cells for CCL25 were seeded in the upper wells and incubated for 20 hours at 37°C. Negative controls were performed without chemokine or serum. Migrated cells were fixed in methanol/acetone, stained with hemacolor (Merck, Germany), and counted microscopically with Image J software.

Histology and immunohistochemistry

To examine chondrogenesis, the high-density micromass pellets were embedded in Tissue-Tek with O.C.T compound (Sakura Finetek, Torrance, USA), and then were frozen in liquid nitrogen and cryosectioned (6-μm thickness). For the cartilage-specific proteoglycan examination, these sections were stained with Alcian blue 8GX (Roth, Karlsruhe, Germany) and counterstained with nuclear fast red (Sigma Aldrich). For the deposition and accumulation of collagen type II in the ECM, cryosections (6 μm) were incubated for 1 hour with primary rabbit anti-human type II collagen antibodies (Acris Antibodies). Subsequently, the sections were processed according to the manufacturer's recommendation with the Envision system peroxidase kit (DAKO, Hamburg, Germany), followed by hematoxylin counterstaining (Merck, Darmstadt, Germany). The stained sections in the control samples were prepared from the chondrogenic control pellets.

To stain the chondrogenic differentiated and dedifferentiated cells, 2×10^5 cells were transferred to each well of the four-well chamber slides (Thermo-scientific, Germany). The cells inside chamber slides were cultured for 3 days under standard conditions to ensure the proper attachment of the cells to the slide surface. For direct staining, the cells were fixed for 5 minutes in already cooled 3.7% formaldehyde in PBS. Subsequently, cells were stained according to the standard procedure, as described for cryosections of the chondrogenic pellets.

RNA isolation and qPCR

For RNA isolation, the MSCs, chondrogenic differentiated, and dedifferentiated cells were mixed with TriReagent (Sigma-Aldrich). While the differentiated chondrogenic pellets [11-17], were first pooled for each individual donor (n = 3) in the 2-ml Eppendorf tube, then the TriReagent was mixed with these pellets and mechanically homogenized with an Ultra-Turrax (IKA, Staufen, Germany). Then 1-bromo-3-chloro-propane (Sigma-Aldrich) was added to all samples, followed by centrifugation (45 minutes, 13,000 *g*), and the upper phase, being free of proteins, was collected and mixed with an equal amount of ethanol. Subsequently, samples were processed with the RNeasy Mini Kit (Qiagen, Hilden, Germany), according to manufacturer recommendation. The quantity and quality of eluted RNA was ensured with NanoDrop measurements (NanoDrop Products, Wilmington, USA).

For qPCR, cDNA was synthesized from 2.5 μg total RNA by using the iScript cDNA synthesis kit (BioRad, Munich, Germany). The TaqMan qPCR was executed in triplicates in 96-well optical plates on a Mastercycler ep Realplex2 S system (Eppendorf, Hamburg, Germany). The gene-expression assays for typical chondrogenic-specific genes was performed with TaqMan probes and primer sets (Applied Biosystems, Darmstadt, Germany). Quantitative gene expression was analyzed for collagen type 2 A1 (*COL2A1*; Hs 00264051_m1), SRY (sex-determining region Y)-box-9 (*SOX9*; Hs 00165814_m1), C-C chemokine receptor type 9 (*CCR9*; Hs 01890924_s1), and glyceraldehyde-3-phosphate dehydrogenase (*GAPDH;* Hs99999905_m1). The expression of *COL2A1* and *SOX9* genes was normalized to the endogenous *GAPDH*

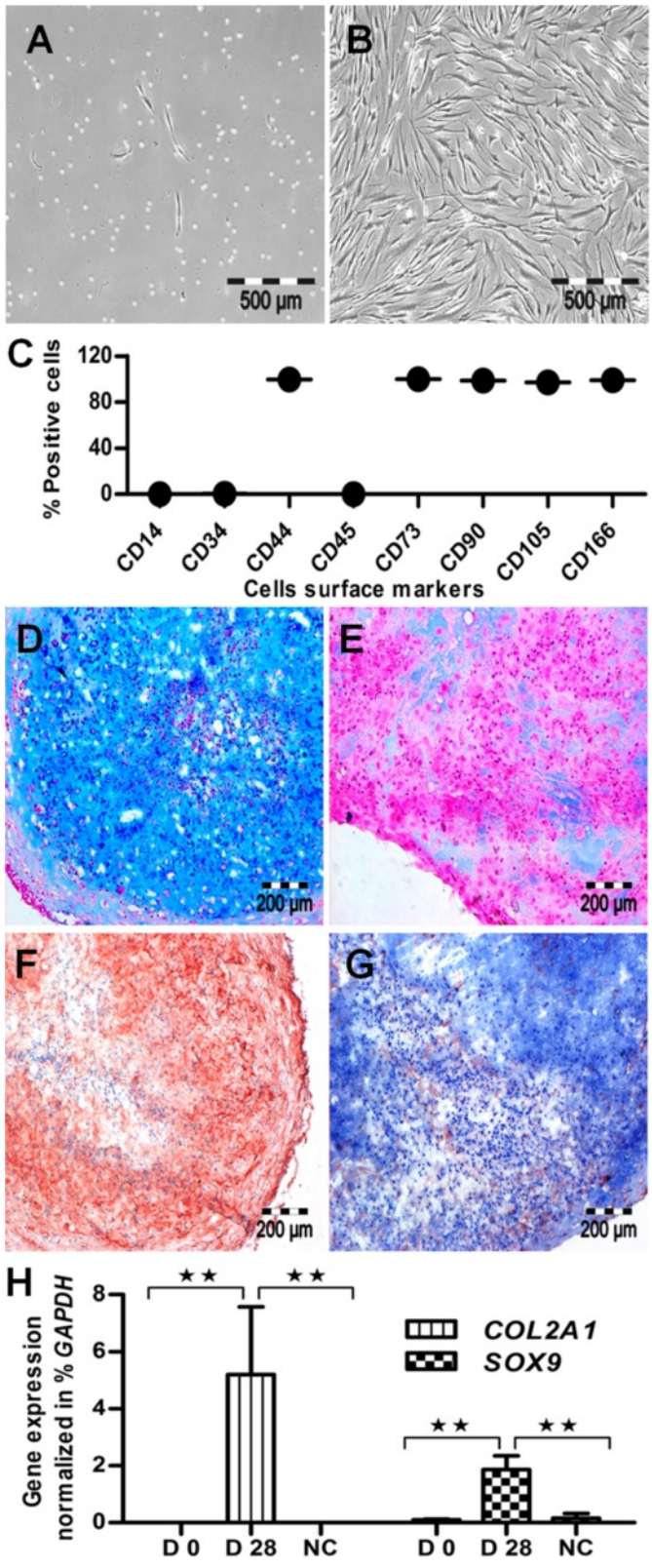

Figure 1 (See legend on next page.)

(See figure on previous page.)
Figure 1 MSC isolation, confirmation, and chondrogenic differentiation. (A) MSCs appeared as single cells in P0, and **(B)** showed uniform growth and fibroblast-like morphology in P3. **(C)** Flow-cytometric analysis revealed positive expression for typical MSC antigens like CD166, CD105, CD90, CD73, and CD44, but negative expression for hematopoietic lineage-specific antigens like CD45, CD34, and CD14 (three biologic replicates; $n = 3$), mean ± SEM. **(D)** On chondrogenic differentiation, they showed positive expression for Alcian blue staining compared with **(E)** control. **(F)** Similarly, they were positive for collagen type II expression compared with **(G)** unstimulated samples. **(H)** On the gene level, the chondrogenic differentiation was confirmed by significantly upregulated expression of *COL2A1* and *SOX9* genes compared with negative controls and undifferentiated MSCs, day 0 ($n = 3$). Student t test was performed for statistical analysis, and asterisks were assigned in the order $P^* < 0.05$, $P^{**} < 0.01$, and $P^{***} < 0.001$; mean ± SEM. Bar A, B, 500 μm; D through G, 200 μm.

expression level and calculated with the 2-ΔΔCt formula in percentage of *GAPDH* expression [61].

Statistical analysis

The statistical analysis was performed by using SigmaStat 3.5 software (Systat Software, USA), whereas GraphPad Prism4 (GraphPad Software) was used for drawing graphs. Simple Student t test was used for statistical assessment, and asterisks were assigned in the order $P^* < 0.05$, $P^{**} < 0.01$, and $P^{***} < 0.001$ for statistically significant values, whereas exact P values were mentioned for statistically nonsignificant data sets. Error bars in all figures represent standard error of the mean.

Results

MSC isolation, authentication, and chondrogenic differentiation

Human MSCs were isolated from bone marrow aspirates, as shown in the form of individual longitudinal cells in P0 (Figure 1A), which became homogeneous with subsequent growth and revealed the typical fibroblast-like morphology in P3 (Figure 1B). The surface screening of MSCs showed a positive expression for CD44, CD73, CD90, CD105, and CD166, and a negative expression for CD14, CD34, and CD45 antigens (Figure 1C). For MSCs, the FACS histogram plots are shown in supplementary Figure 1 (see Additional file 1: Figure S1), and their adipogenic, osteogenic, and chondrogenic potential was shown elsewhere [62]. The comparative flow-cytometric analysis of MSCs showed higher expression for their surface antigens compared with chondrogenic cells, as shown as a mean of three donors (see Additional file 2: Figure S5). Characterized MSCs were then induced to chondrogenic lineage differentiation. After 28 days of chondrogenic stimulation, the 6-μm-thick cryosections of the pellets showed cartilage-specific proteoglycan and were positive for Alcian blue staining (Figure 1D), in contrast to unstimulated control samples (Figure 1E). The chondrogenic ability of these samples was further ensured by the positive expression of cartilage-specific collagen type II (Figure 1F), compared with control samples (Figure 1G). On the gene level, the chondrogenic nature was verified by the expression of cartilage-specific genes *COL2A1* and *SOX9*. Both genes showed significantly upregulated expression in the chondrogenic samples compared with undifferentiated MSCs and controls (Figure 1H). These results confirmed the well-advanced state of chondrogenic differentiation.

Isolation of chondrogenic differentiated cells

After 28 days of chondrogenic differentiation, the cells were isolated from the compact pellets with enzymatic cues consisting of 300 U of collagenase II, 20 U of collagenase P, and 2 mM $CaCl_2$ (Figure 2) [59]. After successful isolation, the cells were cultivated in culture flasks to remove the components of the extracellular matrix, and their differentiated state was maintained in the presence of chondrogenic differentiation stimulus TGF-β3 for 14 days, and 2×10^5 cells were transferred to chamber slides for histologic and immunohistochemical assessment. The chondrogenic potential of cultured cells showed a positive expression of collagen type II (Figure 2A) compared with control samples (Figure 2B). Similarly, the chondrogenic-stimulated samples were positive for Alcian blue staining (Figure 2C) compared with unstimulated control samples (Figure 2D), indicating cartilage-specific proteoglycan in the culture. This indicates that the cell-isolation procedure, removal of extracellular matrix, and subsequent cultivation does not affect the chondrogenic potential of cultured cells.

Similarly, on the gene level, they showed significantly higher expression of *COL2A1* and *SOX9* compared with undifferentiated MSCs and unstimulated controls (Figure 2E). After removing the extracellular components, the cultured cells were isolated with trypsinization (after 3 days) and subsequently analyzed for surface antigens. The surface screening showed a reduced expression for CD44, CD73, CD90, CD105, and CD166 antigens (Figure 2F; see Additional file 3: Figure S2) compared with undifferentiated MSCs (Figure 1H), indicating that MSCs reduce their expression for above-surface CD epitopes on chondrogenic differentiation. This statement is further confirmed by the comparative flow-cytometric analysis of surface antigens for three independent donors, in chondrogenically differentiated cells compared with undifferentiated and dedifferentiated cells (see Additional file 2: Figure S5).

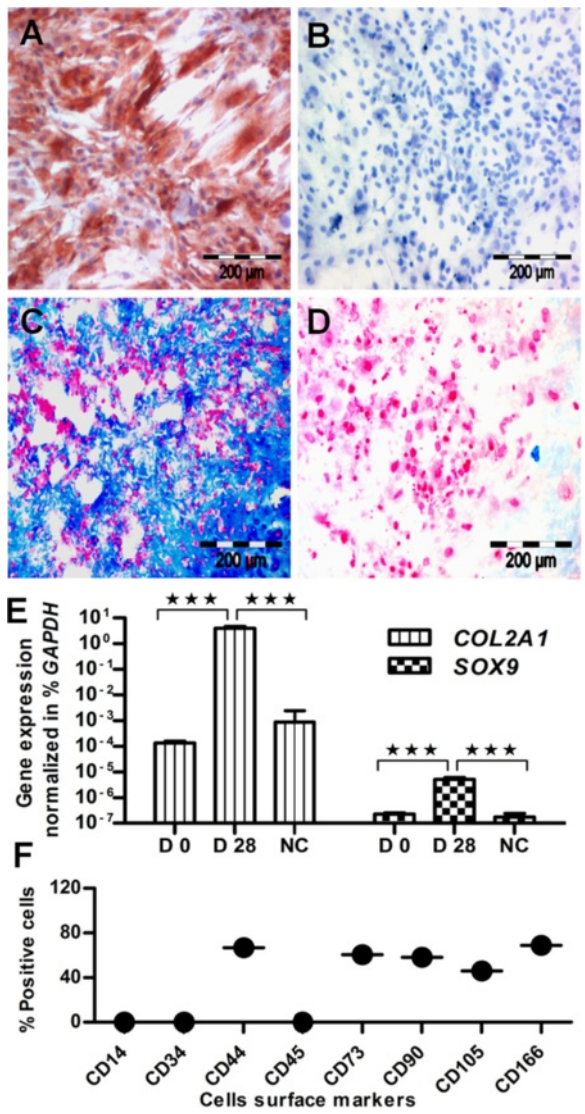

Figure 2 Isolation of chondrogenically differentiated cells and their confirmation. Chondrogenically differentiated cells were isolated from chondrogenic pellets. **(A)** Their chondrogenic character showed a positive collagen type II, **(C)** and Alcian blue staining, whereas the controls were negative for both **(B)** collagen type II **(D)** and Alcian blue staining. **(E)** After 28 days of induction, the chondrogenically differentiated cells showed significantly upregulated expression for cartilage-specific genes like *COL2A1* and *SOX9* compared with controls and undifferentiated cells, day 0 ($n = 3$), mean ± SEM. **(F)** Flow-cytometric analysis showed a relatively lower expression of CD44, CD73, CD90, CD105, and CD166 antigens compared with undifferentiated MSCs ($n = 3$). Student *t* test was performed for statistical analysis, and asterisks were assigned in the order $P^* < 0.05$, $P^{**} < 0.01$, and $P^{***} < 0.001$, mean ± SEM. Bar, 200 µm.

Dedifferentiation of chondrogenic differentiated cells

To measure the chemotaxis potential for different states of MSCs, the isolated chondrogenically differentiated cells were dedifferentiated in the MSC culture/expansion medium, to generate their dedifferentiated progeny. After five passages, they showed intensive proliferation and converted into dedifferentiated progenitor cells. To inspect whether the chondrogenic character is still present in dedifferentiated cells, we examined them for collagen type II expression. The collagen type II staining was almost as negative as that of control samples (Figure 3A and B). Similar to control samples, they showed negative Alcian blue staining (Figure 3C, D), indicating the absence of proteoglycan in dedifferentiated cells. On the gene level, they showed significantly downregulated expression of *COL2A1* and *SOX9* genes compared with chondrogenically differentiated cells (Figure 3E). In conclusion, these results confirmed the well-advanced state of dedifferentiation. Surface analysis of CD antigens again showed higher expression for CD44, CD73, CD90, CD105, and CD166 (Figure 3F; see Additional file 4: Figure S3) compared with chondrogenic differentiated cells, but this is relatively lower than MSC expression. Conclusively, the surface CD profile of MSCs changed with differentiation, but was not completely recovered after dedifferentiation, as confirmed by the quantitative measurement of surface antigens of three independent donors (see Additional file 2: Figure S5).

Migration of undifferentiated, chondrogenic differentiated, and dedifferentiated cells in response to serum-mediated chemotaxis

After generating different states of MSCs (undifferentiated, chondrogenic differentiated, and their derived dedifferentiated state), we performed the chemotaxis assay to determine the relative effect of cell migration on these states. As stem cells-guided migration is considered one crucial parameter among all preclinical characterizing parameters [54,60]. Therefore, migration potential was analyzed with 10% allogenic serum for undifferentiated MSCs, chondrogenic differentiated, and dedifferentiated cells. Undifferentiated MSCs showed intensive hemacolor staining for migrated cells (Figure 4A) compared with control samples (Figure 4B). The quantification-assessment tool of Image J software confirmed the migration of about 3.3×10^4 cells for the undifferentiated state of MSCs (Figure 4C). Similarly, the chondrogenically differentiated cells showed less hemacolor staining for migrated cells (Figure 4D) compared with the undifferentiated state of MSCs (Figure 4A). The control samples were negative (Figure 4E). The quantification assessment confirmed the migration of about 1.3×10^4 cells for the chondrogenic differentiated state of MSCs (Figure 4F), suggesting that the differentiated state limits the rate of cell migration. On subsequent dedifferentiation, the cells again showed higher hemacolor staining (Figure 4G) versus chondrogenic cells (Figure 4D) for migrated cells. The control samples showed negligible cell

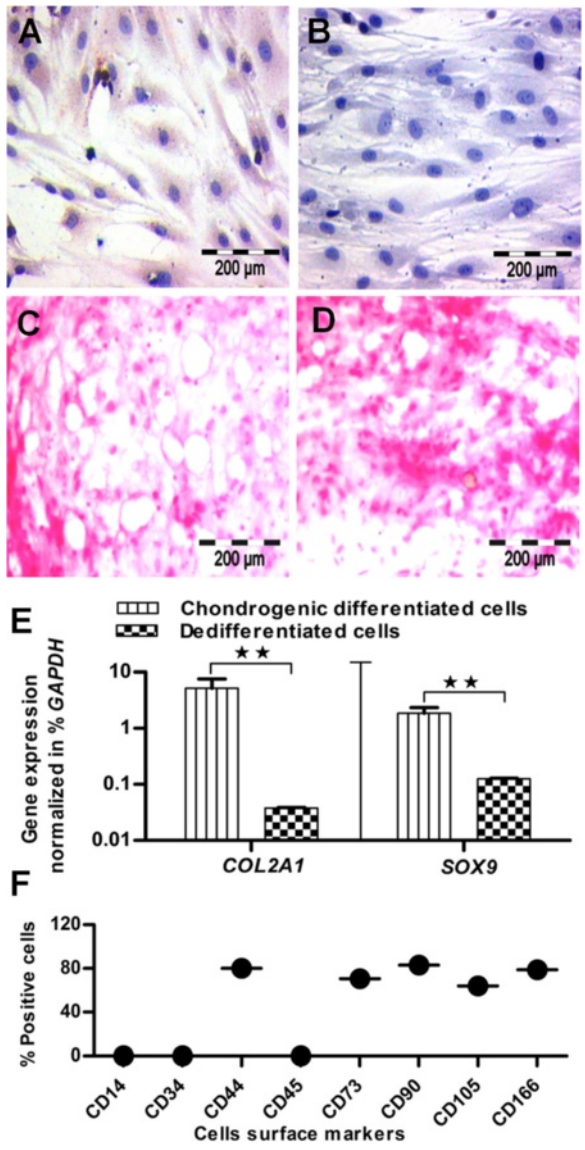

Figure 3 Dedifferentiation of chondrogenically differentiated cells. Chondrogenically differentiated cells were converted to dedifferentiated cells **(A)**, which showed almost the same collagen type II expression as **(B)** in control samples, and similarly **(C)** uniform expression for Alcian blue staining, **(D)** like their unstimulated control samples. **(E)** On the gene level, dedifferentiated cells showed significantly downregulated expression of *COL2A1* and *SOX9* genes, and confirmed the well-advanced state of dedifferentiation ($n = 3$). **(F)** Flow-cytometric profile of CD markers showed a relatively lower expression for dedifferentiated cells compared with the undifferentiated state of MSCs (n = 3), Student *t*test was performed for statistical analysis, and asterisks were assigned in the order P* < 0.05, P** < 0.01, and P*** < 0.001; mean ± SEM. Bar, 200 µm.

migration (Figure 4H). The quantitative calculation ensured the migration of about 3.4×10^4 cells for the dedifferentiated state of MSCs (Figure 4I).

In conclusion, the percentage comparison relative to total cell number (40×10^3) revealed about 33%, 84%, and 85% cell migration for the chondrogenic differentiated, undifferentiated, and dedifferentiated states of MSCs, respectively (Figure 4J). This is in line with the statement that mature chondrocytes have relatively low migration potential *in vivo* for cartilage repair, because of its inherent architectural nature [20,22]. Allogenic 10% serum-mediated chemotaxis recruited relatively more cells for the undifferentiated (84%) and dedifferentiated states (85%), compared with the chondrogenic differentiated state (33%) of MSCs.

Migration of undifferentiated, chondrogenic differentiated, and dedifferentiated cells in response to CCL25-mediated chemotaxis

Biochemically, the serum is a complex and an undefined cue for diverse known and unknown functions, including migration [39-42]. Hence, it emphasizes the need for a known chemokine for guided and targeted cell migration. Moreover, CCL25 is an important chemoattractant and well known to initiate the process of inflammation, cellular mobilization, and migration of cells for effective regeneration [63,64]. In this scenario, CCL25 has been tested by our group [44,54] and reported as an important chemokine for targeted stem cell migration in regenerative medicine. Therefore, we assessed the relative effect of cell migration on different states of MSCs (undifferentiated, differentiated, and dedifferentiated), by using different concentrations of CCL25 (500 n*M*, 750 n*M*, and 1,000 n*M*). At 1,000 n*M* concentration of CCL25, we found almost uniform hemacolor staining for undifferentiated (Figure 5A), chondrogenic differentiated (Figure 5D), and dedifferentiated states of MSCs (Figure 5G) compared with their respective controls (Figure 5B, E, and H). The quantification assessment for different states of MSCs was performed with Image J software. For different concentrations of CCL25 (500 n*M*, 750 n*M*, and 1,000 n*M*), the quantitative analysis confirmed the differences in cell migration for different states of MSCs. For instance, at 1,000 n*M* concentration, about 3.8×10^3 cells showed migration for the chondrogenic differentiated state (Figure 5F), about 4.5×10^3 cells for the undifferentiated state (Figure 5C), and about 4.4×10^3 cells for the dedifferentiated state (Figure 5I) of a total of 30×10^3 cells for each state of MSCs.

To show an obvious comparative representation of cell migration in different states of MSCs, percentage quantification analysis was performed. The percentage quantification assessment with Image J software revealed a cell migration of about 12% for the chondrogenic differentiated state, about 14% for the undifferentiated state, and about 13% for the dedifferentiated state of MSCs of a total 30×10^3 cells (Figure 5J) in response to CCL25-mediated chemotaxis at a concentration of 1,000 n*M* chemokine.

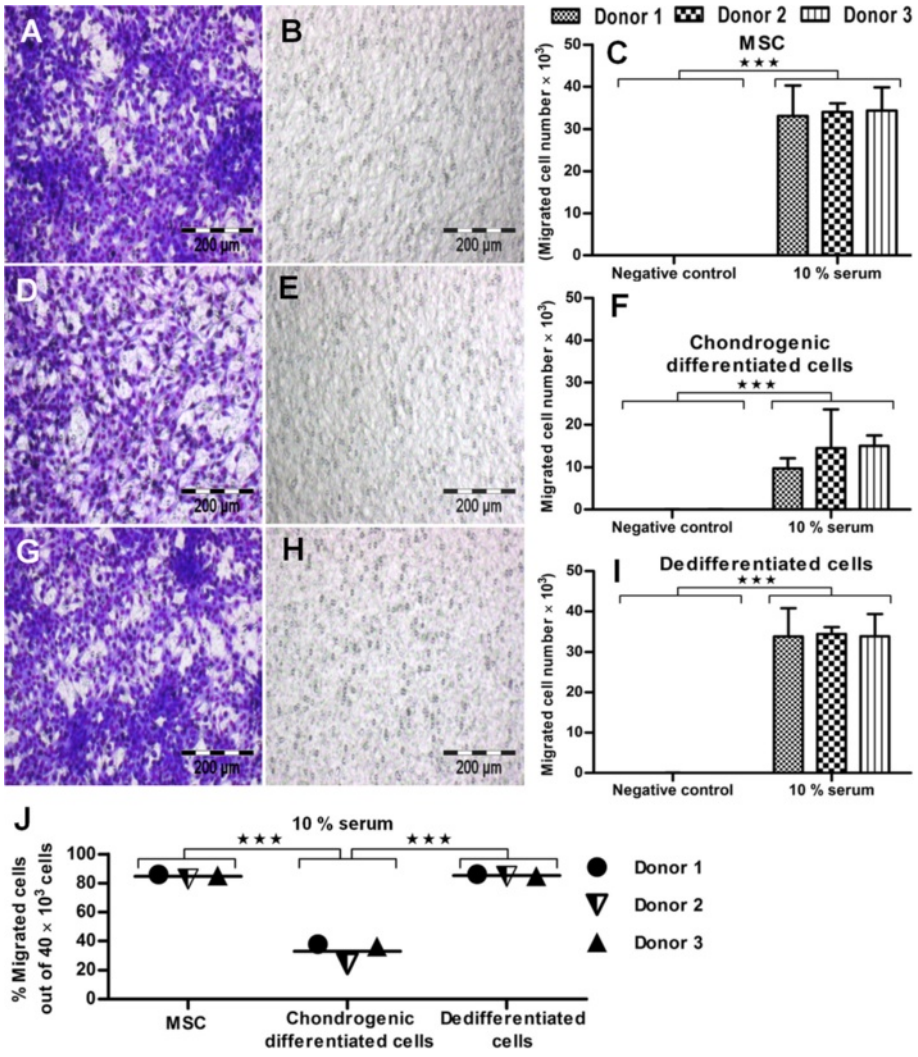

Figure 4 Serum-mediated chemotaxis for undifferentiated, chondrogenic differentiated, and dedifferentiated states of MSCs. (A) Serum-mediated chemotaxis showed higher hemacolor staining for MSCs compared with **(B)** control. **(C)** Quantification assessment with Image J software revealed more migrated cells for undifferentiated MSCs compared with control. **(D)** Chondrogenically differentiated cells showed intermediate hemacolor staining compared with **(E)** control, and **(F)** quantification assessment confirmed their low migration potential (33%). **(G)** Similarly, dedifferentiated cells again showed intense hemacolor staining compared with **(H)** control, **(I),** and the number of migrated cells was confirmed with Image J software. **(J)** The percentage of migrated cells relative to total cell number (40×10^3) is shown for undifferentiated, chondrogenic differentiated, and dedifferentiated states of MSCs ($n = 3$). Student t test was performed for statistical analysis, and asterisks were assigned in the order $P^* < 0.05$, $P^{**} < 0.01$, and $P^{***} < 0.001$, mean ± SEM. Bar, 200 μm.

In conclusion, chondrogenically differentiated cells showed a low migration potential compared with undifferentiated MSCs and dedifferentiated cells in response to serum-mediated chemotaxis. The reason for this low migration potential of chondrogenic differentiated cells may be hidden in the loss/modification of migration-specific receptors to serum, during differentiation. Conversely, chondrogenically differentiated cells had almost equally migrated (12%) compared with undifferentiated MSCs (14%) and dedifferentiated cells (13%) in response to CCL25-mediated chemotaxis. This enhances the value of CCL25 as a guided chemokine for cartilage repair, as its chemotactic activity is not influenced by the differentiated or undifferentiated nature of the cells. Alternatively, the receptors taking part in the CCL25-mediated chemotaxis, perhaps had not lost/modified their expression, during chondrogenic differentiation. However, CCL25 controls cellular trafficking irrespective of the cell architectural nature and the differentiated state, so it is important to investigate CCL25 as a migratory cue, in a broad spectrum, as the concentration of CCL25 (1,000 nM) was maintained similarly for undifferentiated, differentiated, and dedifferentiated states of MSCs.

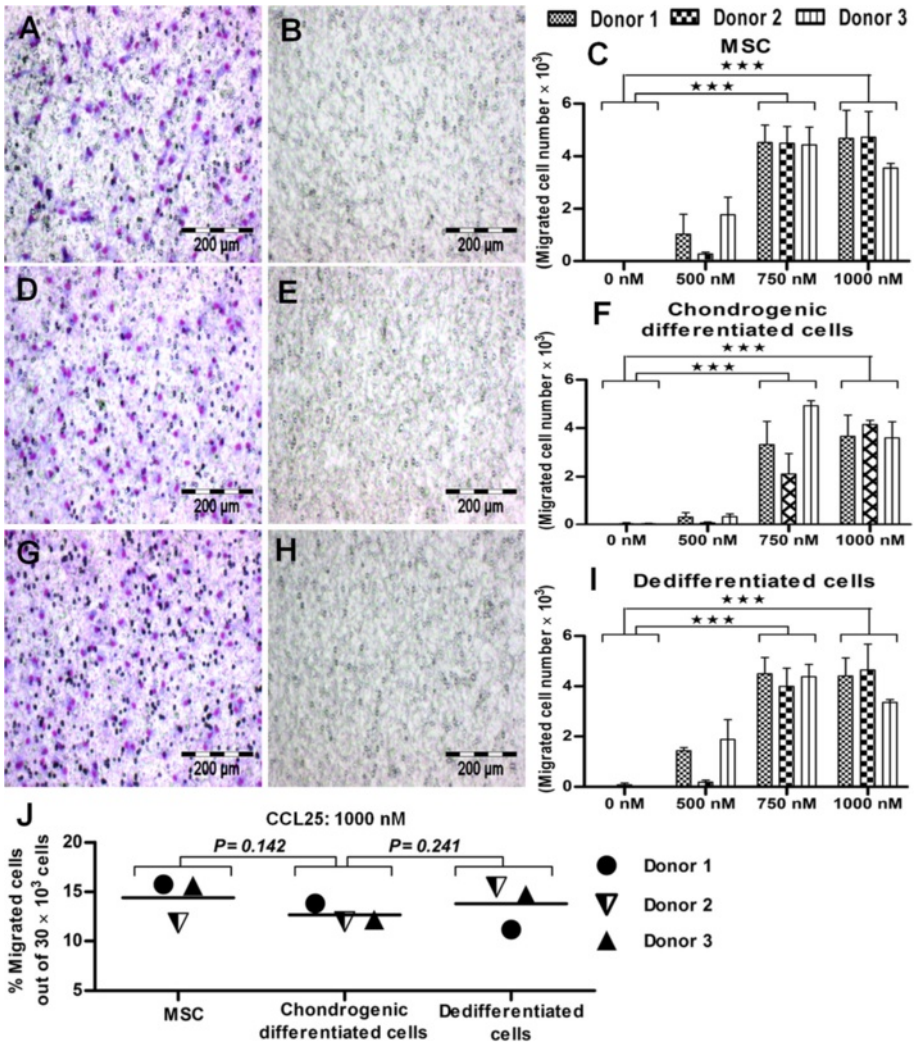

Figure 5 CCL25-mediated chemotaxis for undifferentiated, chondrogenic differentiated, and dedifferentiated states of MSCs. (A) In CCL25-mediated chemotaxis, the cell-migration assay showed almost uniform hemacolor staining for undifferentiated **(D),** chondrogenic differentiated **(G)**, and dedifferentiated states of MSCs compared with their **(B**, **E**, and **H)** respective controls. **(F)** Quantification assessment with Image J software confirmed a relatively low level of migration for chondrogenically differentiated cells (12%) compared with **(C)** undifferentiated and **(I)** dedifferentiated states of MSCs. **(J)** The percentage migration analysis relative to total cell number (30×10^3) is given for undifferentiated, chondrogenic differentiated, and dedifferentiated states of MSCs ($n = 3$). Student t test was performed for statistical analysis, and asterisks were assigned in the order $P^* < 0.05$, $P^{**} < 0.01$, and $P^{***} < 0.001$, mean ± SEM. Bar, 200 μm.

Why did the chondrogenic differentiated state show an almost equal rate of cell migration in CCL25-mediated chemotaxis compared with undifferentiated and dedifferentiated states of MSCs? CCR9, a binding receptor of CCL25 chemokine, was investigated to determine the role in guided cell migration.

Analysis of CCR9, a cellular receptor of CCL25 chemokine

CCL25 is an identified chemokine for stem cells-targeted migration, and CCR9 is its known receptor [54,57,58]. Thus, the undifferentiated, chondrogenic differentiated, and dedifferentiated states of MSCs were examined for CCR9 expression. The undifferentiated state of MSCs showed a bit greater and homogeneous staining for CCR9 receptor (Figure 6A) compared with the chondrogenic differentiated (Figure 6D) and dedifferentiated states (Figure 6G). The corresponding controls were negative for all states of MSCs (Figures 6B, E, and H). This indicates the presence of CCR9 receptor in only undifferentiated, differentiated, and dedifferentiated states of MSCs on a qualitative basis.

For quantitative measurement, flow-cytometric analysis was performed to examine the expression level of CCR9 receptor. However, CCR9 receptor has two distinct domains called extracellular and intracellular; thus flow-cytometric analysis was performed to screen all

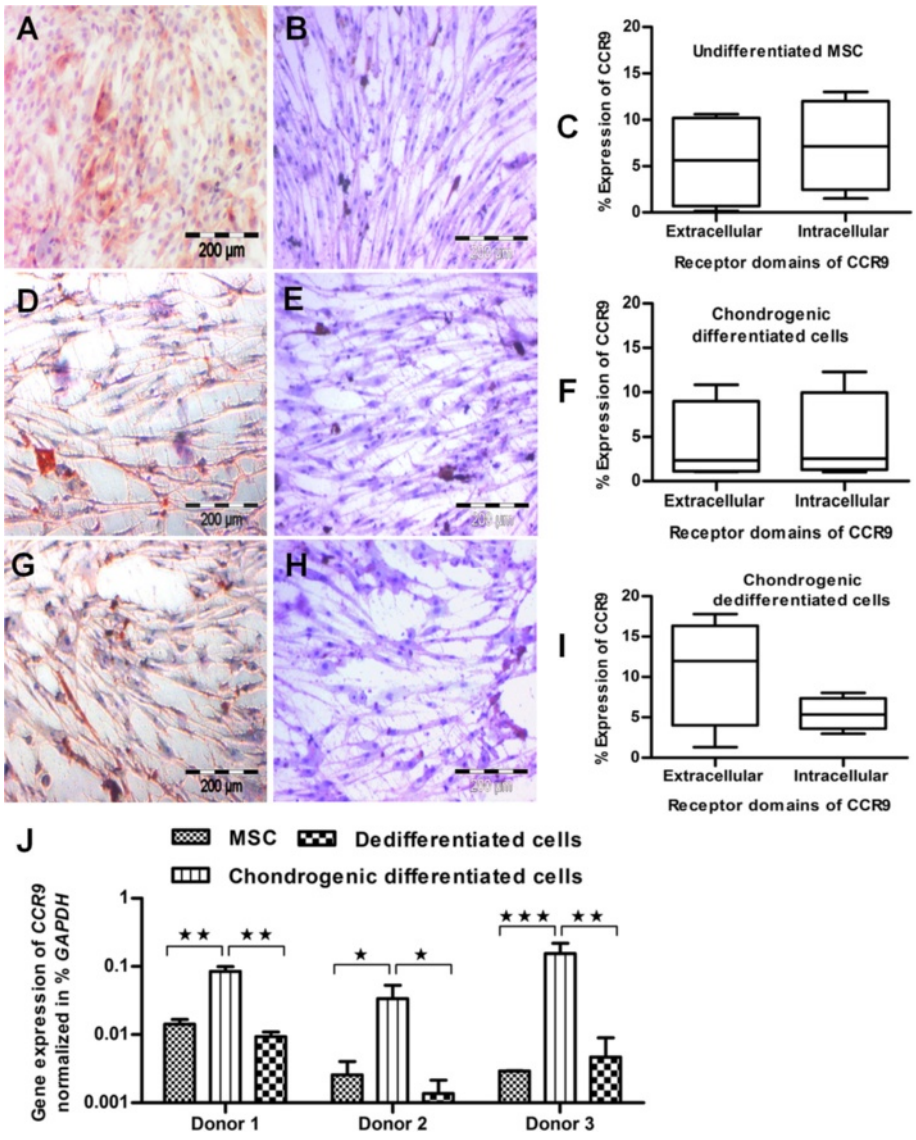

Figure 6 Analysis of CCR9, a cellular receptor of CCL25 chemokine. The immunohistochemical analysis of CCR9 showed greater staining for **(A)** the undifferentiated state compared with **(D)** chondrogenic differentiated and **(G)** dedifferentiated states of MSCs. The percentage flow-cytometric measurement for extracellular and intracellular domains of CCR9 is given in the form of average ($n = 3$) with a horizontal line, and bars represents a minimum or maximum expression for **(C)** undifferentiated state, **(F)** chondrogenic differentiated, and **(I)** dedifferentiated states of MSCs. **(J)** On the gene level, the qPCR analysis revealed significantly upregulated expression for *CCR9* receptor in the chondrogenic differentiated state compared with undifferentiated and dedifferentiated states of MSCs ($n = 3$). Student *t* test was performed for statistical analysis, and asterisks were assigned in the order $P^* < 0.05$, $P^{**} < 0.01$, and $P^{***} < 0.001$, average ± SD. Bar, 200 µm.

states of MSCs for its two domains. After analysis, their expression was quantitatively expressed in the form of averages, along with standard deviations ($n = 3$); here the representative bars are divided to specify a minimum or maximum expression. For undifferentiated (Figure 6C) and chondrogenic differentiated (Figure 6F) states of MSCs, the expression of extracellular and intracellular domains was almost similar and about 10% for each domain, whereas for the dedifferentiated state of MSCs, the expression of extracellular and intracellular domains was about 18% and 5%, respectively (Figure 6I). The detailed histogram plots for extracellular and intracellular domains of CCR9 receptors are in the form of supplemental files, for undifferentiated, chondrogenic differentiated, and dedifferentiated states of MSCs (see Additional file 5: Figure S4).

The expression level of CCR9 was almost homogeneous for extracellular (10%) and intracellular (10%) domains, and collectively about 20% for each undifferentiated and chondrogenic differentiated state of MSCs,

and a bit higher, about 23%, for their dedifferentiated state (Figure 6C, F, and I). On a molecular level, the qPCR analysis was performed for *CCR9* gene expression, which showed significantly upregulated expression for the chondrogenic differentiated state compared with undifferentiated and dedifferentiated states of MSCs (Figure 6J). Here, the protein and gene level expression of *CCR9* confirms the presence of receptor in undifferentiated, differentiated, and dedifferentiated states of MSCs.

Discussion

Guided stem cell migration is a vital approach for cell recruitment to the point of injury or damage. For cartilage regeneration, the endogenous mobilization of chondrogenic cells and subsequent migration could be a promising approach. In this context, the *in vivo* model remains to be proven; however, we performed some primary experiments *in vitro* for guided cell migration of chondrogenic differentiated cells, a step toward the search for the right cells for the job. Cartilage tissue is a combination of progenitor and differentiated cell types, such as chondroblasts, chondrocytes, and dedifferentiated cells [20,29,32]. Therefore, in the current study, we analyzed the chemotactic ability of undifferentiated, chondrogenic differentiated, and dedifferentiated states of MSCs with serum- or CCL25-mediated chemotaxis. Moreover, the surface profile of CD markers was investigated to screen and specify the chondrogenic differentiated state on the basis of typical MSC antigens. The flow-cytometric analysis revealed a low level of expression for CD44, CD73, CD90, CD105, and CD166 antigens in the chondrogenic differentiated state compared with undifferentiated and dedifferentiated states of MSCs, suggesting that chondrogenically differentiated cells reduce their expression for these surface antigens. In addition, these surface antigens are good characterizing markers for chondrogenically differentiated cells and their progeny, and in line with previously published reports, recommending the use of such surface markers for identification of chondrogenic cells [65,66].

Chondrogenically differentiated cells were assessed for cell migration in response to 10% allogenic serum-mediated chemotaxis [39] or an established concentration of 500 n*M*, 750 n*M*, and 1,000 n*M* CCL25-mediated chemotaxis [44,54]. In serum-mediated chemotaxis, we observed a significant decrease in recruited cells for the chondrogenic differentiated state (33%) compared with undifferentiated (84%) and dedifferentiated states (85%) of MSCs. We would recommend the use of chondrogenically differentiated cells for therapeutic repair of cartilage, as they have active signaling pathways, chondrogenic character, and biological paradigms of the differentiated state. For fast-track regeneration, the cartilaginous nature and chemokinetic ability of chondrogenically differentiated cells could be a beneficial asset.

For migration, serum is considered a very good chemoattractant for recruitment of cells; however, its composition is very complex, and its role as yet unknown in several biologic functions [40-42]. Therefore, we applied CCL25 for cell recruitment, a well-known chemokine for targeted stem cell migration [44,54]. Here, we noticed negligibly low migration potential for chondrogenically differentiated cells compared with serum-mediated chemotaxis.

In serum-mediated chemotaxis, we blame the inherent architectural ability of the chondrogenic differentiated state of MSCs for its limited cell migration. As chondrocytes have limited mitotic potential, lack of innervations and vascular supply, and are entrapped in the extracellular matrix, almost no physical contact with each other and restricted migration potential to the point of injury *in vivo* [20-22]. The CCL25-mediated chemotaxis has recruited 14%, 13%, and 12% of cells, respectively for undifferentiated, dedifferentiated, and chondrogenic differentiated states of MSCs. Here, the migration rate of chondrogenically differentiated cells was almost similar to the differentiated or undifferentiated states of MSCs. Perhaps the activation of some receptors and signaling in the chondrogenic differentiated state is the cause of this higher chemotactic ability. In this way, CCL25-mediated chemotaxis favors guided cellular trafficking, and we recommend the use of CCL25 as a migratory cue in regenerative applications. This especially highlights the significant use of chondrogenically differentiated cells for cartilage restoration because they have almost the same migration potential compared with the undifferentiated and dedifferentiated states of MSCs. The collective use of CCL25 chemokine and chondrogenic differentiated states of MSCs could be more beneficial for cartilage regeneration, possibly because of their active signaling, so the use of chondrogenically differentiated cells for cartilage repair could be fruitful.

We propose that chemotactic signals and inflammatory response from injured sites could induce cellular mobilization and create an intermediate pore sizes for subsequent movement of cells to the injured sites. Our suggestion is in line with the reports that inflammation plays a critical role in the regeneration of cartilage tissue [32,67-70].

Cytokine- and especially chemokine-based migration is a crucial step for *in vivo* regenerative application [43,71]. In this context, CCL25/CCR9 is a chemokine/receptor pair and plays a key regulative role in stem cell migration [57,58]. In our study, the immunohistochemical analysis was performed for the assessment of CCR9 receptor, which showed almost uniform staining for undifferentiated, differentiated, and dedifferentiated states of MSCs, indicated the presence of receptors in these

states. However, we have not used the positive controls for immunohistochemical staining of CCR9 receptor, which is a study limitation. For quantitative analysis, flow-cytometric analysis was performed to measure the expression of the extracellular and intracellular domains of the CCR9 receptor. It has been reported that intracellular signaling is required for CCL25 activation and stimulation of chemoattractant ability [45,72]. The expression of extracellular and intracellular domains of CCR9 collectively revealed about 20% expression for the undifferentiated and chondrogenic differentiated states, but about 23% expression for the dedifferentiated state of MSCs.

On the molecular level, we analyzed all states of MSCs for *CCR9* gene expression by performing qPCR, to identify the normalized amount of receptor to *GAPDH* [73]. Gene analysis showed significantly upregulated expression of *CCR9* in the chondrogenic differentiated state compared with the undifferentiated and dedifferentiated states of MSCs. To correlate the protein- and gene-level expression, we propose that any apparent observational change in the protein and gene level of the CCR9 receptor could be the cause of posttranscriptional and posttranslational level modification. In some cases, the protein-level expression of CCR9 does not correlate with mRNA level expression, and such noncorrelation of CCL25/CCR9 has been reported in mucosal immune systems on protein and gene levels [57], and favors our speculation about posttranslational modification. Furthermore, it also supports the Monte Carlo effect, a hypothesis drawn about the biological importance that the level of mRNA expression is not always directly correlated with the protein expression [74]. In addition, the chemotactic ability of CCL25 not only is the result of a cellular receptor of CCR9, but also is receiving signals from other receptors and signaling cascades for activation, stimulation, and cellular migration [64].

The current study generated the knowledge of the comparative surface CD profile, chemotaxis, and migration potential for undifferentiated, chondrogenic differentiated, and dedifferentiated states of MSCs. To understand the molecular mechanisms of migration in different states of MSCs could be valuable to identify the potential targets for wound healing, damage repair, and regeneration.

Conclusions

The chemokines, cytokines, and growth factors in consequence of inflammation facilitate cells homing to the site of injury and improve tissue regeneration [75]. These regenerative strategies emphasize the importance of targeted and guided chemotaxis for cell migration. Therefore, the chondrogenically differentiated cells were investigated for their chemotactic ability. In this context, chondrogenic pellets were generated from MSCs by using chondrogenic differentiation medium for 28 days. The chondrogenic nature of the pellets was confirmed by proteoglycan-specific Alcian blue staining, cartilage-specific collagen type II staining, and significantly upregulated cartilage-specific genes *COL2A1* and *SOX9*. Then differentiated cells were isolated from the intact chondrogenic pellets with enzymatic cues consisting of 300 U of collagenase II, 20 U of collagenase P, and 2 m*M* $CaCl_2$ [59]. After successful isolation, the differentiated cells were again verified for chondrogenic features, and they were positive for Alcian blue staining, collagen type II staining, and showed an upregulated expression of *COL2A1* and *SOX9*.

Afterward, the chondrogenically differentiated cells were washed with PBS, and extracellular matrix was removed; then their surface was analyzed for surface CD antigens. The surface profile of chondrogenically differentiated cells showed a positive expression of CD44, CD73, CD90, CD105, and CD166, but notably this expression was about 40% to 50% lower than that in undifferentiated and dedifferentiated states of MSCs. In serum-mediated chemotaxis, the number of migrated cells was significantly lower for the chondrogenic differentiated state (33%) compared with the undifferentiated (84%) and dedifferentiated (85%) states of MSCs, of a total 40×10^3 cells. In CCL25-mediated chemotaxis, the number of migrated cells was almost the same for the chondrogenic differentiated state (12%) compared with undifferentiated (14%) and dedifferentiated states (13%) of MSCs, of a total of 30×10^3 cells.

The expression of CCR9 was examined with immunohistochemistry and flow-cytometric analysis, which confirmed the presence of CCR9 in undifferentiated, differentiated, and dedifferentiated states of MSCs. On the molecular level, the expression of *CCR9* was significantly upregulated in the chondrogenic differentiated state compared with the undifferentiated and dedifferentiated states of MSCs. We propose that CCL25-mediated chemotaxis is influenced by the expression of CCR9 and stimulates guided cell migration in all states of MSCs. Cell migration as a result of mutual interaction of CCL25 and CCR9 has already been studied [57], and supports our conclusive message of guided chemotaxis. Moreover, the coupling interactions between CCL25 and CCR9 induce cell migration in porcine mucosal tissue and in the immune system during fetal development [57,58].

The *in vivo* migration of chondrogenically differentiated cells remains to be proven; however, *in vitro* oriented cell migration and homing study could provide valuable arguments in this direction for further investigation.

Additional files

Additional file 1: Figure S1. Flow-cytometric analysis of undifferentiated MSCs, isolated from bone marrow. MSCs in passage 3 ($n = 3$) were uniformly positive for typical surface markers like CD166, CD105, CD90, CD73, and CD44, as examples given for a single donor, and were negative for hematopoietic cell markers like CD45, CD34, and CD14.

Additional file 2: Figure S5. Comparative flow-cytometric profile of undifferentiated, chondrogenic differentiated and dedifferentiated cells. The comparative surface profile of CD markers showed a lower expression for chondrogenically differentiated cells compared with undifferentiated and dedifferentiated cells. Generally the undifferentiated, differentiated, and dedifferentiated states of MSCs were positive for CD44, CD73, CD90, CD105, and CD166 and negative for CD14, CD34, and CD45. The Student *t* test was performed for statistical analysis, and asterisks were assigned in the order $P^* < 0.05$, $P^{**} < 0.01$, and $P^{***} < 0.001$, mean ± SEM. Red asterisks represent the statistical comparison of undifferentiated cells versus dedifferentiated cells, whereas black asterisks represent the statistical comparison of undifferentiated cells versus chondrogenic differentiated cells.

Additional file 3: Figure S2. Flow-cytometric analysis of chondrogenically differentiated cells, isolated from chondrogenic pellets. Differentiated cells ($n = 3$) were positive for typical surface markers like CD166, CD105, CD90, CD73, and CD44, as exemplary of a single donor, and were negative for hematopoietic cell markers like CD45, CD34, and CD14. However, their plot expressions were not uniform and showed variations; moreover, chondrogenically differentiated cells significantly reduced their expression (about 40% to 50%) for CD166, CD105, CD90, CD73, and CD44.

Additional file 4: Figure S3. Flow-cytometric analysis of dedifferentiated cells. After dedifferentiation, the cells ($n = 3$) again showed higher expression for typical surface markers like CD166, CD105, CD90, CD73, and CD44, as examples of a single donor, and were negative for hematopoietic cell markers like CD45, CD34, and CD14. However, their plot expressions were not uniform and showed variations; moreover, dedifferentiated cells significantly recovered their expression compared with chondrogenically differentiated cells but still were relatively lower than undifferentiated MSCs.

Additional file 5: Figure S4. Flow-cytometric analysis of CCR9 receptor. Undifferentiated, chondrogenic differentiated and dedifferentiated cells ($n = 3$) were analyzed for CCR9, which is a cognate receptor of CCL25 chemokine. For complete assessment, the CCR9 examination was divided into extracellular and intracellular analysis, as examples of a single donor, which showed relatively lower level of expression for undifferentiated MSCs compared with chondrogenic differentiated and dedifferentiated cells. Moreover, the expression-profile plots, especially for the intracellular domain, were flatter compared with the extracellular domains.

Abbreviations

$CaCl_2$: Calcium chloride; *CCL25*: Chemokine (C-C motif) ligand 25; *CCR9*: C-C chemokine receptor type-9; CD: Cluster of differentiation; *COL2A1*: Collagen type IIα1; FACS: Fluorescence-activated cell sorting; GAPDH: Glyceraldehyde-3-phosphate dehydrogenase; MSC: Mesenchymal stem cell; PBS: Phosphate-buffered saline; PCR: Polymerase chain reaction; *SOX9*: *SRY (sex-determining region Y)-box-9*; TGF: transforming growth factor.

Competing interests

Michael Sittinger is a shareholder of CellServe Ltd. (Berlin, Germany) and BioRetis Ltd. (Berlin, Germany) and works as consultant for BioTissue Technologies Ltd. (Freiburg, Germany), which develops tissue transplants for the regeneration of bone and cartilage. The product activities of the companies are not related to the scientific topics presented here. The other authors indicate no potential conflict of interest. All authors disclose any financial and personal relationship with people or organizations that could inappropriately influence this scientifically oriented *in vitro* study. Therefore, no competing financial interests exist.

Authors' contributions

MU performed experiments, participated in the design and coordination of the study, and prepared the primary draft of the manuscript. MU, JR, and MS evaluated and cross checked the data, helped in the final drafting of manuscript, helped in processing of FACS data, and participated in the design and coordination of study. JE provided the bone marrow samples and helped in the coordination and final drafting of manuscript. All authors read and approved the final manuscript.

Acknowledgements

We thank Barbara Walewska and Anja Wachtel for excellent technical assistance. The study was supported by the Investitionsbank Berlin (IBB) and the European Regional Development Fund (grant number: 10147246), and the Berlin-Brandenburg Center for Regenerative Therapies (Bundesministerium für Bildung und Forschung, grant number: 1315848A). The grant sponsors had absolutely no influence on the study design, in the collection, analysis, and interpretation of data, in the writing of the manuscript, and in the decision to submit the manuscript to *Stem Cells Research and Therapy*.

Author details

[1]Tissue Engineering Laboratory & Berlin-Brandenburg Center for Regenerative Therapies, Department of Rheumatology and Clinical Immunology, Charité-Universitätsmedizin Berlin, Charitéplatz 1, 10117 Berlin, Germany. [2]Department of Hematology and Oncology, Charité-Universitätsmedizin Berlin, Charitéplatz 1, 10117 Berlin, Germany.

Received: 5 March 2013 Revised: 10 June 2013
Accepted: 12 August 2013 Published: 19 August 2013

References

1. Kang SK, Shin IS, Ko MS, Jo JY, Ra JC: **Journey of mesenchymal stem cells for homing: strategies to enhance efficacy and safety of stem cell therapy.** *Stem Cells Int* 2012, **2012:**342968.
2. Koelling S, Kruegel J, Irmer M, Path JR, Sadowski B, Miro X, Miosge N: **Migratory chondrogenic progenitor cells from repair tissue during the later stages of human osteoarthritis.** *Cell Stem Cell* 2009, **4:**324–335.
3. Langenbach F, Naujoks C, Kersten-Thiele PV, Berr K, Depprich RA, Kubler NR, Kogler G, Handschel J: **Osteogenic differentiation influences stem cell migration out of scaffold-free microspheres.** *Tissue Eng Part A* 2010, **16:**759–766.
4. Pranav S, Kelber JA, Lee JW, Wright TN, Vecchio KS, Klemke RL, Chen SC: **Cancer cell migration within 3D layer-by-layer microfabricated photocrosslinked PEG scaffolds with tunable stiffness.** *Biomaterials* 2012, **33:**7064–7070.
5. Trouillas M, Prat M, Doucet C, Ernou I, Laplace-Builhe C, Blancard PS, Holy X, Lataillade JJ: **A new platelet cryoprecipitate glue promoting bone formation after ectopic mesenchymal stromal cell-loaded biomaterial implantation in nude mice.** *Stem Cell Res Ther* 2013, **4:**1.
6. Gurtner GC, Callaghan MJ, Longaker MT: **Progress and potential for regenerative medicine.** *Annu Rev Med* 2007, **58:**299–312.
7. Orlic D, Kajstura J, Chimenti S, Jakoniuk I, Anderson SM, Li B, Pickel J, McKay R, Nadal-Ginard B, Bodine DM, Leri A, Anversa P: **Bone marrow cells regenerate infarcted myocardium.** *Nature* 2001, **410:**701–705.
8. Strauer BE, Schannwell CM, Brehm M: **Therapeutic potentials of stem cells in cardiac diseases.** *Minerva Cardioangiol* 2009, **57:**249–267.
9. Mingliang R, Bo Z, Zhengguo W: **Stem cells for cardiac repair: status, mechanisms, and new strategies.** *Stem Cells Int* 2011, **2011:**310928.
10. Zakharova L, Mastroeni D, Mutlu N, Molina M, Goldman S, Diethrich E, Gaballa MA: **Transplantation of cardiac progenitor cell sheet onto infarcted heart promotes cardiogenesis and improves function.** *Cardiovasc Res* 2010, **87:**40–49.
11. Kang KS, Kim SW, Oh YH, Yu JW, Kim KY, Park HK, Song CH, Han H: **A 37-year-old spinal cord-injured female patient, transplanted of multipotent stem cells from human UC blood, with improved sensory perception and mobility, both functionally and morphologically: a case study.** *Cytotherapy* 2005, **7:**368–373.
12. Liu W, Ren Y, Bossert A, Wang X, Dayawansa S, Tong J, He X, Smith DH, Gelbard HA, Huang JH: **Allotransplanted neurons used to repair peripheral nerve injury do not elicit overt immunogenicity.** *PLoS One* 2012, **7:**e31675.

13. Centeno CJ, Busse D, Kisiday J, Keohan C, Freeman M, Karli D: **Regeneration of meniscus cartilage in a knee treated with percutaneously implanted autologous mesenchymal stem cells.** *Med Hypotheses* 2008, **71:**900–908.
14. Wakitani S, Nawata M, Tensho K, Okabe T, Machida H, Ohgushi H: **Repair of articular cartilage defects in the patello-femoral joint with autologous bone marrow mesenchymal cell transplantation: three case reports involving nine defects in five knees.** *J Tissue Eng Regen Med* 2007, **1:**74–79.
15. De Becker A, Van Hummelen P, Bakkus M, Broek IV, De Wever J, De Waele M, Van Riet I: **Migration of culture-expanded human mesenchymal stem cells through bone marrow endothellum is regulated by matrix metalloproteinase-2 and tissue inhibitor of metalloproteinase-3.** *Haematol-Hematol J* 2007, **92:**440–449.
16. Gutierrez-Fernandez M, Rodriguez-Frutos B, Ramos-Cejudo J, Teresa Vallejo-Cremades M, Fuentes B, Cerdan S, Diez-Tejedor E: **Effects of intravenous administration of allogenic bone marrow- and adipose tissue-derived mesenchymal stem cells on functional recovery and brain repair markers in experimental ischemic stroke.** *Stem Cell Res Ther* 2013, **4:**11.
17. Lee JW, Kim YH, Kim SH, Han SH, Hahn SB: **Chondrogenic differentiation of mesenchymal stem cells and its clinical applications.** *Yonsei Med J* 2004, **45:**41–47.
18. Shekkeris AS, Jaiswal PK, Khan WS: **Clinical applications of mesenchymal stem cells in the treatment of fracture non-union and bone defects.** *Curr Stem Cell Res Ther* 2012, **7:**127–133.
19. Wang S, Qu X, Zhao RC: **Clinical applications of mesenchymal stem cells.** *J Hematol Oncol* 2012, **5:**19.
20. Bhosale AM, Richardson JB: **Articular cartilage: structure, injuries and review of management.** *Br Med Bull* 2008, **87:**77–95.
21. O'Driscoll SW: **The healing and regeneration of articular cartilage.** *J Bone Joint Surg Am* 1998, **80:**1795–1812.
22. Tetteh ES, Bajaj S, Ghodadra NS: **Basic science and surgical treatment options for articular cartilage injuries of the knee.** *J Orthop Sports Phys Ther* 2012, **42:**243–253.
23. Redman SN, Oldfield SF, Archer CW: **Current strategies for articular cartilage repair.** *Eur Cell Mater* 2005, **9:**23–32. discussion 23–32.
24. Ringe J, Haupl T, Sittinger M: **Future of tissue engineering in rheumatic diseases.** *Expert Opin Biol Ther* 2007, **7:**283–287.
25. Ringe J, Sittinger M: **Tissue engineering in the rheumatic diseases.** *Arthritis Res Ther* 2009, **11:**211.
26. Ringe J, Burmester GR, Sittinger M: **Regenerative medicine in rheumatic disease: progress in tissue engineering.** *Nat Rev Rheumatol* 2012, **8:**493–498.
27. Brittberg M, Lindahl A, Nilsson A, Ohlsson C, Isaksson O, Peterson L: **Treatment of deep cartilage defects in the knee with autologous chondrocyte transplantation.** *N Engl J Med* 1994, **331:**889–895.
28. Tang QO, Carasco CF, Gamie Z, Korres N, Mantalaris A, Tsiridis E: **Preclinical and clinical data for the use of mesenchymal stem cells in articular cartilage tissue engineering.** *Expert Opin Biol Ther* 2012, **12:**1361–1382.
29. de la Fuente R, Abad JL, Garcia-Castro J, Fernandez-Miguel G, Petriz J, Rubio D, Vicario-Abejon C, Guillen P, Gonzalez MA, Bernad A: **Dedifferentiated adult articular chondrocytes: a population of human multipotent primitive cells.** *Exp Cell Res* 2004, **297:**313–328.
30. Barbero A, Ploegert S, Heberer M, Martin I: **Plasticity of clonal populations of dedifferentiated adult human articular chondrocytes.** *Arthritis Rheum* 2003, **48:**1315–1325.
31. Lin L, Shen Q, Zhang C, Chen L, Yu C: **Assessment of the profiling microRNA expression of differentiated and dedifferentiated human adult articular chondrocytes.** *J Orthop Res* 2011, **29:**1578–1584.
32. Morales TI: **Chondrocyte moves: clever strategies?** *Osteoarthritis Cartilage* 2007, **15:**861–871.
33. Ringe J, Strassburg S, Neumann K, Endres M, Notter M, Burmester GR, Kaps C, Sittinger M: **Towards in situ tissue repair: human mesenchymal stem cells express chemokine receptors CXCR1, CXCR2 and CCR2, and migrate upon stimulation with CXCL8 but not CCL2.** *J Cell Biochem* 2007, **101:**135–146.
34. Hara Y, Stolk M, Ringe J, Dehne T, Ladhoff J, Kotsch K, Reutzel-Selke A, Reinke P, Volk HD, Seifert M: **In vivo effect of bone marrow-derived mesenchymal stem cells in a rat kidney transplantation model with prolonged cold ischemia.** *Transpl Int* 2011, **24:**1112–1123.
35. Orbay H, Tobita M, Mizuno H: **Mesenchymal stem cells isolated from adipose and other tissues: basic biological properties and clinical applications.** *Stem Cells Int* 2012, **2012:**461718.
36. Nejadnik H, Hui JH, Feng Choong EP, Tai BC, Lee EH: **Autologous bone marrow-derived mesenchymal stem cells versus autologous chondrocyte implantation: an observational cohort study.** *Am J Sports Med* 2010, **38:**1110–1116.
37. Dhinsa BS, Adesida AB: **Current clinical therapies for cartilage repair, their limitation and the role of stem cells.** *Curr Stem Cell Res Ther* 2012, **7:**143–148.
38. Kamei G, Kobayashi T, Ohkawa S, Kongcharoensombat W, Adachi N, Takazawa K, Shibuya H, Deie M, Hattori K, Goldberg JL, Ochi M: **Articular cartilage repair with magnetic mesenchymal stem cells.** *Am J Sports Med* 2013, **41:**1255–1264.
39. Kalwitz G, Andreas K, Endres M, Neumann K, Notter M, Ringe J, Sittinger M, Kaps C: **Chemokine profile of human serum from whole blood: migratory effects of CXCL-10 and CXCL-11 on human mesenchymal stem cells.** *Connect Tissue Res* 2010, **51:**113–122.
40. Psychogios N, Hau DD, Peng J, Guo AC, Mandal R, Bouatra S, Sinelnikov I, Krishnamurthy R, Eisner R, Gautam B, Young N, Xia J, Knox C, Dong E, Huang P, Hollander Z, Pedersen TL, Smith SR, Bamforth F, Greiner R, McManus B, Newman JW, Goodfriend T, Wishart DS: **The human serum metabolome.** *PLoS One* 2011, **6:**e16957.
41. Rajala K, Lindroos B, Hussein SM, Lappalainen RS, Pekkanen-Mattila M, Inzunza J, Rozell B, Miettinen S, Narkilahti S, Kerkelä E, Aalto-Setälä K, Otonkoski T, Suuronen R, Hovatta O, Skottman H: **A defined and xeno-free culture method enabling the establishment of clinical-grade human embryonic, induced pluripotent and adipose stem cells.** *PLoS One* 2010, **5:**e10246.
42. Mannello F, Tonti GA: **Concise review: no breakthroughs for human mesenchymal and embryonic stem cell culture: conditioned medium, feeder layer, or feeder-free; medium with fetal calf serum, human serum, or enriched plasma; serum-free, serum replacement nonconditioned medium, or ad hoc formula? All that glitters is not gold!** *Stem Cells* 2007, **25:**1603–1609.
43. Christopherson K 2nd, Hromas R: **Chemokine regulation of normal and pathologic immune responses.** *Stem Cells* 2001, **19:**388–396.
44. Endres M, Andreas K, Kalwitz G, Freymann U, Neumann K, Ringe J, Sittinger M, Haupl T, Kaps C: **Chemokine profile of synovial fluid from normal, osteoarthritis and rheumatoid arthritis patients: CCL25, CXCL10 and XCL1 recruit human subchondral mesenchymal progenitor cells.** *Osteoarthritis Cartilage* 2010, **18:**1458–1466.
45. Parmo-Cabanas M, Garcia-Bernal D, Garcia-Verdugo R, Kremer L, Marquez G, Teixido J: **Intracellular signaling required for CCL25-stimulated T cell adhesion mediated by the integrin alpha4beta1.** *J Leukoc Biol* 2007, **82:**380–391.
46. Liu Z, Klominek J: **Chemotaxis and chemokinesis of malignant mesothelioma cells to multiple growth factors.** *Anticancer Res* 2004, **24:**1625–1630.
47. Vertelov G, Kharazi L, Muralidhar MG, Sanati G, Tankovich T, Kharazi A: **High targeted migration of human mesenchymal stem cells grown in hypoxia is associated with enhanced activation of RhoA.** *Stem Cell Res Ther* 2013, **4:**5.
48. Raheja LF, Genetos DC, Wong A, Yellowley CE: **Hypoxic regulation of mesenchymal stem cell migration: the role of RhoA and HIF-1alpha.** *Cell Biol Int* 2011, **35:**981–989.
49. Seton-Rogers S: **Cytokine cues.** *Nat Rev Cancer* 2011, **11:**690.
50. Silva TA, Garlet GP, Fukada SY, Silva JS, Cunha FQ: **Chemokines in oral inflammatory diseases: apical periodontitis and periodontal disease.** *J Dent Res* 2007, **86:**306–319.
51. Baggiolini M, Dahinden CA: **Cc-chemokines in allergic inflammation.** *Immunol Today* 1994, **15:**127–133.
52. Penido C, Costa MFS, Souza MC, Costa KA, Candea ALP, Benjamim CF, Henriques MDMO: **Involvement of CC chemokines in gamma delta T lymphocyte trafficking during allergic inflammation: the role of CCL2/CCR2 pathway.** *Int Immunol* 2008, **20:**129–139.
53. Gonzalo JA, Lloyd CM, Wen DY, Albar JP, Wells TNC, Proudfoot A, Martinez C, Dorf M, Bjerke T, Coyle AJ, Gutierrez-Ramos JC: **The coordinated action of CC chemokines in the lung orchestrates allergic inflammation and airway hyperresponsiveness.** *J Exp Med* 1998, **188:**157–167.

54. Stich S, Loch A, Leinhase I, Neumann K, Kaps C, Sittinger M, Ringe J: **Human periosteum-derived progenitor cells express distinct chemokine receptors and migrate upon stimulation with CCL2, CCL25, CXCL8, CXCL12, and CXCL13.** *Eur J Cell Biol* 2008, **87:**365–376.
55. Phinney DG, Prockop DJ: **Concise review: mesenchymal stem/multipotent stromal cells: the state of transdifferentiation and modes of tissue repair: current views.** *Stem Cells* 2007, **25:**2896–2902.
56. Binger T, Stich S, Andreas K, Kaps C, Sezer O, Notter M, Sittinger M, Ringe J: **Migration potential and gene expression profile of human mesenchymal stem cells induced by CCL25.** *Exp Cell Res* 2009, **315:**1468–1479.
57. Meurens F, Whale J, Brownlie R, Dybvig T, Thompson DR, Gerdts V: **Expression of mucosal chemokines TECK/CCL25 and MEC/CCL28 during fetal development of the ovine mucosal immune system.** *Immunology* 2007, **120:**544–555.
58. Meurens F, Berri M, Whale J, Dybvig T, Strom S, Thompson D, Brownlie R, Townsend HG, Salmon H, Gerdts V: **Expression of TECK/CCL25 and MEC/CCL28 chemokines and their respective receptors CCR9 and CCR10 in porcine mucosal tissues.** *Vet Immunol Immunopathol* 2006, **113:**313–327.
59. Ullah M, Hamouda H, Stich S, Sittinger M, Ringe J: **A reliable protocol for the isolation of viable, chondrogenically differentiated human mesenchymal stem cells from high-density pellet cultures.** *BioRes Open Access* 2012, **1:**297–305.
60. Stich S, Haag M, Haupl T, Sezer O, Notter M, Kaps C, Sittinger M, Ringe J: **Gene expression profiling of human mesenchymal stem cells chemotactically induced with CXCL12.** *Cell Tissue Res* 2009, **336:**225–236.
61. Pfaffl MW: **A new mathematical model for relative quantification in real-time RT-PCR.** *Nucleic Acids Res* 2001, **29:**e45.
62. Ullah M, Stich S, Notter M, Eucker J, Sittinger M, Ringe J: **Transdifferentiation of mesenchymal stem cells-derived adipogenic-differentiated cells into osteogenic- or chondrogenic-differentiated cells proceeds via dedifferentiation and has a correlation with cell cycle arresting and driving genes.** *Differentiation* 2013, **85:**78–90.
63. Vicari AP, Figueroa DJ, Hedrick JA, Foster JS, Singh KP, Menon S, Copeland NG, Gilbert DJ, Jenkins NA, Bacon KB, Zlotnik A: **TECK: a novel CC chemokine specifically expressed by thymic dendritic cells and potentially involved in T cell development.** *Immunity* 1997, **7:**291–301.
64. Wurbel MA, McIntire MG, Dwyer P, Fiebiger E: **CCL25/CCR9 interactions regulate large intestinal inflammation in a murine model of acute colitis.** *PLoS One* 2011, **6:**e16442.
65. Lee HJ, Choi BH, Min BH, Park SR: **Changes in surface markers of human mesenchymal stem cells during the chondrogenic differentiation and dedifferentiation processes in vitro.** *Arthritis Rheum* 2009, **60:**2325–2332.
66. Chang CB, Han SA, Kim EM, Lee S, Seong SC, Lee MC: **Chondrogenic potentials of human synovium-derived cells sorted by specific surface markers.** *Osteoarthritis Cartilage* 2013, **21:**190–199.
67. Lu YL, Dhanaraj S, Wang ZW, Bradley DM, Bowman SM, Cole BJ, Binette F: **Minced cartilage without cell culture serves as an effective intraoperative cell source for cartilage repair.** *J Orthop Res* 2006, **24:**1261–1270.
68. Kouri JB, Jimenez SA, Quintero M, Chico A: **Ultrastructural study of chondrocytes from fibrillated and non-fibrillated human osteoarthritic cartilage.** *Osteoarthr Cartilage* 1996, **4:**111–125.
69. Qiu W, Murray MM, Shortkroff S, Lee CR, Martin SD, Spector M: **Outgrowth of chondrocytes from human articular cartilage explants and expression of alpha-smooth muscle actin.** *Wound Repair Regen* 2000, **8:**383–391.
70. Maumus M, Guerit D, Toupet K, Jorgensen C, Noel D: **Mesenchymal stem cell-based therapies in regenerative medicine: applications in rheumatology.** *Stem Cell Res Ther* 2011, **2:**14.
71. Mortier A, Gouwy M, Van Damme J, Proost P: **Effect of posttranslational processing on the in vitro and in vivo activity of chemokines.** *Exp Cell Res* 2011, **317:**642–654.
72. Hoffmann R: **Using the iHOP information resource to mine the biomedical literature on genes, proteins, and chemical compounds.** *Curr Protoc Bioinformatics* 2007, **Chapter 1:**Unit1 16.
73. Balcells I, Cirera S, Busk PK: **Specific and sensitive quantitative RT-PCR of miRNAs with DNA primers.** *BMC Biotechnol* 2011, **11:**70.
74. Karrer EE, Lincoln JE, Hogenhout S, Bennett AB, Bostock RM, Martineau B, Lucas WJ, Gilchrist DG, Alexander D: **In situ isolation of mRNA from individual plant cells: creation of cell-specific cDNA libraries.** *Proc Natl Acad Sci USA* 1995, **92:**3814–3818.
75. Van Linthout S, Stamm C, Schultheiss HP, Tschope C: **Mesenchymal stem cells and inflammatory cardiomyopathy: cardiac homing and beyond.** *Cardiol Res Pract* 2011, **2011:**757154.

doi:10.1186/scrt310
Cite this article as: Ullah *et al.*: Mesenchymal stem cells and their chondrogenic differentiated and dedifferentiated progeny express chemokine receptor CCR9 and chemotactically migrate toward CCL25 or serum. *Stem Cell Research & Therapy* 2013 **4**:99.

11. CURRICULUM VITAE

Mein Lebenslauf wird aus daten schutzrechtlichen Gründen in der electornischen Version meiner Arbeit nich veröffentlicht.

“For reasons of data protection, the Curriculum vitae is not published in the online version”.

12. Complete List of Publications:

1. Ullah M, Stich S, Notter M, Eucker J, Sittinger M, Ringe J. Transdifferentiation of mesenchymal stem cells-derived adipogenic-differentiated cells into osteogenic- or chondrogenic-differentiated cells proceeds via dedifferentiation and have a correlation with cell cycle arresting and driving genes. Differentiation. 2013. [doi: 10.1016/j.diff.2013.02.001] Impact Factor: 3.01.

2. Ullah M, Sittinger M, Ringe J. Transdifferentiation of adipogenically differentiated cells into osteogenically or chondrogenically differentiated cells: Phenotype switching via dedifferentiation. The International Journal of Biochemistry & Cell Biology. 2013. [In Press] Impact Factor: 4.91.

3. Ullah M, Stich S, Häupl T, Eucker J, Sittinger M, Ringe J. Reverse differentiation as a gene filtering tool in genome expression profiling of adipogenesis for fat marker gene selection and their analysis. PLoS One. 2013. [doi: 10.1371/journal.pone.0069754] Impact Factor: 4.09.

4. Hamouda H, **Ullah M**, Berger M, Sittinger M, Tauber R, Ringe J, Blanchard V. N-Glycosylation Profile of Undifferentiated and Adipogenically Differentiated Human Bone Marrow Mesenchymal Stem Cells - Towards a Next Generation of Stem Cell Markers. Stem Cells and Development. 2013. [doi:10.1089/scd.2013.0108] Impact Factor: 4.67.

5. Ullah M, Hamouda H, Stich S, Sittinger M, Ringe J. A reliable protocol for the isolation of viable, chondrogenically differentiated human mesenchymal stem cells from high-density pellet cultures. BioResearch Open Access. 2012. [doi: 10.1089/biores.2012.0279].

6. Ullah M, Sittinger M, Ringe J. Extracellular matrix of adipogenically differentiated mesenchymal stem cells reveals a network of collagen filaments, mostly interwoven by hexagonal structural units. Matrix Biology. 2013. [doi: 10.1016/j.matbio.2013.07.001] Impact Factor: 3.56.

7. Ullah M, Eucker J, Sittinger M, Ringe J. Mesenchymal stem cells and their chondrogenic differentiated and dedifferentiated progeny express chemokine receptor CCR9 and chemotactically migrate towards CCL25 or serum. Stem Cell Research & Therapy. 2013. [doi:10.1186/scrt310] Impact Factor: 3.65.

8. Ullah M, Eucker J, Sittinger M, Ringe J. Mesenchymal stem cells and their chondrogenic differentiated and dedifferentiated progeny express chemokine receptor CCR9 and chemotactically migrate towards CCL25 or serum. Stem Cell Research & Therapy. 2013. [doi:10.1186/scrt310] Impact Factor: 3.65.

9. Shafique M, Ahmad N, Awan FR, Mustafa T, **Ullah M**, Qureshi JA. Investigating the concurrent presence of HCV in serum, oral fluid and urine samples from chronic HCV patients in Faisalabad, Pakistan. *Archives* of *Virology*. 2009. [doi: 10.1007/s00705-009-0477-7] Impact Factor: 2.11.

10. Stich S, Tanzil G.S, Ibold Y, Stoll C, Abbas A, Kohl B, **Ullah M**, John T, Sittinger M, Ringe J. Continuous Cultivation of Human Hamstring Tenocytes on Microcarriers in a Spinner Flask Bioreactor System. Biotechnology Progress. 2013. [In revision] Impact Factor: 1.85.

Oral Presentations

Invited Key-note presentation:
Given an invited key-note talk at international conference for Tissue Engineering and Regenerative Medicine, TERMIS, Vienna, Austria, 2012.

Oral presentation:
Given an oral presentation at international conference for Tissue Engineering and Regenerative Medicine, TERMIS, Istanbul, Turkey, 2013.

Abstract Papers:

1. **Ullah M**, Stich S, Sittinger M, Ringe J. In vitro analysis of the transdifferentiation of adipogenic differentiated mesenchymal stem cells towards the osteogenic and chondrogenic lineage via dedifferentiation. Journal of Tissue Engineering & Regenerative Medicine. 2012.

2. Ullah M, Wloka Y, Sommerkamp S, Sittinger M, Ringe J. Structure and function of extracellular fat matrix generated by human mesenchymal stem cells. Journal of Tissue Engineering & Regenerative Medicine. 2013.

3. Ringe J, **Ullah M**, Sittinger M. Differentiation, dedifferentiation and transdifferentiation potential and mechanisms of human bone marrow-derived mesenchymal stem cells. Cell Journal, Vol.15. 2013.

4. Ringe J, Dehne T, Andreas K, Naderi-Meshkin H, **Ullah M**, Gulich K, Sittinger M. Migration and differentiation capacity of mesenchymal stem cells from patients with osteoarthritis. Towards In Situ Join Cartilage Tissue Engineering. Cell Journal, Vol.15. 2013.

5. Hamouda H, **Ullah M**, Kaup M, Blanchard V, Tauber R, Ringe J, Sittinger M. The N-glycome as a potential marker to differentiate human mesenchymal stem cells from adipocytes. Glycobiology. 2012.

Posters:

Ullah M, Stich S, Wloka Y, Sommerkamp S, Sittinger M, Ringe J. Genomic and proteomic analysis of extracellular fat matrix reveals a uniform structural and functional network for cellular interactions. 2013.

13. Acknowledgements

I am sincerely honored to pay thanks to my worthy supervisor Prof. Michael Sittinger for his acceptance to supervise my doctoral thesis and for his subsequent support, motivation, freedom in the lab and encouragement. He has helped me in critical thinking of research projects and in how to design and convert basic research into clinically oriented products. Moreover, he educated me in research grant writing, in how to collaborate the lab research products with industry, and in how to protect the clinical research translational products and patents.

I am deeply grateful to my worthy co supervisor Dr. Jochen Ringe. I really benefited immensely from his intriguing questions, suggestions and comments that he had raised in events such as manuscript writing, project proposal, research progress reports and seminar papers. He helped me allot in the designing of my personal and professional thinking for a challenging carrier. During, working with German colleagues and co-workers, I have learnt a lot which for sure will help me in my future career development. Such support and guidance were not limited only to my doctoral studies but also were extended to my personal life in Germany.

I am deeply indebted to all of my colleagues and especially members of the Tissue Engineering laboratory for their incredible support and help in a number of ways. It is also my pleasure to say thanks to all persons working in the Trans Tissue Technology for their support. Moreover, I am grateful to our collaborator Dr. Markus Berger and Houda Hamouda, who provided their support in a number of ways in the successful accomplishment of my Project.

I wish to express my love and gratitude to my beloved family members as well.